Implementation of High Performance Concrete in Washington State

WA-RD 530.1

Research Final Report
December 2001

Washington State Department of Transportation

Washington State Transportation Commission
Planning and Capital Program Management
in cooperation with:
U.S. DOT - Federal Highway Administration

Research Final Report

for
Research Project T9902-29
Implementation of High Performance
Concrete in Washington State

IMPLEMENTATION OF HIGH PERFORMANCE CONCRETE IN WASHINGTON STATE

by

Eyad Masad and Lisa James
Washington State Transportation Center (TRAC)
Department of Civil and Environmental Engineering
Washington State University
Pullman, WA 99164

Washington State Department of Transportation
Technical Monitor
David Jones, Assistant Roadway Construction Engineer

Prepared for

Washington State Transportation Commission
Department of Transportation
and in cooperation with
US Department of Transportation
Federal Highway Administration

December, 2001

TECHNICAL REPORT STANDARD TITLE PAGE

1. REPORT NO. WA-RD 530.1	2. GOVERNMENT ACCESSION NO.	3. RECIPIENT'S CATALOG NO.
4. TITLE AND SUBTITLE IMPLEMENTATION OF HIGH PERFORMANCE CONCRETE IN WASHINGTON STATE		5. REPORT DATE December , 2001 6. PERFORMING ORGANIZATION CODE
7. AUTHOR(S) Eyad Masad and Lisa James		8. PERFORMING ORGANIZATION REPORT NO.
9. PERFORMING ORGANIZATION NAME AND ADDRESS Washington State Transportation Center (TRAC) Civil and Environmental Engineering; Sloan Hall, Room 101 Washington State University Pullman, Washington 99164-2910		10. WORK UNIT NO. 11. CONTRACT OR GRANT NO. T9902-29
12. SPONSORING AGENCY NAME AND ADDRESS Research Office Washington State Department of Transportation Transportation Building, MS 7370 Olympia, Washington 98504-7370 Keith Anderson, Project Manager (360) 709-5405		13. TYPE OF REPORT AND PERIOD COVERED Final Report 14. SPONSORING AGENCY CODE

15. SUPPLEMENTARY NOTES

This study was conducted in cooperation with US Department of Transportation, Federal Highway Administration.

16. ABSTRACT

In this study, the performance of five typical mix designs from four different regions in Washington State is assessed. The performance characteristics that are evaluated include four durability properties: freeze-thaw durability, scaling resistance, abrasion resistance, chloride penetration, and one strength related property: compressive strength.

Determination of the current level of performance of existing concrete mixes is the first step toward fully implementing performance-based specifications. Knowing the level of durability of existing mix designs will give WSDOT a starting point in defining new levels of durability for higher performance mixes. Previously, the selection of appropriate mix designs was based solely on the flexural or compressive strength of the mix. The results of this study enable mix designs to be selected by matching the performance grade with exposure conditions.

A map of the state of Washington outlining freeze-thaw zones is presented to indicate exposure conditions. This may be used to match pavement performance grades with actual field conditions. Recommendations based on experimental findings and the literature review are provided for improving the durability of the mixes.

17. KEY WORDS Key words: Concrete, Performance, Freeze-thaw, Scaling, Abrasion, Permeability	18. DISTRIBUTION STATEMENT No restrictions. This document is available to the public through the National Technical Information Service, Springfield, VA 22616

19. SECURITY CLASSIF. (of this report)	20. SECURITY CLASSIF. (of this page)	21. NO. OF PAGES	22. PRICE
None	None	130 pages	

DISCLAIMER

TABLE OF CONTENTS

Section **Page**

TABLES

FIGURES

Figure		Page

SUMMARY

In this study, the performance of five typical mix designs from four different regions in Washington State is assessed. The performance characteristics that are evaluated include four durability properties: freeze-thaw durability, scaling resistance, abrasion resistance, chloride penetration, and one strength related property: compressive strength.

Determination of the current level of performance of existing concrete mixes is the first step toward fully implementing performance-based specifications. Knowing the level of durability of existing mix designs will give WSDOT a starting point in defining new levels of durability for higher performance mixes. Previously, the selection of appropriate mix designs was based solely on the flexural or compressive strength of the mix. The results of this study enable mix designs to be selected by matching the performance grade with exposure conditions.

A map of the state of Washington outlining freeze-thaw zones is presented to indicate exposure conditions. This may be used to match pavement performance grades with actual field conditions. Recommendations based on experimental findings and the literature review are provided for improving the durability of the mixes.

CHAPTER 1: INTRODUCTION

1.1 Problem Statement

Concrete mixes for pavements have been specified in the State of Washington based on their compressive or flexural strength. However, several studies have shown that durability characteristics should be taken into consideration when specifying pavement concrete mixes. Therefore, the Washington State Department of Transportation (WSDOT) is in the process of implementing performance-based specifications for concrete based on the Federal Highway Administration (FHWA) definition of High Performance Concrete (HPC). FHWA defines HPC by durability and strength parameters that can be measured using standardized tests and given a performance grade (Goodspeed et al. 1996). The performance characteristics include four durability properties: freeze-thaw durability, scaling resistance, abrasion resistance, chloride penetration, and four strength related properties: compressive strength, elasticity, shrinkage, and creep as shown in Table 1.1 (Goodspeed et al. 1996). Testing method details for determining HPC performance grades are given in Table 1.2. The recommended HPC grades based on field exposure conditions are given in Table 1.3.

Prior to developing new specifications for concrete mix durability, it is necessary to establish a baseline that defines the durability of typical mixes used in concrete pavements in the state. This would assist WSDOT and the industry in identifying methods for adjusting mix designs in order to achieve desirable durability levels. It will also give a starting point for developing reasonable specifications that consider the current durability levels.

1.2. Objectives

The objectives of the proposed research are:

1. To experimentally evaluate the performance grades of existing concrete mixes in Washington State based on their durability and compressive strength.
2. To investigate the relationship between freeze-thaw durability and compressive strength for typical mixes used in Washington State.
3. To create a map of the state of Washington that outlines freeze-thaw exposure conditions by region.
4. To make conclusions on the effect of various constituents of a concrete mix on its performance grade.
5. To propose recommendations for improving the durability and compressive strength of existing mixes based on the findings of this study and the literature review.

1.3. Task Summary

Task 1: Literature Review

The first task is to perform a literature review on the relationship between the mix constituents and its compressive strength and durability properties. The emphasis of the review is based on the results of SHRP C-103 and SHRP C-205 research.

Task 2: Experimental Plan

The second task is to acquire typical mixes from the state. Also, a laboratory work plan is developed in this task to evaluate the performance parameters of these concrete mixes.

Task 3: Testing and Analysis

The third task includes conducting the experiments for evaluating the mix properties in terms of compressive strength, resistance to freezing and thawing, chloride permeability, scaling, and abrasion. It also includes analyzing climatic data in the state to determine freeze-thaw exposure levels.

Task 4: Guidelines Development

The fourth task is to develop guidelines for improving the performance of concrete mixes. These guidelines will be based on critical review of the literature and research results.

Table 1.1: Grades of Performance Characteristics for High Performance Structural Concrete[1]

Performance Characteristic[2]	Standard test Method	FHWA HPC performance grade[3]			
		1	2	3	4
Freeze-thaw durability[4] (*x*=relative dynamic modulus of elasticity after 300 cycles	AASHTO T 161 ASTM C 666 Proc. A	60%≤*x*<80%	80%≤*x*		
Scaling resistance[5] (*x*=visual rating of the surface after 50 cycles)	ASTM C 672	*x*=4,5	*x*=2,3	*x*=0,1	
Abrasion resistance[6] (*x*=avg. Depth of wear in mm)	ASTM C 944	2.0> *x*≥1.0	1.0> *x*≥0.5	0.5>*x*	
Chloride penetration[7] (*x*=coulombs)	AASHTO T 277 ASTM C 1202	3000≥*x*>2000	2000≥*x*>800	800≥*x*	
Strength (*x*=compressive strength)	AASHTO T 2 ASTM C 39	41≤*x*<55 Mpa (6≤*x*<8 ksi)	55≤*x*<69 MPa (8≤*x*<10 ksi)	69≤*x*<97 MPa (10≤*x*<14 ksi)	*x*≥97 MPa (*x*≥14 ksi)
Elasticity[10] (*x*=modulus of elasticity)	ASTM C 469	28≤*x*<40 Gpa (≤*x*<6x10^6 psi)	40≤*x*<50 Gpa (6≤*x*<7.5x10^6 psi)	*x*≥50 Gpa (*x*≥7.5x10^6 psi)	
Shrinkage[8] (*x*=microstrain)	ASTM C 157	800>*x*≥600	600>*x*≥400	400>*x*	
Creep[9] (*x*=microstrain/pressure unit)	ASTM C 512	75≥*x*>60/Mpa (0.52*x*>0.41/psi)	60≥x>45/MPa (0.41≥x0.31/psi)	45≥x>30/MPa (0.31≥x0.21/psi)	30 MPa≥x (0.21 psi≥x)

[1]This table does not represent a comprehensive list of all characteristics that good concrete should exhibit. It does list characteristics that can quantifiably be divided into different performance groups.

[2]All tests to be performed on concrete samples moist or submersion cured for 56 days. See Table 2 for additional information and exceptions.

[3]A given HPC mix design is specified by a grade for each desired performance characteristic. For example, a concrete may perform at Grade 4 in strength and elasticity, Grade 3 in shrinkage and scaling resistance, and Grade 2 in all other categories.

[4]Based on SHRP C/FR-91, p. 3.52.

[5]Based on SHRP S-360.

[6]Based on SHRP C/FR-91-103.

[7]Based on *PCA Engineering Properties of Commercially Available High-Strength Concretes.*

[8]Based on SHRP C/FR-91-103, p. 3.25.

[9]Based on SHRP C/FR-91-103, p. 3.30.

[10]Based on SHRP C/FR-91-103, p. 3.17.

Table 1.2: Details of Test Methods for Determining HPC Performance Grades.

Performance Characteristic	Standard Test Method	Notes[1]
Freeze/Thaw Durability	AASHTO T 161 ASTM C 666 Proc. A	1. Test specimen 76.2 x 76.2 x 279.4 mm (3 x 3 x 11 in.,) cast or cut from 152.4 x 304.8 mm (6 x 12 in.) cylinder. 2. Acoustically measure dynamic modulus until 300 cycles.
Scaling Resistance	ASTM 672	1. Test specimen to have a surface area of 46.451 mm^2 (72 in^2) 2. Perform visual inspection after 50 cycles.
Abrasion	ASTM C 944	1. Concrete shall be tested at 3 different locations. 2. At each location, 98 Newtons, for three, 2 minute, abrasion periods shall be applied for a total of 6 minutes of abrasion time per location. 3. The depth of abrasion shall be determined per ASTM C 799 Procedure B.
Chloride Penetration	AASHTO T 277 ASTM C 1202	1. Test per standard test method.
Strength	AASHTO T 22 ASTM C 39	1. Molds shall be rigid metal or one time use rigid plastic. 2. Cylinders shall be 100 mm dia. X 200 mm long (4 x 8 in.) or 150 mm dia. X 300 mm long (6.0 x 12.0 in.). 3. Ends shall be capped with high strength capping compound, ground parallel, or placed onto neoprene pads per AASHTO Specifications for Concretes. 4. Use of neoprene pads on early age testing of concrete exceeding 70 Mpa at 56 days should use neoprene pads on the 56 day test. 5. The 56 day strength is recommended.
Elasticity	ASTM C 469	1. Test per standard test method.
Shrinkage	ASTM C 157	1. Use 76.2 x 76.2 x 285 mm *3 x 3 x 11.25 in.) specimens. 2. Shrinkage measurements are to start 28 days after moist curing and be taken for a drying period of 180 days.
Creep	ASTM C 512	1. Use 152 x 305 mm (6 x 12 in.) specimens. 2. Cure specimens at 73 F and 50 percent RH after 7 days until loading at 28 days. 3. Creep measurements to be taken for a creep loading period of 180 days.

[1]See footnote to Table 1 for the curing period to be used before testing.

Table 1.3: Recommendations for the Application of HPC Grades.

	Recommended HPC Grade for Given Exposure Condition				
Exposure condition	N/A[2]	Grade 1	Grade 2	Grade 3	Grade 4
Freeze/Thaw Durability Exposure (x=F/T cycles per year)[1]	$x<3$	$3\leq x<50$	$50\leq x$		
Scaling Resistance Applied Salt [3] (x=tons/lane-mile-year)	$x<5.0$	$5.0\leq x$			
Abrasion Resistance (x=average daily traffic, studded tires allowed)	No studs/chains	$x \leq 50{,}000$	$50{,}000<x<$ 100,000	$100{,}000\leq x$	
Chloride Penetration Applied Salt[2] (x=tons/lane-mile-year)	$x<1$	$1.0\leq x<3.0$	$3.0\leq x<6.0$	$6.0\leq x$	

[1]F/T stands for "freeze/thaw." A freeze/thaw cycle is defined as an event where saturated concrete is subjected to an ambient temperature which drops below –2.2°C (28°F) followed by a rise in temperature above freezing.

[2] N/A stands for "not applicable" and indicates a situation in which specification of an HPC performance grade is unnecessary.

[3]As defined in SHRP S-360.

CHAPTER 2: LITERATURE REVIEW

This literature review focuses on the mix properties evaluated in this study: namely compressive strength, freeze-thaw resistance, chloride permeability, abrasion, and scaling. It highlights the relationship between these properties and mix constituents. To facilitate the use of the information related to HPC properties evaluated in this report, a summary of the literature research findings is provided in Table 2.1.

2.1. Freeze-Thaw Resistance

Air-entrainment, void-spacing factor (the average distance between air bubbles), aggregate durability, paste properties, and alkalinity are among the many aspects affecting the freeze-thaw durability of concrete. Air-entrainment is the introduction of very tiny air bubbles into the concrete mixture. The entrained air reduces the hydraulic pressures caused by freezing water, and consequently, increases the freeze-thaw resistance. The amount of air that should be added to the concrete to protect against freeze and thaw depends on the maximum coarse aggregate size. As the size of the coarse aggregate is reduced the paste volume becomes larger, which requires increased amounts of air-entrainment. Zia et al. (1993) found that 5% air-entrainment is sufficient to protect high performance concrete against freezing and thawing.

Some studies show the effect of air-entrainment to be dependent on the mix components. For example, Galeota (1991) compared air-entrained to non-air-entrained concrete mixes that contained Type I Portland cement, high silica fume content, a maximum coarse aggregate size of 20mm, and water to cement ratio (w/c) between 0.35 to 0.55. Silica fume is spherical glassy particles obtained from coal residue in electric arc furnaces that produce silicon or ferro-silicon alloys. Galeota et al., (1991) found that these mixes were not freeze-thaw durable, even when they were air-entrained. Mixes with 20% silica fume had less resistance to freezing and thawing than a control concrete without silica fume.

The spacing and size of the air voids significantly affect the durability of the concrete (e.g. Stark 1989). The American Concrete Institute (2000) recommends that air voids should be spaced no more than 0.008 in. Attiogbe et al. (1992), however, found that superplasticized and properly air-entrained mixes can be freeze-thaw durable even at spacing factors greater than the ACI recommended maximum of 0.008 in.

Smaller coarse aggregates are being used in concrete to increase freeze-thaw durability. Failure of the concrete due to freezing and thawing is usually caused by aggregate deterioration. Therefore, the use of durable coarse aggregate is essential to improve the freeze-thaw resistance. Pitt (1992) found that unsatisfactory pore structure of the coarse aggregate could reduce freeze-thaw durability. In some cases, paste can be the first component to fail due to freezing and thawing. Pitt (1992) concluded that the mortar could fail depending on the salt concentration during freezing and thawing.

Cementitious materials, including pozzolans, are usually used in concrete mixes and they have been found to influence their freeze-thaw properties. The most common pozzolonic materials used are fly ash and silica fume. Fly ash is a powder containing spherical silicate glass particles that consist of alumina, iron, and calcium. It is obtained from remaining coal particles after combustion in electric power generating plants. There are two types of fly ash, referred to as class C and class F. Class C fly ash has higher calcium content than class F fly ash. Mixes without fly ash contain pores with water and air that contribute no strength to the hardened concrete. However, when fly ash is added to the mix, it chemically combines with water, filling in some of the pores and hardening into an impenetrable solid. Fly ash increases the resistance to chemical breakdown of the concrete by increasing the density of the mix, and making it less permeable.

In 1990, Malhotra reported that Class F fly ash improves the freeze-thaw durability of concrete, and that high silica fume concretes do not resist freezing and thawing even when air-entrained. Nasser and Lai (1992) found that 20% replacement of cement with Class C fly ash improves the resistance to freezing and thawing. However, freeze-thaw resistance was found to decrease when 35-50% of Class C fly ash was used in concrete containing 6% air. Bilodeau et al. (1994a) found that normal weight concretes with high amounts of fly ash demonstrate high resistance to freezing and thawing.

Bowser et al. (1996) indicated that the freeze-thaw resistance of normal weight concrete decreases as the percentage of cementitious material increases. He reported that this decrease could be caused by an increase in alkalinity or an increase in density. Alkalinity causes concrete to expand during freezing. On the other hand, they observed that increasing the percentage of cementitious materials in lightweight mixes improves the freeze-thaw resistance. The recommendation by Bowser et al. (1996) was to keep the percentage of cementitious materials in a lightweight mix about 12-15%, and to keep fly ash quantities approximately 45%-50% of the cementitious material. They also pointed out that replacing some of the cement solution in concrete with silica fume would reduce the level of alkalinity, and consequently, increase the resistance to damage caused by freezing. This contradicts with the findings of Malhotra (1990) who reported that high silica fume concretes do not resist freezing and thawing.

The w/c ratio is another important factor that influences the resistance to freeze-thaw damage. Kashi and Weyers (1989) found that reducing w/c increases the freeze-thaw durability of high strength concrete in comparison to ordinary concrete. They also determined that with a w/c ratio less than 0.3, high strength silica fume concrete would be freeze-thaw resistant even without air-entrainment. However, concrete containing silica fume and w/c equal to 0.32 requires air-entrainment to be freeze-thaw durable. Van Dam and Aldrich (1998) recommended that w/c should not exceed 0.45 to provide freeze-thaw resistance.

Li, et al. (1994) experimented with mixes containing Type I Portland cement, 5% silica fume of the total mix, superplasticizer, a maximum coarse aggregate size of 14mm, and no air-entrainment. They showed that the freeze-thaw resistance of concrete was dependent on the w/c ratio. The use of w/c of 0.24 yielded concrete with excellent freeze-thaw durability, while concretes with w/c greater than 0.24 did not adequately resist freezing and thawing damage (Li et al., 1994).

Siebel (1989) found that mixes containing superplasticizer are freeze-thaw resistant when the air content of the fresh concrete is increased proportionately with the amount of superplasticizer. The increased air content is required because the superplasticizer alters the pore structure by increasing the number of pores that are at least 0.5mm and decreasing the number of pores that are less than 0.3mm.

2.2 Chloride Ion Penetration Resistance

The term "permeability" refers to the amount of water, liquid, gas, or ions that can penetrate the concrete. Chloride ion penetration is a major cause for corrosion of steel reinforcement. Decreasing permeability will improve the concrete's ability to resist chloride ion penetration. Chloride ions are introduced into the concrete by deicers or seawater. In general, the use of fly ash, silica fume, and lightweight concrete were found to improve chloride ion penetration resistance.

According to Ozyildirim (1998), concretes containing air-entrainment, pozzolans or slag, and a w/c ratio less than 0.45 have very low permeability. Torii and Kawamura's (1991) work also showed that mixes containing silica fume or fly ash are resistant to chloride ion permeability. Bilodeau et al. (1994b) experimented with 16 air-entrained mixes prepared with w/c = 0.33 and two types of fly ash. For each fly ash, two concrete mixtures were prepared using Type I and Type III Portland cement. All concretes exhibited high resistance to chloride-ion penetration. Ellis (1991) found that Class F fly ash improves concrete's resistance to chloride permeability better than Class C fly ash.

Naik et al. (1994a) analyzed mixtures containing Type I cement, class C fly ash, a maximum coarse aggregate size of 25 mm, superplasticizer, and an air-entraining agent. Their results showed that the replacement of up to 70% of cement with class C fly ash reduces the permeability of chloride ions at an age of 91-days. In 1995, Naik et al. observed that high-volumes of Class C fly ash increase chloride ion permeability resistance.

Zhang and Gjorv (1991) found that the permeability of high-strength lightweight concrete appeared to be more dependent on the porosity of the mortar mix than the porosity of the lightweight aggregate. Pigeon et al., (1991) studied the influence of drying of HPC on the chloride ion permeability, and concluded that silica fume at w/c = 0.25 or less will resist chloride ion penetration unless they are not adequately protected against freezing and thawing.

2.3 Abrasion Resistance

Abrasion resistance is necessary to reduce skidding or slipping on pavements. Many aspects of the mix design influence abrasion resistance, such as the type of aggregate, water/cement ratio, and the compressive strength.

Laplante et al. (1991) stated that the coarse aggregate is the most important factor affecting the abrasion resistance of concrete. Very hard aggregate, such as granite, exhibited very small amounts of abrasion in comparison to softer aggregates such as limestone. If coarse aggregate and mortar have the same abrasion resistance, the concrete will wear uniformly and cause skidding or slipping problems when wet. Fine aggregates should be 25% siliceous to be abrasion resistant. Laplante et al. (1991) also found that the w/c ratio significantly affects abrasion resistance because abrasion resistance decreases as w/c increases. A low w/c (0.30 or less) will produce abrasion resistant concrete.

Gjorv et al. (1990) used an accelerated loading facility that has four truck wheels with studded tires running at a speed up to 70 km/h to determine the abrasion resistance of different concrete mixes. Their results indicated that increasing compressive strength would increase abrasion resistance. In addition, they reported that the aggregate type has significant influence on abrasion resistance.

Naik et al., (1994a) found that abrasion resistance is predominantly influenced by the compressive strength. Their research also showed that concrete without fly ash experienced higher abrasion resistance during accelerated testing than concrete with 50 to 70 percent cement replacement. However, later work by Naik et al., (1995) showed that the abrasion resistance of concrete was dependent on the compressive strength regardless of the fly ash content.

De Almeida (1994) found that when 100% Portland cement was used, the concrete was abrasion resistant. The addition of silica fume to the concrete reduced the abrasion resistance. However, when silica fume and superplasticizer were added, abrasion resistance was improved. Thus, De Almedia (1994) concluded that the abrasion resistance of concrete containing pozzolans is improved with the addition of superplasticizing admixtures. Without superplasticizer the mineral admixtures will require more water and the abrasion resistance will decrease.

2.4 Surface Scaling Resistance

Scaling of concrete occurs when deicers cause a weak layer of paste at the surface of the concrete to flake off. Using a good mix design, and ensuring proper placing, finishing, and curing before applying deicing salts will improve scaling resistance. In general, mineral admixtures increase surface scaling, while low w/c content will improve concretes resistance to scaling.

Gagne et al. (1991) observed that concretes made of Type I and certain Type III Portland cements had sufficient salt scaling resistance without air entrainment. A study by Li et al. (1994) showed that non-air-entrained concrete had excellent scaling resistance when w/c of 0.27 was used, but suffered serious scaling when the w/c was 0.30 or 0.33 (Li et al., 1994).

Bilodeau et al. (1991) tested fly ash concretes and found that up to 30% replacement did not adversely influence the scaling resistance. They, however, attributed the scaling durability to an adequate air void system. Bilodeau and Malhotra (1994b) stated that high-volume Class F fly ash concretes do not protect against salt scaling. Later research by Bilodeau et al. (1994a) reported that fly ash concrete suffers from surface scaling.

McDonald and Perenchio (1997) tested the effect of various salts on scaling. They found that a proprietary salt solution caused the least amount of scaling and the salts containing potassium chloride resulted in the most scaling. The proprietary salt solution contained significant amounts of magnesium and the authors suspected that this was the cause of the scaling. The high strength concrete specimens experienced more scaling than the low strength mixtures when ponded with the proprietary salt.

2.5 Compressive Strength

Compressive strength is a measure of the maximum resistance a concrete specimen can maintain against axial loading. It is one of the primary parameters for concrete quality control testing. Although very high compressive strengths can be easily obtained, it is important to understand how the addition of pozzolans, w/c ratio, age, and the type of cement affect the compressive strength of concrete.

Bilodeau and Malhotra (1994b) found that high-volume class F fly ash made with Type I cement could obtain a compressive strength of 43 MPa at 91 days. They also noted that the strengths could be increased significantly within 3 days by using Type III cement. However, Langely et al. (1989) found that early-age strength development of concrete made with Type I portland cement and Type III cement are comparable. Both of the mixes they tested contained high volumes of Class F fly ash.

In 1990, Naik and Ramme found that concrete mixtures containing Type I cement and up to 30% Class C fly ash cement replacement would increase early age strength when compared to no fly ash concrete. Naik et al. (1994b) experimented with mixes containing Type I cement and Class C fly ash and found that 50% to 70% cement replacement reduces the strength of the concrete.

Zhang and Gjorv (1991) concluded that lightweight aggregate strength has the greatest influence on the strength of the high-strength lightweight concrete. Galeota et al. (1991) found that adding very high percentages of silica fume increases the compressive strength at 28 days. Li et al. (1994) also found that silica fume increases the compressive strength.

Siebel (1989) found that the addition of superplasticizer would increase compressive strength. Rear and Chin's (1990) research shows that non-chloride accelerating admixtures are effective in increasing early compressive strength with both cement and cement-fly ash combinations. Kashi and Weyers (1989) found that reducing w/c from 0.32 to 0.25 caused a 37% increase in compressive strength after 56 days of curing for mixtures containing Type I portland cement, silica fume, air-entrainment, and superplasticizer. Their research also showed that air-entrained mixtures have lower strength than non-air-entrained mixtures and typically a 1% increase in air content caused a 5% decease in compressive strength.

Table 2.1: Summary of research findings on HPC properties discussed in this report.

Author	Reference	Key Findings
	Freeze-thaw durability	
Kashi And Weyers	(1989). "Freezing and thawing durability of high strength silica fume concrete." *Structural Materials. Proc., Sessions at the ASCE Structures Congress '89*, San Francisco, CA; Ed. By James F. Orofino; ASCE, New York, 138-148.	High strength silica fume concrete with w/c less than 0.3, is freeze and thaw resistant (without air-entrainment). Concrete containing silica fume and w/c = 0.32 requires air-entrainment to be freeze-thaw durable. Without silica fume, the same concrete will not need air-entrainment. Reducing w/c increases the freeze-thaw durability in comparison to ordinary concrete.
Siebel	(1989). "Air-void characteristics and freezing and thawing resistance of superplasticized air-entrained concrete with high workability." *Superplasticizers and Other Chemical Admixtures in Concrete. Proc. Third Int.Conf.*, Ottawa, Canada, American Concrete Institute, ACI SP-119, 297-319.	Superplasticized mixes are freeze/thaw resistant if the air content of the fresh concrete is increased proportionately with the superplasticizer.
Malhotra	(1990). "Durability of concrete incorporating high-volume of low-calcium (ASTM class F) Fly ash." *Cement and Concrete Composites*, 12(4), 271-277.	High silica fume concretes do not resist freezing and thawing even when air-entrained.
Attiogbe et al.	(1992). "Air-void system parameters and freeze-thaw durability of concrete containing superplasticizers." *Concrete Int.*, 14(7), 57-61.	Superplasticized and air-entrained mixes can be freeze-thaw durable at spacing factors greater than 0.008 in.
Nasser and Lai	(1992). "Resistance of fly ash concrete to freezing and thawing." *Fly Ash, Silica Fume, Slag, and Natural Pozzolans in Concrete. Proc., Fourth Int. Conf.*, Istanbul, Turkey, ACI SP-132, 1, 205-226.	20% Class C fly ash improves freeze-thaw resistance. 35-50% of Class C fly ash in concrete containing 6% air, decreased freeze-thaw resistance.
Pitt	(1992). "Reliability-based design for freeze-thaw concrete." Materials Performance and Prevention of Deficiencies and Failures." *Proc., Materials Engr. Congress*, ASCE, 462-475.	Unsatisfactory pore structure of coarse aggregate reduces freeze-thaw durability.
Bowser et al.	(1996). "Freeze-thaw durability of high-performance concrete masonry units." *ACI Materials J.*, 93(4), 386-394.	Cementitious materials improve freeze-thaw resistance of lightweight concrete and decreases freeze-thaw resistance of normal weight concrete.

Author	Reference	Key Findings
	Compressive Strength	
Kashi and Weyers	(1989). "Freezing and thawing durability of high strength silica fume concrete." *Structural Materials. Proc., Sessions at the ASCE Structures Congress '89*, San Francisco, CA; Ed. By James F. Orofino; ASCE, New York, 138-148.	Reducing w/c increases compressive strength after 56 days of curing for mixtures containing Type I Portland cement, silica fume, air-entrainment, and superplasticizer. Air-entrained mixtures have lower strength than non-air-entrained mixtures and typically a 1% increase in air content caused a 5% decease in compressive strength.
Langely et al.	(1989). "Structural concrete incorporating high volumes of ASTM Class F fly ash." *ACI Materials J.*, 86(5), 507-514.	Type I and Type III cement with high volumes of Class F fly ash affect early-age strength comparably.
Siebel	(1989). "Air-void characteristics and freezing and thawing resistance of superplasticized air-entrained concrete with high workability." *Superplasticizers and Other Chemical Admixtures in Concrete. Proc. Third Int.Conf.*, Ottawa, Canada, American Concrete Institute, ACI SP-119, 297-319.	Superplasticizer increases compressive strength
Naik and Ramme	(1990). "High early strength concrete containing large quantities of fly ash." *Serviceability and Durability of Construction Materials. Proc. First Materials. Engr. Congress*, Denver, CO, Suprenant; 2, 1039-1050.	Type I cement with up to 30% Class C fly ash cement replacement increase early age strength when compared to no fly ash concrete.
Rear and Chin	(1990). "Non-chloride accelerating admixtures for early compressive strength." *Concrete Int.* 12(10), 55-58.	Non-chloride accelerating admixtures are effective in increasing early compressive strength with both cement and cement-fly ash combinations.
Galeota	(1991). "Freezing and thawing resistance of non air-entrained and air-entrained concretes containing a high percentage of condensed silica fume." *Durability of Concrete. Second Int., Conf.*, Montreal, Canada, American Concrete Institute, Detroit, MI, 1, 249-261.	Very high percentages of silica fume increase the compressive strength at 28 days.
Zhang and Gjorv	(1991). "Permeability of high-strength lightweight concrete." *ACI Mater. J.*, 88(5), 463-469.	Lightweight aggregate strength has the greatest influence on the strength of the high-strength lightweight concrete.
Bilodeau and Malhotra	(1994). "High-performance concrete incorporating large volumes of ASTM class F fly ash." *High-Performance Concrete. Proc., ACI Int. Conf.*, Singapore, ACI SP-149, 177-193.	Type I cement with high-volume Class F fly ash can obtain 43 MPa at 91 days. Type III cement increases strength.

Author	Reference	Key Findings
	Compressive Strength (continued)	
Li et al.	(1994). "Freezing and thawing: Comparison between non-air-entrained and air-entrained high-strength concrete." *High-Performance Concrete. Proc., ACI Int. Conf.*, Singapore, American Concrete Institute, Detroit, MI, ACI SP-149, 545-560.	Silica fume increases compressive strength.
Naik et al.	(1994b). "Abrasion resistance of concrete as influenced by inclusion of fly ash." *Cement and Concrete Res.*, 24(2), 303-312.	50% and 70% Class C fly ash reduces the strength of the concrete.
	Chloride Permeability	
Ellis	(1991). "Comparative results of utilization of fly ash, silica fume and GGBFS in reducing the chloride permeability of concrete." *Durability of Concrete. Second Int., Conf.*, Montreal, Canada, ACI SP-126, 1, 443-458.	Class F fly ash improves concrete's resistance to chloride permeability better than Class C fly ash.
Pigeon et al.	(1991) "Freezing and thawing tests of high-strength concretes." *Cement and Concrete Res.*,12(5), 844-852.	Silica fume with w/c = 0.25 or less will resist chloride ion penetration unless they are not adequately protected against freezing and thawing.
Torii and Kawamura	(1991). "Pore structure and chloride permeability of surface layers of concrete." *Trans. Japan Concrete Inst.*, 13, 195-202.	Pozzolans resistant chloride ion permeability.
Zhang and Gjorv	(1991). "Permeability of high-strength lightweight concrete." *ACI Mater. J.*, 88(5), 463-469.	Permeability of high-strength lightweight concrete is more dependent on the porosity of mortar mix than the porosity of lightweight aggregate.
Naik et al.	(1994a). "Permeability of concrete containing large amounts of fly ash." *Cement and Concrete Res.*, 24(5), 913-922.	Up to 70% Class C fly ash reduces the permeability of chloride ions at an age of 91-days.
Naik et al.	(1995). "Abrasion resistance of high-strength concrete made with Class C fly ash." *ACI Materials J.*, 92(6), 649-659.	High-volumes of Class C fly ash increases chloride ion permeability resistance.
Ozyildirim	(1998). "Permeability specification for high performance concrete decks." *Transportation Res. Rec.*, 1610, 1-5.	Concretes containing air-entrainment, pozzolans or slag, and a w/c ratio less than 0.45 have very low permeability.

Author	Reference	Key Findings
	Scaling	
Gagne et al.	(1991). "Deicer salt scaling resistance of high strength concretes made with different cements." *Concrete Durability. Second Int., Concrete*, Montreal Canada, ACI SP-126, 1, 185-199.	Type I and certain Type III Portland cements are resistant to salt scaling without air entrainment. Salt scaling durability decreases in non-air-entrained concretes when the air content is high.
McDonald and Perenchio	(1997). "Effects of salt type on concrete scaling." Concrete International, 19(7), 23-26.	Proprietary salt solutions cause less scaling than salts containing potassium chloride.
	Abrasion	
Gjorv et al.	(1990). "Abrasion resistance of high-strength concrete pavements." *Concrete International: Design and Construction*, 12(1), 45-48.	Increasing compressive strength will reduce abrasion to concrete. Aggregate type has significant influence on abrasion resistance.
Laplante et al.	(1991). "Abrasion resistance of concrete." *J. Materials. Div. Engr.*, 3(1), 19-28.	Fine aggregates should be 25% siliceaous to be abrasion resistant. W/c ratio significantly affects abrasion resistance.
De Almeida	(1994). "Abrasion Resistance of high strength concrete with chemical and mineral admixtures." *Durability of Concrete. Proc., Third Int. Conf.*, Nice, France, ACI SP-145, 1099-1113.	Abrasion resistance is improved with the combination of pozzolans and superplasticizers. Without superplasticizer, pozzolans will cause abrasion.
Naik et al.	(1994a). "Permeability of concrete containing large amounts of fly ash." *Cement and Concrete Res.*, 24(5), 913-922.	Abrasion resistance is predominantly influenced by compressive strength. Fly ash reduces abrasion resistance.
Naik et al.	(1995). "Abrasion resistance of high-strength concrete made with Class C fly ash." *ACI Materials J.*, 92(6), 649-659.	Abrasion resistance of concrete is dependent on the compressive strength regardless of the fly ash content. Abrasion increases with the addition of more than 30% fly ash.

CHAPTER 3: MATERIALS AND TESTING METHODS

3.1 Mix Design Specifications

The properties of each mix design used in this study are shown in Tables 3.1 – 3.5 including mixture ID, design strength, and materials. These mixes were selected based on consultation with WSDOT to ensure that they are representative of those used in highway projects across the state. Mix designs were selected from four Geographic regions in the state: (1) northeast, (1) southeast, (1) northwest, and (2) southwest. The specific location of each highway project is provided as part of the mix design. Materials sufficient to produce test specimens were shipped from mixing plants to WSU.

3.2 Freeze-Thaw Experiments (ASTM C 666)

Concrete expands and may rupture when it is exposed to cycles of freezing and thawing. To estimate the resistance of concrete to this type of damage, saturated concrete is exposed to rapidly repeated cycles of freezing and thawing according to the test procedure outlined in ASTM C 666. This test is useful for comparing the durability of different mixture designs. In this project, three replicate molded beam specimens (see Figure 3.1) were prepared according to each mix design and cast into 3x4x16 inch aluminum molds. The specimens were cured in limewater for 14 days according to ASTM C 192. Each specimen was tested for fundamental longitudinal frequency, weighed, and the average length and cross section dimensions were determined. The specimens were then inserted into aluminum containers and placed in the freeze-thaw machine (Humboldt, Norridge Ill.) as shown in Figure 3.2.

A control specimen was prepared and positioned near the center of the machine. Figure 3.3 shows the control specimen being drilled so probes could be inserted into its center. A thermometer was placed in one end of the specimen to measure temperature. Another probe was inserted into the opposite end of the control specimen to regulate the cycles of freezing and thawing. When this probe sensed that the center of the control specimen had reached specified freezing temperature it would trigger the temperature control unit to switch to thaw mode and back to freezing when the thawed state was reached.

Water was poured over the specimens on all sides to a depth of 1/8 inch. The temperature control unit was set to cycle between 0 and 40°F as specified in ASTM C 666. Approximately every 26 cycle the specimens were removed from the machine, weighed, measured, and visually examined. The mix deterioration was evaluated by measuring the change in the fundamental longitudinal frequency to determine the Relative Dynamic Modulus of Elasticity (RDME). A description of the method used to measure the RDME is given in the following section. The specimens were turned end-for-end and returned to the clean aluminum containers in a different place in the machine according to a predetermined rotation scheme. These steps were repeated until approximately 300 freeze-thaw cycles were completed.

Table 3.1 Mix Design A

Mix ID: 5065/4000 28Mpa 4000 PSI @28 days Compressive Strength Project: Burnt Br. Cr. /78th street/Vancouver WA Construction Type: Cast in Place Placement: Pour or Pump		
Weights per Cubic Yard (saturated, surface-dry)		
	lbs.	Yield, ft^3
Type I-II cement	565	2.87
Class F Flyash	141	1.00
Sand (Class 2)	947	5.88
Agg. ¾" (aashto#67/#57)	2002	11.88
Water	250	4.01
Total Air, %	5.0 +/- 1.5	1.35
	Total	27.00 ft^3
WATER REDUCING AGENT WRA POZZ 80,ounces	35.3	
AIR ENTRAINMENT AE-90, ounces	4.9	
Water/cement ratio	0.35	
Slump, in.	4.00	
Concrete Unit Weight, lbs./ft^3	144.60	

Table 3.2 Mix Design B

Mix ID: 6095 1 Day 650 PSI @ flexural Strength Project: 395 1 Day Paving Construction Type: Slipform Concrete Pavement Placement: Dump Truck and Chute		
Weights per Cubic Yard (saturated, surface-dry)		
	lbs.	Yield, ft^3
Type III cement	708	3.60
R-101 WSDOT Class 1 Sand	1108	6.58
R-101 WSDOT Agg. #5	1170	6.87
R-101 WSDOT Agg. #4	780	4.58
Water	251	4.02
Total Air, %	5.0 +/- 1.5	1.35
	Total	27.00
WATER REDUCING AGENT 200 N WRA, ounces	28.32	
STABILIZER Delvo, ounces	21.24	
AIR ENTRAINMENT AE-90 AEA, ounces	17.70	
Water/cement ratio	0.35	
Slump, in.	3.00	
Concrete Unit Weight, lbs./ft^3	148.80	

Table 3.3 Mix Design C

Mix ID: 7831A 14 Day 650 PSI @14 days Flexural Strength Project: Sprague Avenue to Argonne-WSDOT #5637 Construction Type: Slipform Concrete Pavement Placement: Dump Truck and Chute		
Weights per Cubic Yard (saturated, surface-dry)		
	lbs.	Yield, ft^3
Type I-II cement	452	2.30
Class F Flyash	113	0.79
Coarse Sand	711	4.30
Fine Sand	472	2.86
Agg. 1 ½"	689	4.09
Agg. ¾"	1177	7.01
Agg. 3/8"	98	0.58
Water	215	3.45
Total Air, %	6.0 +/- 1.5	1.62
	Total	27.00
WATER REDUCING AGENT WRDA 64/Type A, ounces	22.60	
AIR ENTRAINMENT Daravair 1000, ounces	10.70	
Water/cement ratio	0.38	
Slump, in.	2.00	
Concrete Unit Weight, lbs./ft^3	145.40	

Table 3.4 Mix Design D

Region: Southwest Washington State		
4000 PSI @28 days Compressive Strength		
Weights per Cubic Yard (saturated, surface-dry)		
	lbs.	Yield, ft^3
Type I-II cement	611	3.108
Sand	1165	7.235
Agg. ¾"	1843	10.980
Water	270	4.327
Total Air, %	5	1.35
	Total	27.00
WATER REDUCING AGENT WRA POZZ 82 Meets ASTM C260, ounces per yard	5	
AIR ENTRAINMENT AE-90 Meets ASTM C494, ounces per yard	37	
Water/cement ratio	0.44	
Slump, in.	4.00	

Table 3.5 Mix Design E

Mix ID: 7028 650 PSI @ 3 days Flexural Strength Project: 1999 SeaTac Airport Phase 2 & 3 Construction Type: 3 day/ night paving		
Weights per Cubic Yard (saturated, surface-dry)		
	lbs.	Yield, ft^3
Type I-II cement ASTM C 150, lbs	658	3.35
Sand ASTM C 33, lbs	1261	7.77
Agg. ¾" ASTM C 33 #67, lbs	1016	5.96
Agg. 1 ½" ASTM C 33 #4, lbs	838	4.92
Water, lbs	231	3.70
Total Air, %	5.5	1.50
	Total	27.00
WATER REDUCING AGENT WRDA-64 ASTM C 494 Type A, ounces	29.61	
AIR ENTRAINMENT Daravair ASTM C 260, ounces	6.6	
Water/cement ratio	0.35	
Slump, in.	1.50	
Concrete Unit Weight, lbs./ft^3	147.20	

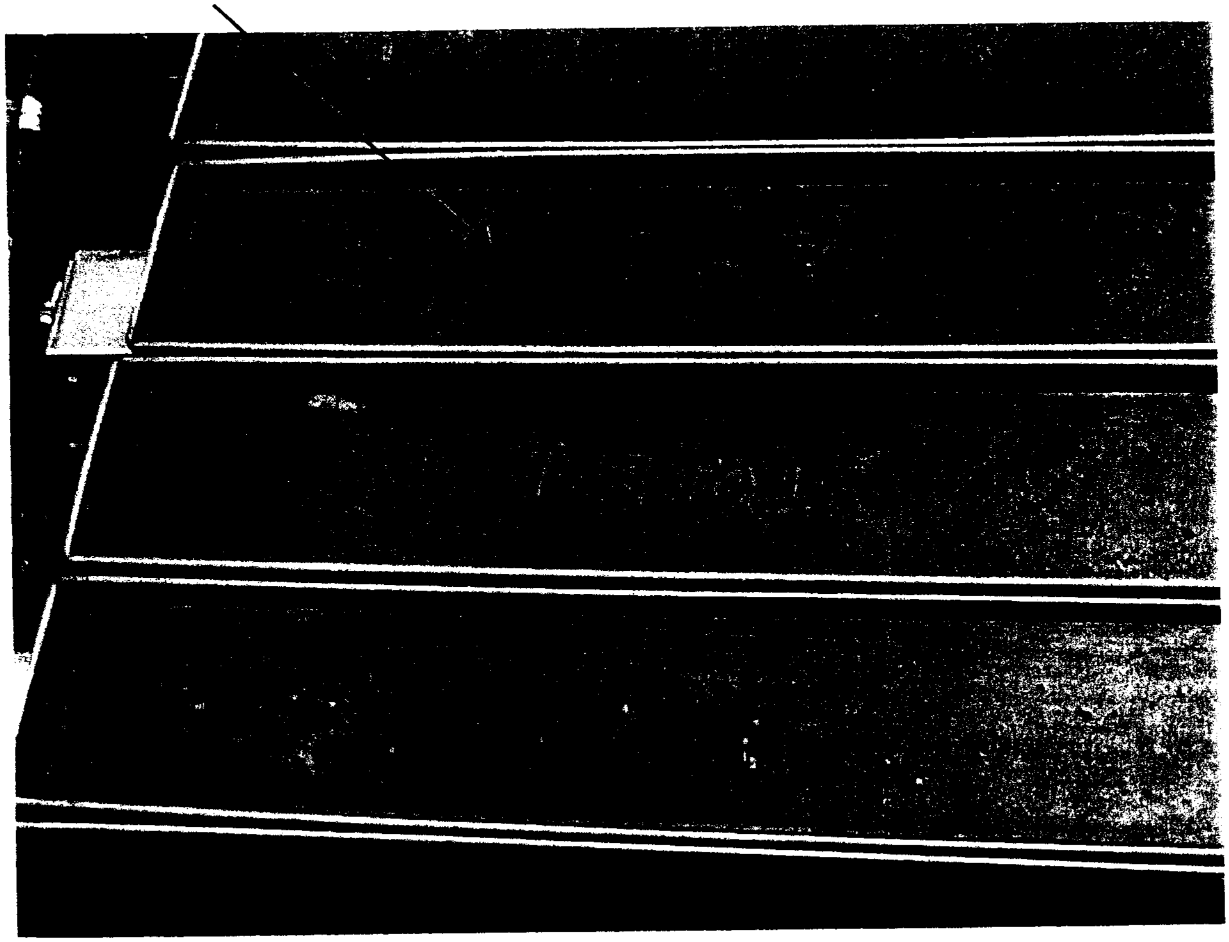

Figure 3.1. Specimens in Freeze-Thaw Machine

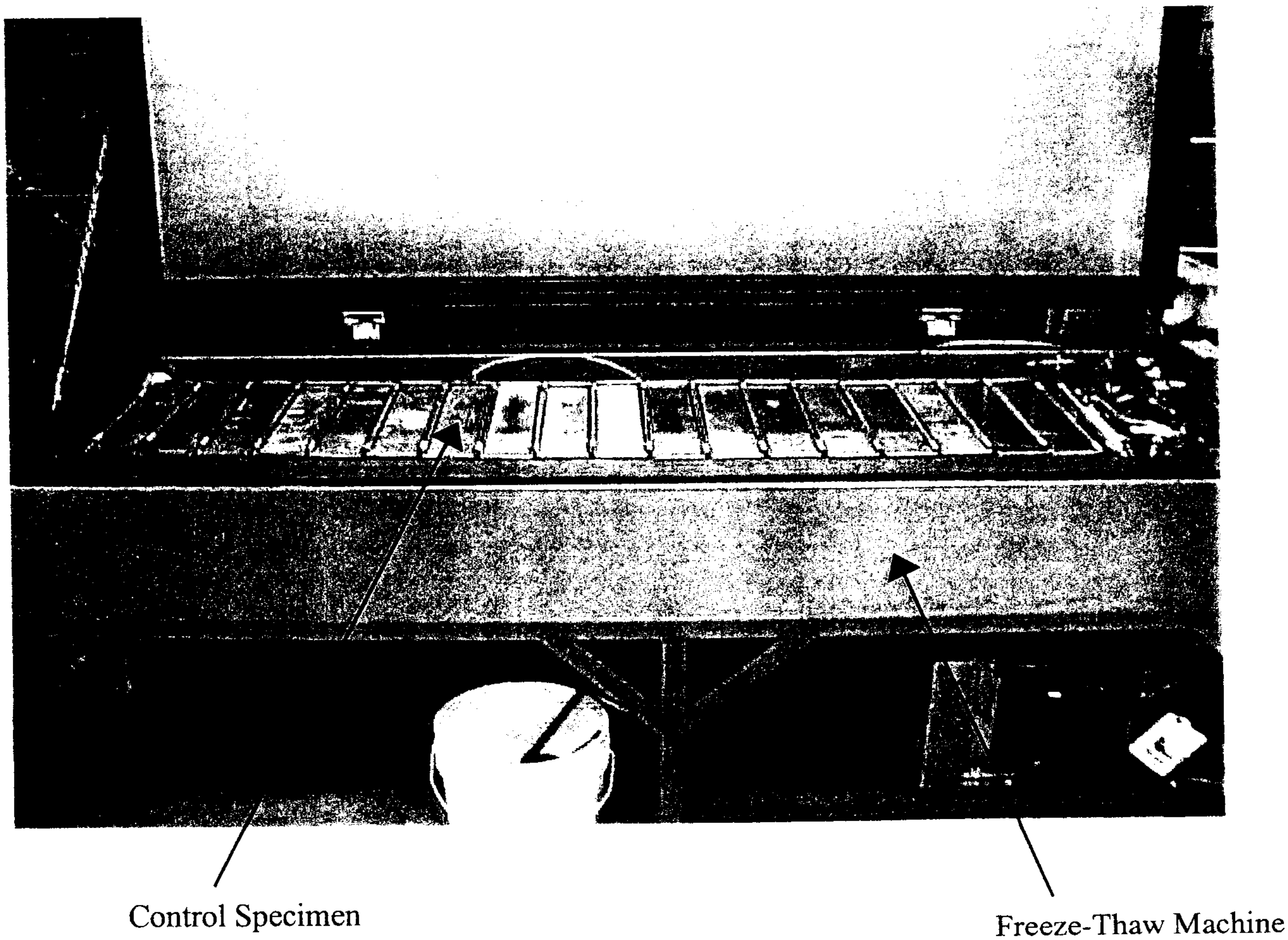

Figure 3.2. Freeze-Thaw Machine with Test Specimens.

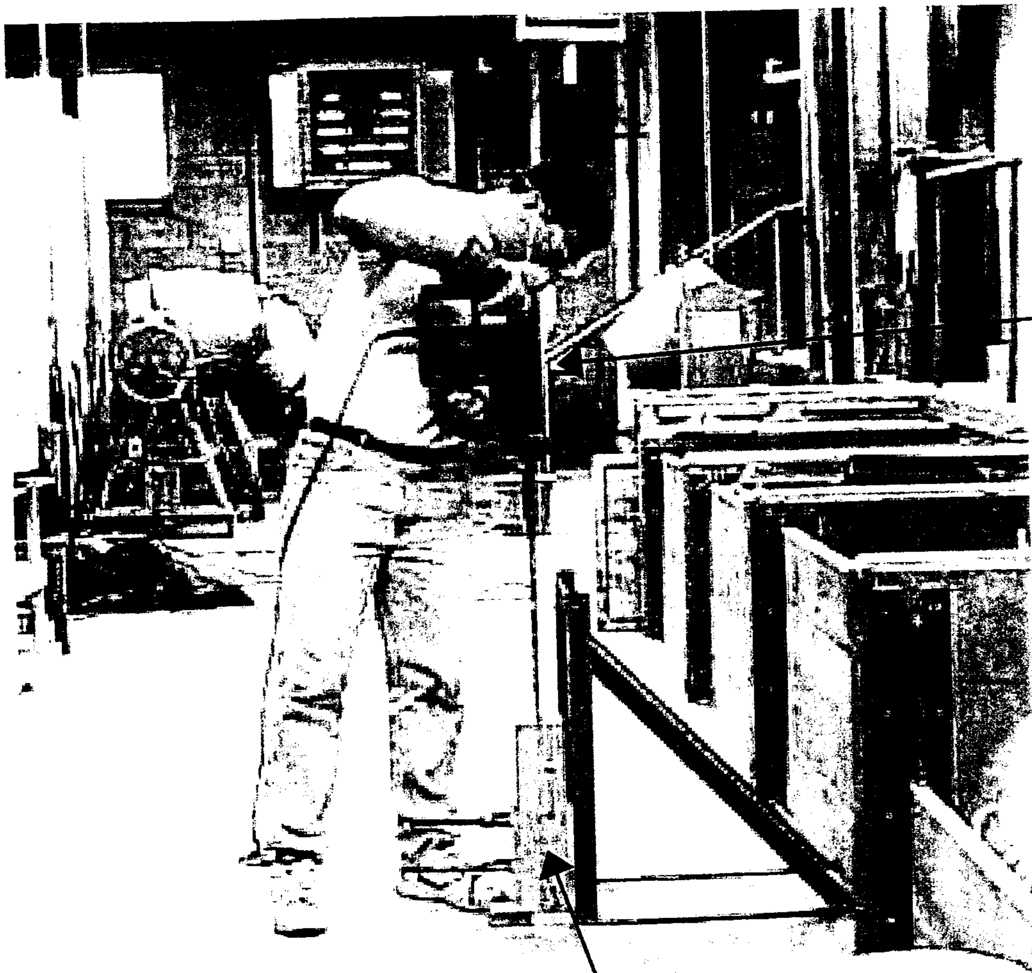

Figure 3.3 Drilling Control Specimen.

3.2.1 Relative Dynamic Modulus of Elasticity

The relative dynamic modulus of elasticity can be determined as a function of specimen weight, length, cross section dimensions, and fundamental frequency. The fundamental frequency may be determined by taking either longitudinal or transverse measurements. The ASTM C 666 standard procedure for freeze-thaw testing specifies the transverse frequency measurement to determine the relative dynamic modulus of elasticity of each specimen. The standard also specifies that longitudinal frequency measurements may be made to verify that the transverse frequency readings are valid.

ASTM C 215 describes the impact resonance method for determining both transverse and longitudinal resonance frequency measurements. The primary components for this testing set up include the specimen supports, pickup unit, impactor, and waveform analyzer. For both methods, the specimen is supported at the nodal points where no vibration occurs. In the transverse test there are two nodal points located at 0.224 of the length of the beam from each end. Only one nodal point in the center of the length of the beam is present for the longitudinal setup. In place of specimen supports, the beam may be placed on a thick pad of sponge rubber. The supports (or sponge pad) are required to have a resonant frequency range that falls outside the range of use, which is 100 to 10, 000 Hz. In this test a sponge pad was used beneath the specimens.

Maximum vibration for the transverse and longitudinal setups occurs near the end of the specimen, where the pickup unit is located. Either a piezoelectric or magnetic pickup unit is required to be capable of generating a voltage proportional to the displacement, velocity, or acceleration of the test specimen. The mass of the vibrating parts is required to be small in comparison with the mass of the specimen (ASTM C 215).

An impactor made of steel or rigid plastic is used to strike the appropriate surface of the specimen. The impactor should make contact perpendicular to the center of the surface.

In the transverse test, the specimen is struck mid length of the beam on the side. In the longitudinal test, the specimen is struck at the end of the beam opposite the accelerometer near the center. Figure 3.4 shows the location of the impactor and the pickup device. Once the specimen is vibrated using the impactor, the resonant frequency is recorded using the waveform analyzer. The test is repeated twice and the average frequency is recorded.

ASTM C 215 describes using an accelerometer as a pickup device and attaching it to the specimen using soft wax, glue, or grease. However, this is difficult to accomplish with wet specimens after freeze-thaw testing. For this reason, alternative methods, including the use of piezoelectric film, were sought for determining the resonant frequency of the specimens.

Piezoelectric film is a unique material that exhibits dielectric properties. Dielectric material is defined by its ability to store charge when the material is contained between two conductive materials. The magnitude of the stored charge is the capacitance and is directly related to the voltage. Figure 3.5 is a schematic diagram of a dielectric material (Askeland, 1994). Additional charges may be stored in the dielectric material as polarization occurs. Polarization may take place when atoms act like egg-shaped particles rather than spheres, when bonds between ions change length, or by distortion due to the orientation of the permanent dipoles in the material (Askeland, 1994). Piezoelectric film displays what is termed 'reversible behavior', where polarization changes the dimensions of the dielectric material and a voltage is created. Mechanical Vibration, such as sound waves or induced frequency in a medium, produces strain in a piezoelectric material (Askeland, 1994).

The piezoelectric film has been used in several experiments in the Wood Materials and Engineering Laboratory at WSU to measure the longitudinal frequency of different wood composite materials. This method was found to provide reliable measurements of the material frequency of vibration (Tucker et al., 1999). The USDA Forest Service has also used piezoelectric films for nondestructive testing of biologically degraded wood (Ross et al., 1994). In their research, the film was attached to wood beams using double-sided adhesive tape. A stress wave was induced through a pendulum and the longitudinal frequency of vibration recorded using a digital storage oscilloscope. It was concluded that this method was successful in determining dynamic modulus of elasticity (and estimating strength properties through empirical relationships.

Piezoelectric film is a transducer material that is able to convert one form of energy into another. In the freeze-thaw test, the specimen is impacted in such a way that a longitudinal vibration (with a characteristic frequency) is transmitted through the concrete to the piezoelectric film.

Piezoelectric film is attached to the specimen using dual sided tape as illustrated in Figure 3.7. The frequency of the transmitted wave causes the piezo material to strain. This mechanical energy is converted to a voltage. The piezoelectric film is connected to the BNC board where the signal is converted from voltage to analog signal. The BNC board is connected to the data acquisition card that is inserted in the computer where the signal is read (Figure 3.8). A computer program was created using LabVIEW software (LabVIEW Version 6.0, National Instruments, Austin, Texas) to read and display the peak frequency of vibration of the specimen. The LabVIEW software enabled the waveform to be viewed similarly to the way an oscilloscope would display it. The captured waveform was analyzed using the Fast Fourier Transform. The maximum amplitude was obtained by plotting the results of the Fourier Transform against frequency. The maximum amplitude, or resonant frequency, occurs when the driving angular frequency is equivalent to the natural angular frequency of the concrete (Halliday et al. 1993).

It has been shown in the literature that dynamic modulus of elasticity calculations made from longitudinal frequencies are equivalent to those made from transverse frequency measurements (Malhotra and Carino, 2000). Figure 3.8 shows a comparison of the dynamic modulus of elasticity determined from longitudinal and transverse frequency measurements. The relationship between these measurements is linear and validates using longitudinal frequency measurements to determine the dynamic modulus of elasticity. Based on these findings, the longitudinal frequency was measured in this study using the piezoelectric film as a pick up device as depicted in Figure 3.9. The dynamic modulus of elasticity is calculated according to the following equation (ASTM C 215):

$$E = DW(n')^2 \tag{3.1}$$

where E is the dynamic Modulus of Elasticity (psi), W is the weight of specimen (lbs), n' is the fundamental longitudinal frequency (cycles per second), $D = 0.01038\frac{L}{t * b^2}$ (sec^2 / in^2), L is the length of specimen (in.), and t, b = dimensions of cross section of prism (in.).

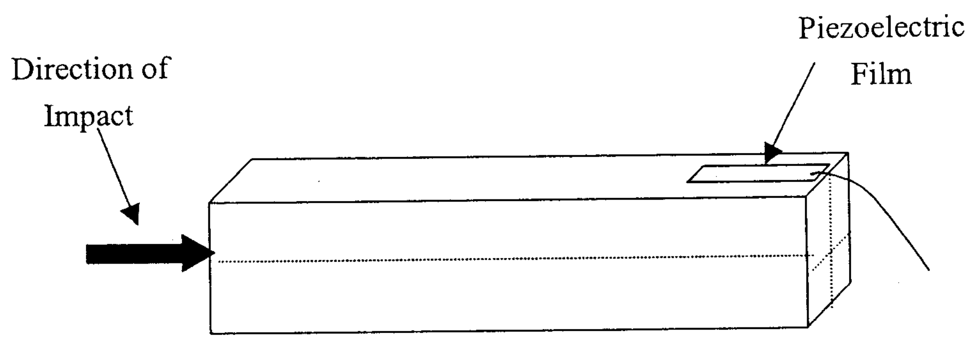

Figure 3.4 Direction of impact: Longitudinal

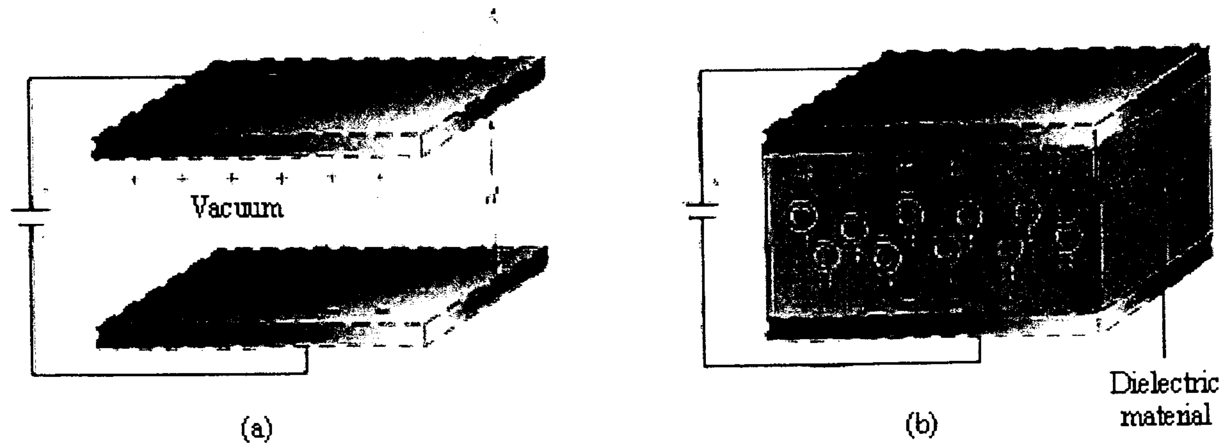

Figure 3.5 Dielectric Material: A charge can be stored at the conductor plates in a vacuum (a). However, when a dielectric is placed between the plates (b), the dielectric polarizes and additional charge is stored. (Askeland, 1994).

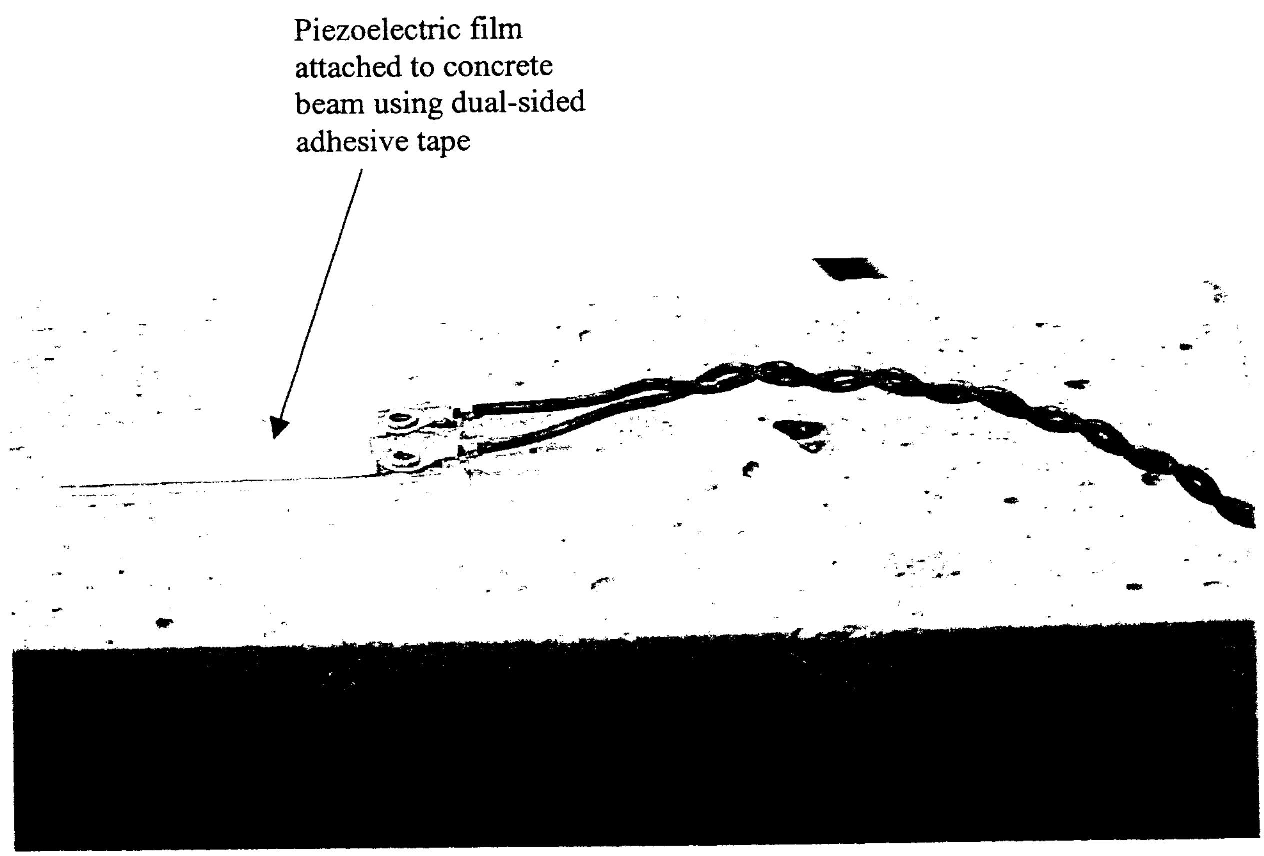

Figure 3.6 Piezoelectric Film Attached to a Concrete Beam

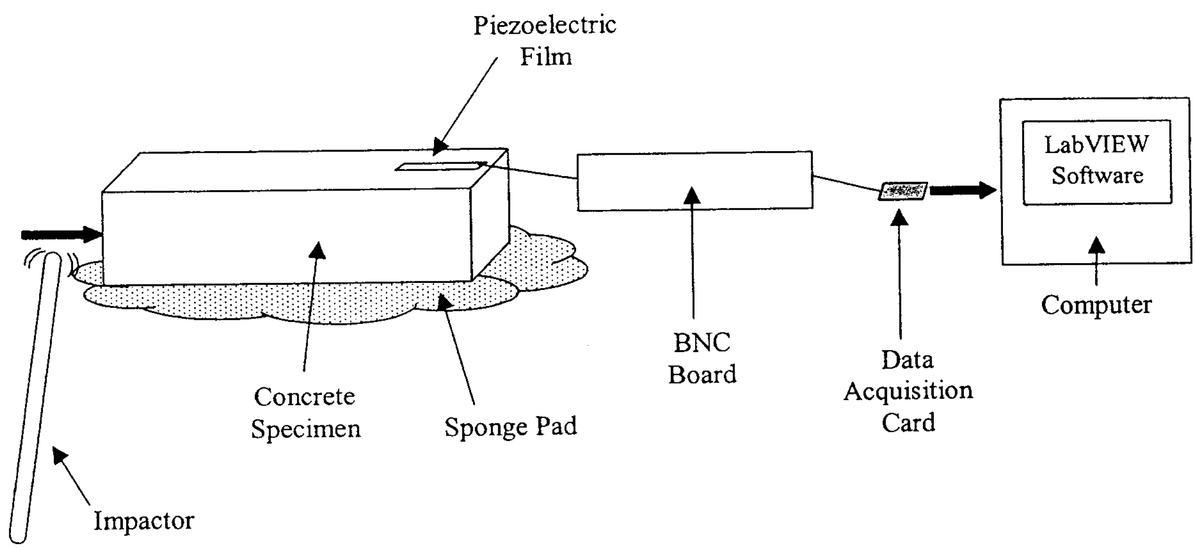

Figure 3.7 Dynamic Modulus of Elasticity Data Acquisition

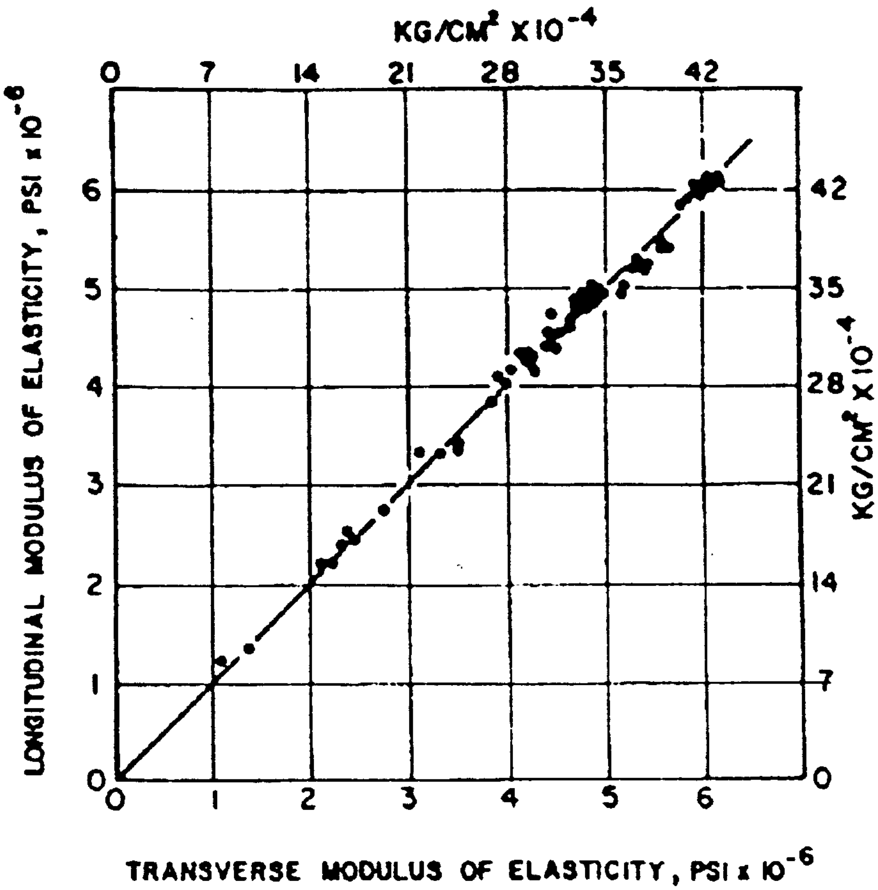

Figure 3.8 Linear Relationship for the Modulus of Elasticity determined by Transverse and Longitudinal Frequency Measurements. (V.M. Malhotra and N.J. Carino, 2000).

3.3 Chloride Permeability Experiments (ASTM C 1202)

Excessively permeable concrete causes reinforcing steel to corrode as chloride ions enter the paste. Permeability is related to water-cement ratio and the degree of cement hydration or length of moist curing. Permeability also affects the ability of saturated concrete to resist breakdown by freezing.

In this test, two replicate 4x8-inch cylinders were made from each mix design and cured in lime water for 56 days. Each specimen was carefully wrapped in wet towels, sealed in plastic bags, and transported to WSDOT Materials Testing Laboratory where they were tested according to ASTM C 1202.

Prior to the beginning of the test each specimen was conditioned for placement in the test cell. Using a water saw with diamond tip blade, a 2-inch slice was cut from the top of each cylinder. The test specimen was a slice of the cylinder made by a parallel cut from the top of the core. A belt sander was used to remove any burrs on the end of the specimen. Two coats of epoxy were applied to the outside of the specimens. After setting for two hours an additional coat of epoxy was applied to ensure that no air bubbles remained. The specimens were then saturated and the air was vacuumed out. The epoxy was sanded down on each specimen until they were able to fit into the testing container. Clay was used to seal the specimen in the container.

The side of the cell (Figure 3.10) containing the top end of the specimen was filled with 3.0% NaCl solution. This side of the cell was connected to the negative terminal of the power supply. The bottom side of the cell was filled with 0.3 M NaOH and was connected to the positive terminal of the power supply (figure 3.11). The power supply was set for 60.0 volts after the electrical connections were made.

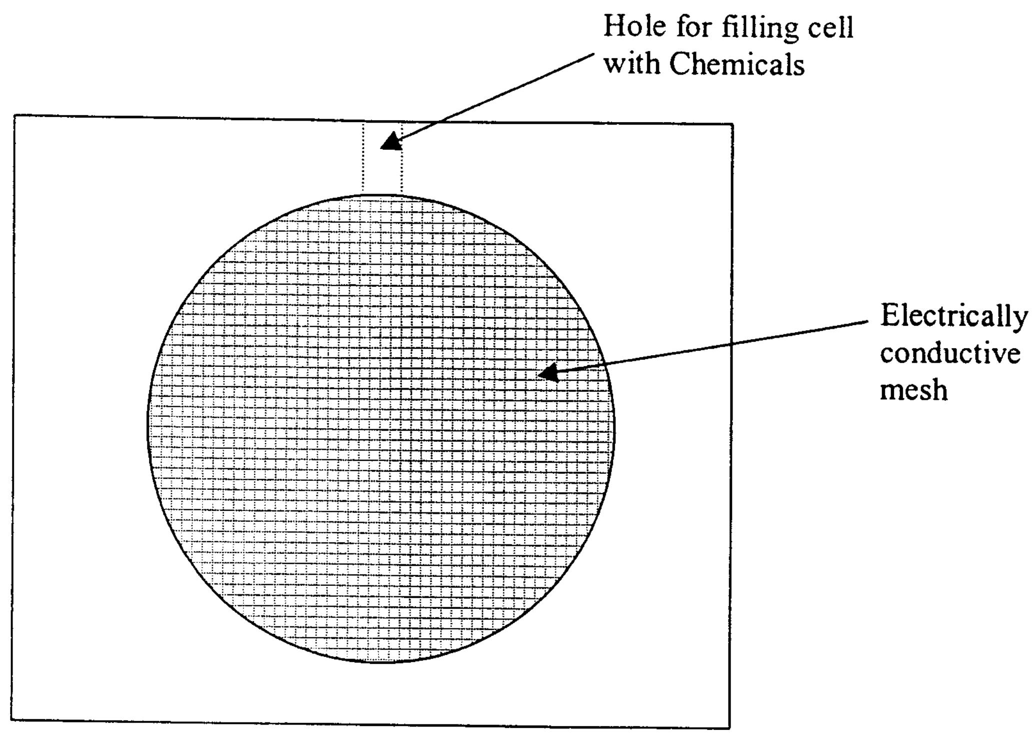

Figure 3.9 Plan View: Chloride Permeability Specimen Cell

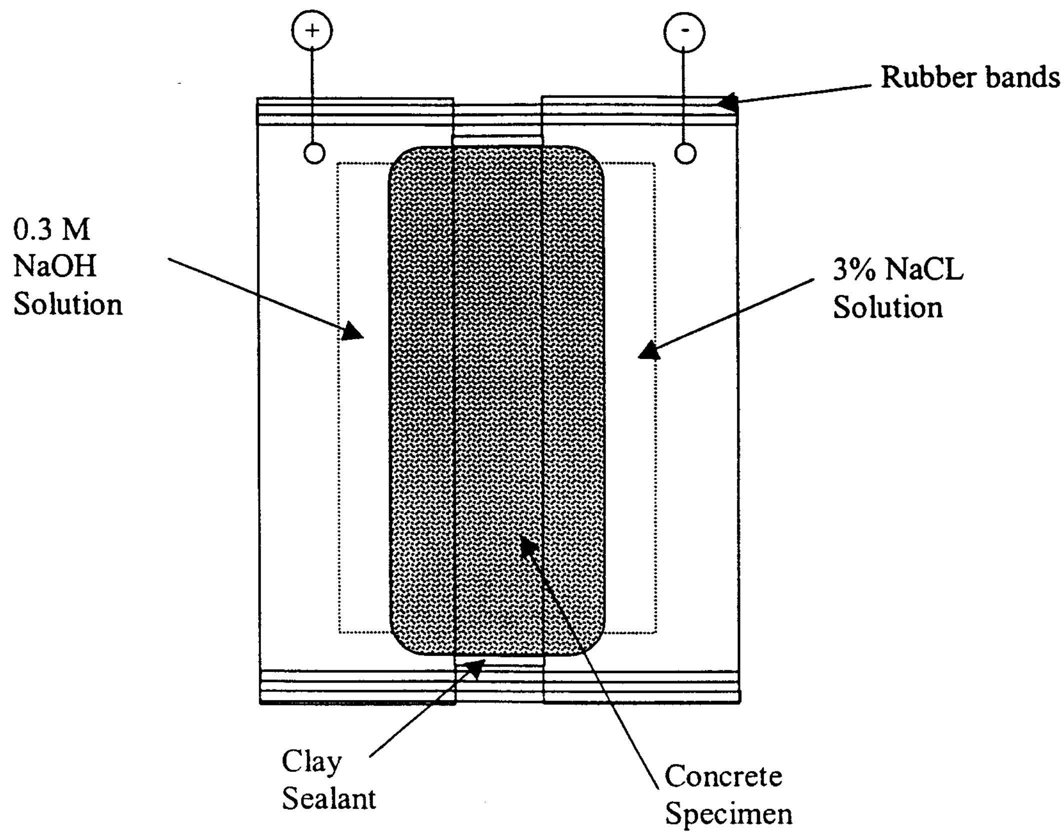

Figure 3.10 Chloride Permeability Experimental Set Up

Every 30 minutes the charge passed in Coulombs through the specimen were recorded. The higher the charge, the greater the chloride permeability. The test was terminated after 6 hours. For mix D, the test was terminated earlier because the temperature exceeded 190 degrees F.

3.4 Abrasion Experiments (ASTM C 944)

As vehicles travel on the highway, tires rub or scrape against the concrete creating friction forces that cause the concrete to wear down or "abrade". The rotating-cutter method described in ASTM C 944 for determining abrasion resistance of concrete was adopted by the FHWA for comparing the relative wear resistance of different concretes as part of HPC criteria. The method was used in this study to measure abrasion resistance.

According to ASTM C944, the abrasion device is a drill press (see Figure 3.12) equipped with a chuck capable of holding and rotating the abrading cutter at a speed of 200 rev/min and exerting a force of 89 N on the test specimen surface. This applies a concentrated friction force to a circular area that is 82.5 mm (3 ¼ in.) in diameter. The abrasion testing equipment is not available commercially. Therefore, the machine was assembled in the concrete laboratory at WSU using a modified drill press. A rotating cutter device as described in ASTM C944 was purchased and attached to the drill press. All springs that would affect the applied vertical force were removed from the machine. A 10 inch diameter aluminum pulley system was built for the drill to produce the required 200 revolutions per minute at the chuck. The press was also fitted with a Plexiglas safety shield to meet Occupational Health and Safety Administration machine safety standards. With the drill press assembled, a digital scale was placed under the

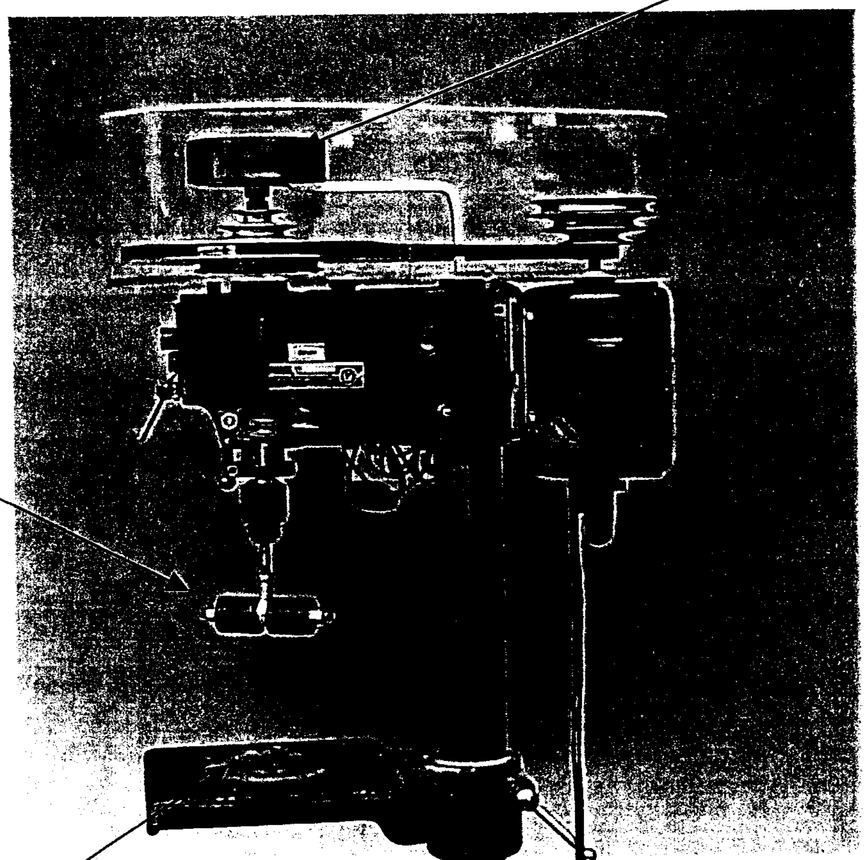

Figure 3.11 Abrasion Testing Equipment Assembled at WSU.

chuck to determine the portion of the required load that the equipment applies. The measured weight of the chuck was subtracted from the total force to be applied during the test. A mass was then machined to apply the remainder of the load.

For each mix design, three replicate 3x4x16 inch prisms were cured in lime water for 56 days. Each concrete beam surface was subjected to the rotating cutter device at three different locations for three 2-minute intervals at each location. The total abrasion time per location was 6 minutes. Each specimen was weighed before being abraded and in-between each abrasion cycle. The results of this test are described in section 4.4.

3.5 Scaling Experiments (ASTM C 672)

Deicing chemicals cause the surface of highways to scale off as they are exposed to cycles of freezing and thawing. Washington State Department of Transportation applies Calcium Magnesium Acetate to the western regions of Washington State and Calcium Chloride to the eastern regions of the state.

Four cylinders with 72-inch diameter and 3 inch height were prepared for each mix design and cured in lime water for 28 days. Two specimens of each mix were exposed to a solution of water and Calcium Magnesium Acetate, while the remaining two of each mix were exposed to a solution of water and Calcium Chloride. The molds had higher thickness than the specimens to allow applying a solution of 0.25 inch thickness at the top of specimens. The specimens were frozen for 16 to 18 hours and thawed for 6 to 8 hours as described in ASTM C 672. Proper depth of solution was maintained by adding water between cycles as necessary. Every five days, the specimens were washed clean, visually inspected for scaling, photographed with a digital camera, and then the chemicals were reapplied. A total of 70 freeze-thaw cycles were used for this test.

Two methods for examining the amount of scaling were utilized in this research. The first method is the qualitative visual approach described in ASTM C 672, and was completed by four individuals independently. The visual scale is as follows:

0 - no scaling,

1 - very slight scaling (1/8 inch depth maximum, no coarse aggregate visible),

2 - slight to moderate scaling,

3 - moderate scaling (some coarse aggregate visible),

4 - moderate to severe scaling,

5 - severe scaling (coarse aggregate visible over entire surface).

In addition to the standard (qualitative) procedure, a quantitative image analysis technique was used to determine the amount of scaling. This new procedure uses digital images of the concrete surface after different scaling cycles to determine the extent of scaling as the test progresses. This method relies on the fact that scaling causes the paste to deteriorate and creates a rough surface on the specimen and sometimes exposes coarse aggregates. Consequently, an image of a concrete surface with scaling would show more variation in gray color intensity compared to the one that has no scaling effects. The variation of gray intensity as a function of cycle number was taken as the parameter to quantify concrete scaling.

In order to obtain the new scaling parameter, a digital color image of the concrete surface was taken at the end of every 5 freeze-thaw cycles for the first 25 cycles. Images were also taken at cycles 50 and 70. Each color image was converted to grayscale for analysis (Figure 3.12). Imaging analysis software (Image-Pro Plus Version 4.0, Media Cybernetics, Silver Spring, MD) was utilized to generate a spatial histogram of different gray intensities on an image. The histogram represents the frequency distribution of different gray intensities. A gray intensity of 0 represents black, while a gray intensity of 255 represents the white color. The coefficient of variation (standard deviation/average) of the histogram was determined for each specimen. The new scaling parameter was taken as the ratio of the coefficient of variation for each specimen at N cycles to the coefficient of variation for the same specimen at cycle 0 (prior to scaling test).

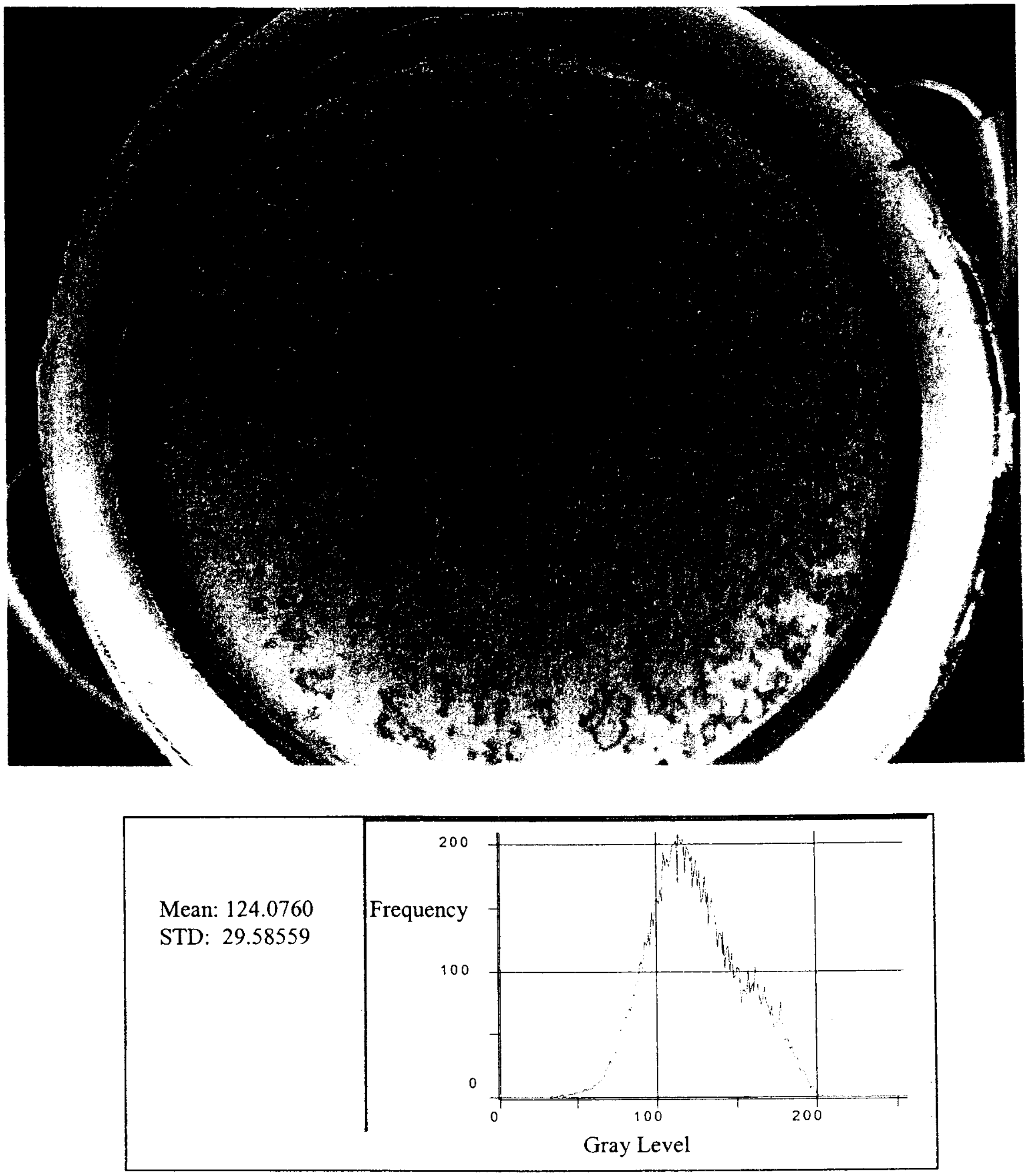

Figure 3.12 A specimen converted to Grayscale for Image Analysis and Corresponding Histogram

This was necessary to normalize the measurements and minimize the effect of any surface roughness that might have been caused by specimen preparation.

3.6 Compressive Strength Experiments (ASTM C 39)

Adequate compressive strength of concrete is essential for supporting traffic loads. Compressive strength of concrete is also related to abrasion resistance. ASTM C 39 was used in this study to determine the compressive strength of the mixes. For each mixture three replicate 6x12 inch cylinders were cured in limewater to 56-day strength. Specimens in moist condition were tested for compressive strength using the machine from SATEC, Model 400 QC Prism-1007, Grove City, PA. Each specimen was capped with a neoprene pad. The axis of the specimen was properly aligned with the thrust of the spherically seated block. The rate of loading was continuous. The maximum load carried by the specimen during the test was recorded as well as the type of failure and appearance of the concrete.

CHAPTER 4: TEST RESULTS

4.1 Mix Characteristics

The characteristics of each mix when the specimens were prepared at WSU are described in Table 4.1. All specimens were prepared according to their mix design as closely as possible. Actual air content and slump were measured for each mix when the specimens were made. In some cases, the measured properties deviated slightly from the values given in the mix designs.

4.2 Freeze-Thaw Test Results

Although the temperature unit was set to maintain temperatures between 0 and 40°F (+/- 3°F), this was not always accomplished due to the limitations of the machine. All temperatures were monitored closely in regular intervals to ensure that freeze-thaw temperatures were achieved. Some problems were encountered in controlling the freeze-thaw range. In these situations, the test was stopped and all specimens were kept under freezing conditions per ASTM C 666. Cycles that did not completely reach freezing and thawing temperatures were not counted towards the 300th cycle at which the test was stopped. An example of the recorded temperature values for one set of approximately 30 freeze-thaw cycles is presented in Figure 4.1.

The measured data such as frequency, specimen dimensions, and visual inspection of specimen condition are given in Appendix A. The dynamic modulus of elasticity was determined based on three repeated frequency measurements of three replicate concrete prisms (9 total measurements) as shown in Table 4.2. Table 4.3 and Figure 4.2 show the decline in relative dynamic modulus of elasticity for each specimen from 0 to 300 freeze-thaw cycles. The relative dynamic modulus of elasticity (RDME) was calculated as the ratio of the dynamic modulus at N cycles to the initial value before freeze-thaw cycling.

With the exception of mix D, all mixes had RDME greater than 80%, which met HPC performance grade 2 requirements. Mix D had RDME of about 70%, which met the HPC performance grade 1 requirement. According to Goodspeed et al. (1996), Grade 2 performance would be required for areas that experience 50 or more freeze-thaw cycles a year.

Factors such as water/cement ratio, air content, and the presence of fly ash affect the ability of concrete to resist damage due to cycles of freezing and thawing. Deterioration is caused by excess water that is expelled from aggregates or is already existing in the mix and expands into ice crystals while freezing. The growth of crystals within the capillary voids causes pressure to build in the paste or in the aggregate. If there are no air voids nearby the capillaries will rupture. For this reason, entrained air is a critical component to improve freeze-thaw durability. Excess water in the mix may be greatly reduced by decreasing the water/cement ratio.

In general, all of the mixes tested contained air-entrainment admixtures. They contained between 5 and 6 percent air-entrainment, which seems to be sufficient to protect against 300 cycles of freezing and thawing.

As shown in Figure 4, the freeze-thaw durability of Mix D was almost 20% lower than all other mixes tested. Also, Mix D degraded more rapidly than the other mixes. This mix did not contain fly ash and it had the highest w/c ratio. This finding agrees with most studies that have shown that lowering the water/cement ratio and adding pozzolans increases freeze-thaw durability (Kashi and Weyers, 1989).

Table 4.1. Mix Characteristics

Mix Characteristic	A	B	C	D	E
w/c ratio	0.35	0.35	0.38	0.44	0.35
Air content, %	5	5	6	5	5.5
Slump, in.	4	3	2	4	1.5
Cement Type	I-II	I-II	I-II	I-II	III
Contains Fly Ash	Yes	No	Yes	No	No
Freeze-Thaw Performance Grade	2	2	2	1	2

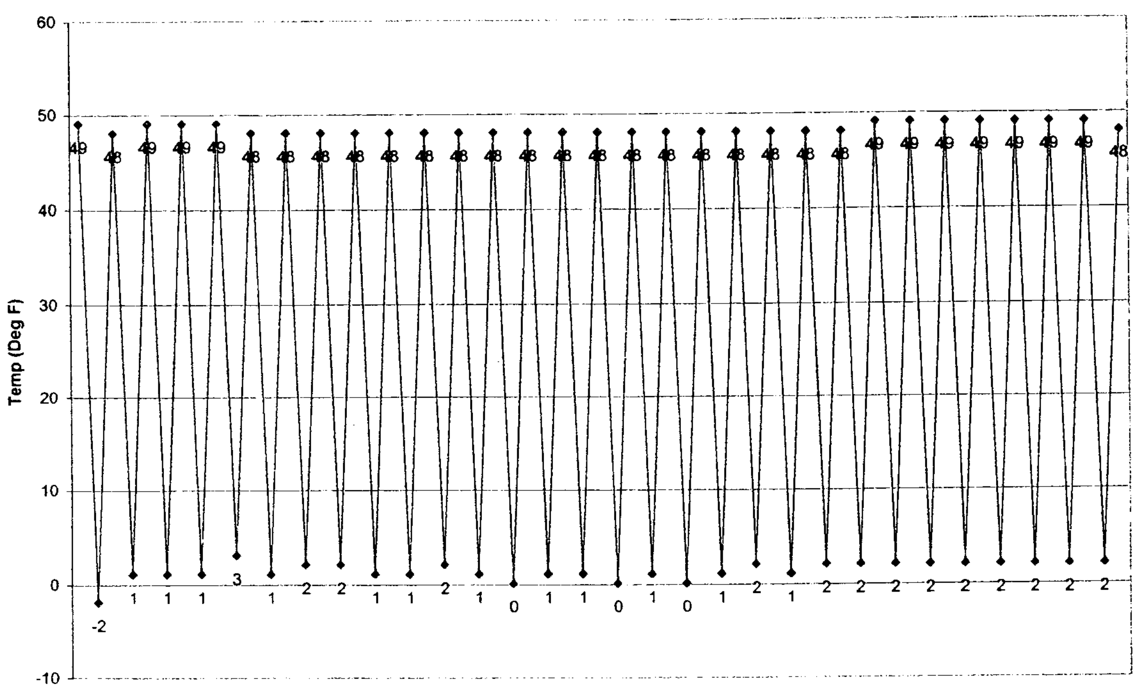

Figure 4.1. Temperature Range for 30 cycles

Table 4.2a Dynamic Modulus of Elasticity Mixes A and B

	Mix A				Mix B			
Cycle	1	2	3	Average	1	2	3	Average
0	4279653	4372244	4427471		4390408	4399994	4789999	
	4279653	4362485	4417620		4380817	4382662	4789999	
	4279653	4362485	4429442	4356745	4390408	4399994	4749466	4519305
30	4259251	4267430	4378289		4344268	4344268	4731283	
	4249681	4286744	4368463		4353851	4344268	4731283	
	4259251	4286744	4368463	4302702	4363444	4344268	4739360	4477366
60	4232481	4228933	4331222		4363444	4334696	4749466	
	4213412	4202089	4331222		4373047	4344268	4721196	
	4232481	4228933	4341007	4260198	4353851	4334696	4731283	4478438
92	4240121	4182967	4282464		4344268	4344268	4739360	
	4222941	4202089	4282464		4307950	4373047	4731283	
	4240121	4163888	4292193	4234361	4325134	4344268	4731283	4471207
125	4268832	4238541	4265367		4325134	4260865	4640981	
	4259251	4238541	4246041		4334696	4287377	4660929	
	4222941	4211666	4246041	4244136	4307950	4279794	4670919	4418738
149	4168801	4202167	4228933		4382662	4251417	4241468	
	4204645	4185010	4238541		4325134	4315874	4270091	
	4178219	4165987	4192522	4196092	4363444	4344465	4296893	4401520
182	4195198	4147008	4211666		4325394	4051729	4371996	
	4149997	4175493	4202089		4315874	4068341	4640981	
	4105042	4156492	4238541	4175725	4260865	4325394	4335326	4299544
212	4159394	4066148	4163888		3996604	4241978	4688928	
	4159394	4047457	4202089		4241978	4241978	4660929	
	4168801	4092387	4219336	4142099	4241978	4270324	4660929	4360625
242	4159394	4148898	4211666		4287377	4306365	4371996	
	4204645	4092387	4211666		4287377	4260865	4553716	
	4204645	4130018	4211666	4174998	4296866	4287377	4631022	4364774
272	4132385	4056833	4219336		4270324	4259171	4371996	
	4104410	4021512	4202089		4251417	4278033	4621075	
	4113724	4012242	4154365	4156700	4251417	4268597	4631022	4355895
300	4176659	4083891	4175240		4062353	4308971	4273552	
	4167213	4102728	4158020		4265628	4289892	4246693	
	4157777	4083891	4158020	4140382	4301902	4308971	4162828	4246754

Table 4.2b Dynamic Modulus of Elasticity Mixes C and D

	Mix C				Mix D			
Cycle	1	2	3	Average	1	2	3	Average
0	5804620	5788905	5700240		5044910	4931710	4838866	
	5793129	5700240	5688922		5055437	4931710	4838866	
	5827636	5734261	5700240	5748688	5044910	4931710	4838866	4939665
30	5660759	5502688	5482847		4882115	4841166	4779912	
	5660759	5524962	5460591		4861436	4841166	4779912	
	5649378	5524962	5449480	5546270	4882115	4859618	4779912	4834150
60	5647051	5589810	5493992		4822269	4790093	4749431	
	5669753	5589810	5482847		4822269	4810490	4741319	
	5647051	5601028	5505149	5580721	4760748	4788056	4710962	4777293
92	5672153	5536116	5438380		4760748	4761611	4700864	
	5615301	5524962	5460591		4760748	4731189	4700864	
	5649378	5513819	5449480	5540020	4750533	4741319	4700864	4734304
125	5440332	5491066	5438349		4691502	4700864	4660900	
	5581474	5513248	5416251		4671232	4690778	4650888	
	5615345	5468930	5394198	5484355	4671232	4700864	4650888	4676572
149	5692500	5589000	5558457		4219057	4391266	4439220	
	5637983	5589000	5547280		4380287	4325189	4232481	
	5647051	5589000	5634753	5609447	4399916	4457844	4259251	4344946
182	5793129	5687799	5589810		4275047	4286554	4203893	
	5658396	5566666	5536116		4255698	4381517	4203893	
	5647051	5524356	5569644	5619218	4294439	4352336	4409941	4295924
212	5647051	5633801	5536116		4134812	4334875	4409941	
	5669753	5544377	5601028		4125293	4221273	4101778	
	5647051	5566666	5623500	5607705	4106286	4230841	4409941	4230560
242	5558950	5513248	5547280		4199836	4401025	5183652	
	5604043	5535474	5352421		4199836	4477521	4545427	
	5549953	5544377	5427295	5514782	3674070	4457844	4439220	4397603
272	5647051	5555516	5547280		4163888	4400203	4392420	
	5747279	5566666	5536116		4035311	4363296	4392420	
	5637983	5566666	5547280	5594649	4080461	4458793	4392420	4297690
300	5652266	5645261	5543916		4115933	4421912	4097540	
	5663688	5633942	5575435		4032440	4250733	4078662	
	5675122	5624895	5564168	5619855	4144593	4221891	4069239	4159216

Table 4.2c Dynamic Modulus of Elasticity Mix E

Cycle	Mix E			
	1	2	3	Average
0	6532060	6566563	6978439	
	6519760	6554230	6978439	
	6507472	6566563	6991240	6688307
30	6470675	6470675	6940106	
	6458433	6482929	6927352	
	6482929	6482929	6917158	6625910
60	6424216	6495194	6904425	
	6412018	6495194	6917158	
	6363341	6458433	6904425	6690842
92	6399831	6458433	6891703	
	6399831	6458433	6853610	
	6375492	6446202	6853610	6570794
125	6363341	6446202	6866296	
	6363341	6446202	6853610	
	6363341	6458433	6840936	6555745
149	6424216	6436426	6780263	
	6399831	6387656	6755062	
	6387656	6424216	6792881	6532023
182	6329377	6129888	6853610	
	6037255	6399831	6285163	
	6139428	6070426	6830805	6341754
212	6329377	6424216	6755062	
	6424216	6446202	6792881	
	6412018	6458433	6694772	6526353
242	6399831	6363341	6792881	
	6387656	6082296	6805510	
	6458433	6436426	6830805	6506353
272	6256904	6001319	6597376	
	5898458	5919278	6694772	
	6351200	6301339	6878994	6322182
300	6267907	5921872	6235180	
	6433679	6354501	6225490	
	5940497	6400799	6213389	6221479

Table 4.3 Relative Dynamic Modulus of Elasticity (%)

Cycle	A	B	C	D	E
0	100.0	100.0	100.0	100.0	100.0
30	97.5	98.2	93.1	95.8	98.1
60	95.6	98.2	94.2	93.5	97.3
92	94.5	97.9	92.9	91.9	96.5
125	93.6	95.2	94.6	81.3	87.4
149	92.8	91.0	95.2	77.4	95.4
182	91.9	90.5	95.5	75.6	89.9
212	90.4	93.1	95.2	73.4	95.2
242	91.8	93.3	92.0	79.3	94.6
272	89.1	92.9	94.7	75.7	89.4
300	90.3	88.3	95.6	70.9	86.5

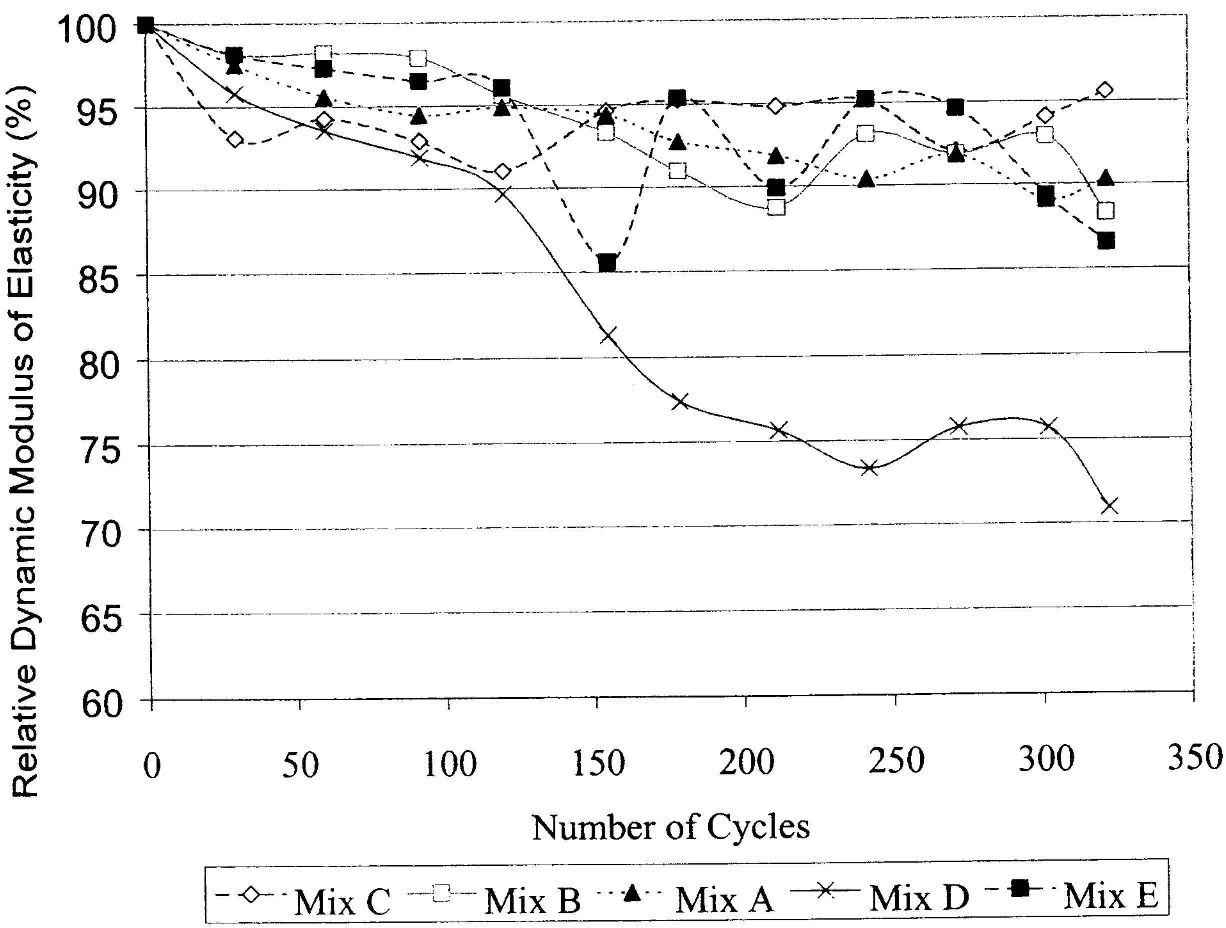

Figure 4.2 Change in Relative Dynamic Modulus of Elasticity with Freezing Thawing Cycles

4.3 Chloride Permeability Test Results

Two replicate 4x8 inch cylinders (56-day cure) were tested at WSDOT according to ASTM C 1202 as described in section 3.3 of this report. The results of chloride ion penetration of each mix design are listed in Table 4.4.

Mix C is the only design that meets one of the FHWA HPC performance grade requirements for chloride permeability. This mix is more resistant to chloride penetration than the other mixes. It is noted that mix C had w/c ratio of 0.38, and contained fly ash. This finding is in agreement with research results reported in the literature. Ozyildirim (1998) showed that mixes with fly ash, air-entrainment, and w/c <0.45 have very low permeability. Torii and Kawamura (1991) as well as Bilodeau (1994) demonstrated that the use of fly ash improves resistance to chloride permeability.

Mix D has very low penetration resistance and low freeze-thaw durability. This might be attributed to the combined effect of relatively high w/c and not including fly ash in the design. Naik et al. (1994) and Pigeon (1991) observed that mixes with low freeze-thaw durability also have low chloride ion penetration resistance. Mixes A, B, and E achieved similar levels of permeability. It is noticed that these mixes have similar water/cement ratio. It was surprising to see that Mix A did not meet any of the performance grades although it has relatively low w/c ratio and contains fly ash. Mix A's average permeability is 3945 Coulombs, but with a difference of 2309 between the two replicates.

Table 4.4 Chloride Permeability Test Results.

Mix Design	Chloride Penetration (Coulombs)			FHWA HPC Performance Grade
	1	2	Average	
A	2790	5099	3945	N/A
B	3749	3840	3795	N/A
C	1707	1546	1627	2
D	10997	9486*	10242	N/A
E	2796	4490	3643	N/A

* Test terminated after 286 minutes due to temperature of solution exceeding 190 degrees Fahrenheit as per test procedure.

This difference is too high compared with the other mixes. It is suspected that an error might have happened during the measurements of the chloride permeability of the second specimen of mix A. The value of the first specimen is more representative of what one might expected for the permeability of this mix.

The results show that high chloride permeability might cause a problem when these mixes are used in reinforced pavements where steel corrosion might occur due to chloride ion penetration. In general, based on the literature and our testing results, low chloride permeability can be achieved with a low w/c ratio and fly ash (Aitcin 1998). It is believed that a low water/cement ratio is the controlling factor for obtaining good permeability results.

4.4 Abrasion Test Results

In this test, three locations on each of the two specimens (Figure 4.3) per mix design were abraded as described in section 3.5. Average loss in grams of abraded material for each mix is listed in Table 4.5. The loss of weight was negligible for all mixes indicating excellent abrasion durability. All mix designs meet, the highest, FHWA HPC performance grade 3.

Compressive strength, w/c ratio, and coarse aggregate all influence abrasion. Laplante et al. (1991) emphasized that the coarse aggregate is the most important factor effecting abrasion resistance. Typical aggregates used in Washington State are igneous rock, which are very hard and abrasion resistant. Although these mixes contain a wide variation in their composition, they all had excellent abrasion resistance as shown in Table 4.5. It is likely that this resistance is mainly due to the hardness of the aggregate.

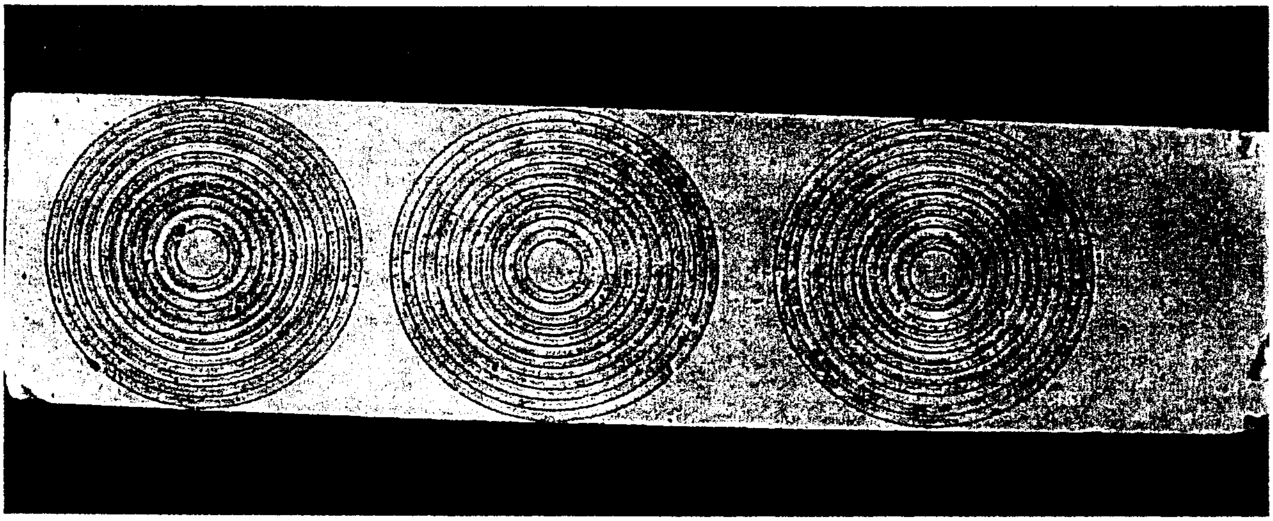

Figure 4.3 Abrasion Specimen After Testing

Table 4.5 Abrasion Test Results.

Mix	Specimen	Initial Mass (g)	Final Mass (g)	Change in Mass (g)	Average Loss of Mass (g)	FHWA HPC Performance Grade
A	1	7338.8	7338.3	0.5	0.3	3
		7338.3	7338.0	0.3		
		7338.0	7337.8	0.2		
	2	7373.7	7373.4	0.3		
		7373.4	7373.2	0.2		
		7373.2	7373.1	0.1		
E	1	7483.8	7483.6	0.2	0.2	3
		7483.6	7483.6	0.0		
		7483.6	7483.2	0.4		
	2	7438.7	7438.7	0.0		
		7438.7	7438.3	0.4		
		7438.3	7438.2	0.1		
D	1	7361.6	7361.5	0.1	0.1	3
		7361.5	7361.4	0.1		
		7361.4	7361.3	0.1		
	2	7331.3	7331.0	0.3		
		7331.0	7330.9	0.1		
		7330.9	7330.9	0.0		
C	1	7228.4	7228.2	0.2	0.2	3
		7228.2	7227.8	0.4		
		7227.8	7227.5	0.3		
	2	7191.2	7191.2	0.0		
		7191.2	7191.0	0.2		
		7191.0	7191.0	0.0		
B	1	7319.8	7319.6	0.2	0.2	3
		7319.6	7319.4	0.2		
		7319.4	7319.3	0.1		
	2	7345.0	7344.8	0.2		
		7344.8	7344.5	0.3		
		7344.5	7344.4	0.1		

The water/cement ratio for four of the mixes is below the recommended 0.35 for HPC, which also helps to improve abrasion resistance. In the literature, abrasion resistance was usually evaluated after subjecting the mixes to higher loads and for longer times than those specified in the FHWA definition of HPC and used in this study. This might suggest that the loading levels currently used in defining HPC are not high enough to differentiate between among mixes with different abrasion durability.

4.5 Scaling Test Results

Scaling test results were determined by two different methods: the first method is a qualitative visual inspection as described in ASTM C 672, and the second is a quantitative method based on image analysis techniques. These methods are described in more detail in section 3.6.

Scaling occurs because salt enters into capillaries just beneath the concrete surface and causes build up of osmotic pressures. This pressure is in addition to the hydraulic pressures previously described in freezing and thawing (section 5.1). It is vital that entrained air be present in the mix to allow the osmotic and hydraulic pressures a place to expand in the voids without rupturing the mix. The water/cement should also be kept at a minimum to avoid excess water from causing additional hydraulic pressures in the mix. ACI 201 recommends w/c less than or equal to 0.45 and air entrainment between 4.5 and 5.5% to ensure scaling resistance. Li et al. (1994) showed that the combination of non-air-entrained concrete with a w/c above 0.30 would suffer serious scaling.

The visual ratings as completed independently by four persons are given in Appendix B. A summary of the average visual inspections by the 4 evaluators is shown in Table 4.6 and Figures 4.4 and 4.5. All mixes tested in this study contained approximately 5% entrained air and had w/c less than or equal to 0.45. As shown in Figures 4.4 and 4.5, all mixes were resistant to scaling after 70 freeze-thaw cycles and achieved the highest performance grade of 3. (In general, the average ratings conformed to the findings of the literature).

The visual inspection results exhibit high variability among the four evaluators (figures 4.6 and 4.7). This demonstrates the subjectivity of the current method described in ASTM C 672. It should be noted that the visual inspection of scaling is based on the visibility of coarse aggregates at the surface. Therefore, it is difficult to rate specimen performance prior to the development of severe scaling.

The results of the scaling measurements using the image analysis techniques are in appendix C. Summary of the results is shown in Figures 4.8 and 4.9. The scaling parameter is taken as the ratio of the coefficient of variation in gray intensities on the surface (at certain number of cycles) to the original coefficient of variation prior to the scaling test. As can be seen in Figure 4.9, all specimens treated with $MgCl_2$ except for Mix E showed some increase in scaling. It is expected that a wide range would have been measured for the new scaling parameter if specimens had experienced severe scaling.

The new scaling parameter is quantitative which is advantageous over the current qualitative visual rating. Also, the new method is based on the variation of gray level on image, which is caused by the loss of paste on the surface. Consequently, it would capture concrete scaling at early stages even before coarse aggregates become visible.

4.6 Compressive Strength Test Results

The average compressive strength of each mix design is listed in Table 4.7. Three replicate 6x12 inch cylinders (56-day cure) were tested under a compressive axial load to failure according to ASTM C 39 as described in Materials and Methods. The standard deviation for all sets of specimens are within the acceptable range listed in ASTM C 39. Mix B had the highest compressive strength of all the mixes. Mix B is also the only mix that contained Type III cement. All of the other mixes contained Type I-II cement. As discussed in the literature review, Bilodeau & Malhotra (1994) found that Type III cement increases compressive strength. It is known that decreasing the w/c ratio will significantly increase compressive strength even if Type I cement is used.

Currently, pavement concrete mixes are specified in Washington State based on their compressive or flexural strength. The underlining assumption is that high compressive strength would improve the mix durability especially for freeze-thaw damage. However, as shown in Figure 4.11, there is no direct relationship between freeze-thaw durability and compressive strength for the test mixes. Consequently, durability of concrete mixes should be evaluated independently from strength. Also, specifications for pavement concrete mixes should consider mix durability.

Table 4.6a Image Analysis and Visual Inspection for Mixes A and B

Mix	Deicing Chemical	Cycle #	Image Analysis Scaling Factor	ASTM Visual Inspection	HPC Performance Grade
Mix A	CMA	0	1.00	0	3
		5	1.33	1	
		10	1.11	1	
		15	1.25	1	
		25	1.46	1	
		50	1.40	1	
		70	1.56	2	
	$MgCl_2$	0	1.00	0	3
		5	1.44	1	
		10	1.44	1	
		15	1.22	1	
		25	1.31	1	
		50	1.21	1	
		70	1.37	2	
Mix B	CMA	0	1.00	0	3
		5	1.44	1	
		10	1.40	1	
		15	1.19	1	
		25	1.40	1	
		50	1.40	2	
		70	1.28	2	
	$MgCl_2$	0	1.00	0	3
		5	1.39	0	
		10	1.28	1	
		15	1.36	1	
		25	1.62	1	
		50	1.79	1	
		70	1.47	2	

Table 4.6b Image Analysis and Visual Inspection for Mixes C and D

Mix	Deicing Chemical	Cycle #	Image Analysis Scaling Factor	ASTM Visual Inspection	HPC Performance Grade
Mix C	CMA	0	1.00	0	3
		5	1.29	0	
		10	1.08	0	
		15	1.16	1	
		25	1.38	1	
		50	1.22	1	
		70	1.41	1	
	$MgCl_2$	0	1.00	0	3
		5	1.81	0	
		10	1.06	1	
		15	1.14	1	
		25	1.26	1	
		50	1.15	1	
		70	1.65	2	
Mix D	CMA	0	1.00	0	3
		5	1.48	0	
		10	1.50	1	
		15	1.36	1	
		25	1.58	1	
		50	1.44	2	
		70	1.76	2	
	$MgCl_2$	0	1.00	0	3
		5	1.39	1	
		10	1.22	1	
		15	1.17	1	
		25	1.41	1	
		50	1.20	2	
		70	1.18	2	

Table 4.6c Image Analysis and Visual Inspection for Mix E

Mix	Deicing Chemical	Cycle #	Image Analysis Scaling Factor	ASTM Visual Inspection	HPC Performance Grade
Mix E	CMA	0	1.00	0	3
		5	1.19	0	
		10	1.23	0	
		15	1.34	1	
		25	1.40	1	
		50	1.53	1	
		70	1.40	1	
	$MgCl_2$	0	1.00	0	3
		5	0.89	0	
		10	0.93	0	
		15	1.00	0	
		25	0.98	0	
		50	0.92	1	
		70	1.02	1	

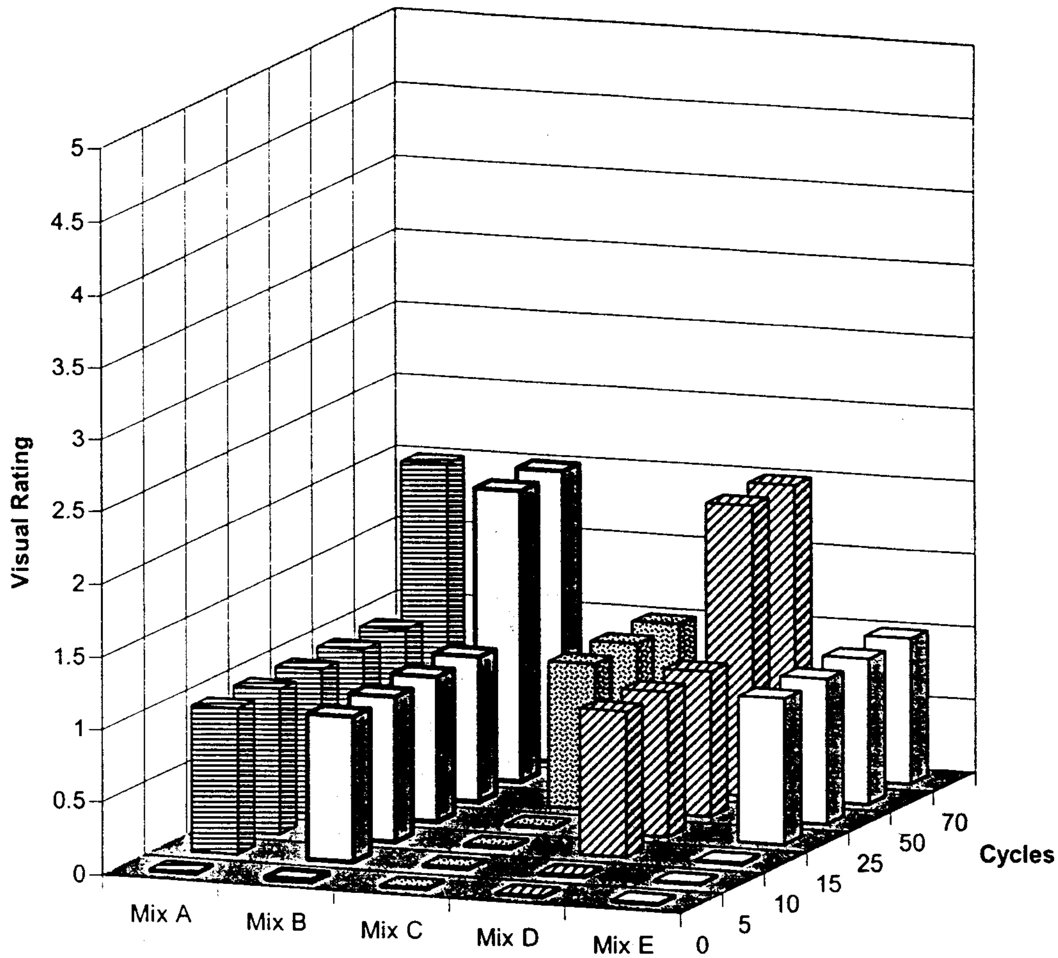

Figure 4.4 Visual Ratings for Specimens Scaled with CMA

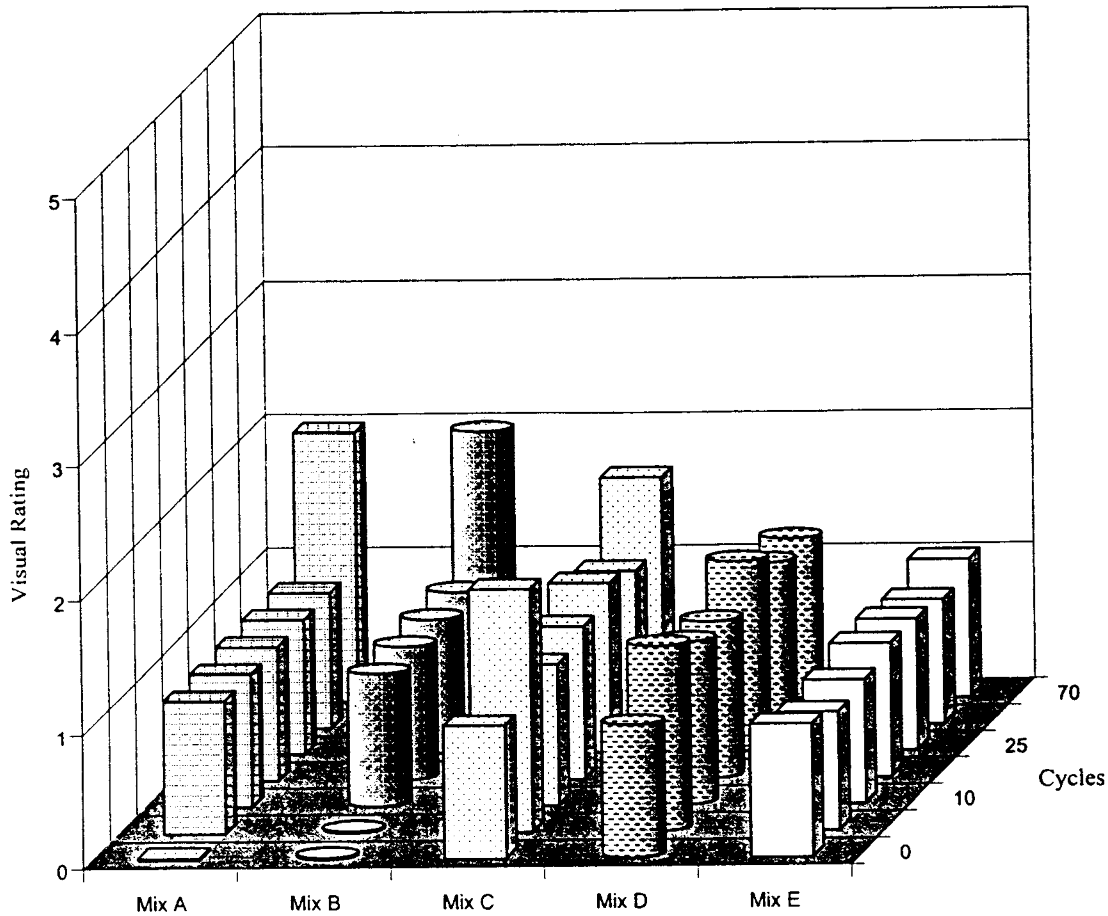

Figure 4.5 Visual Ratings for Specimens Scaled with $MgCl_2$

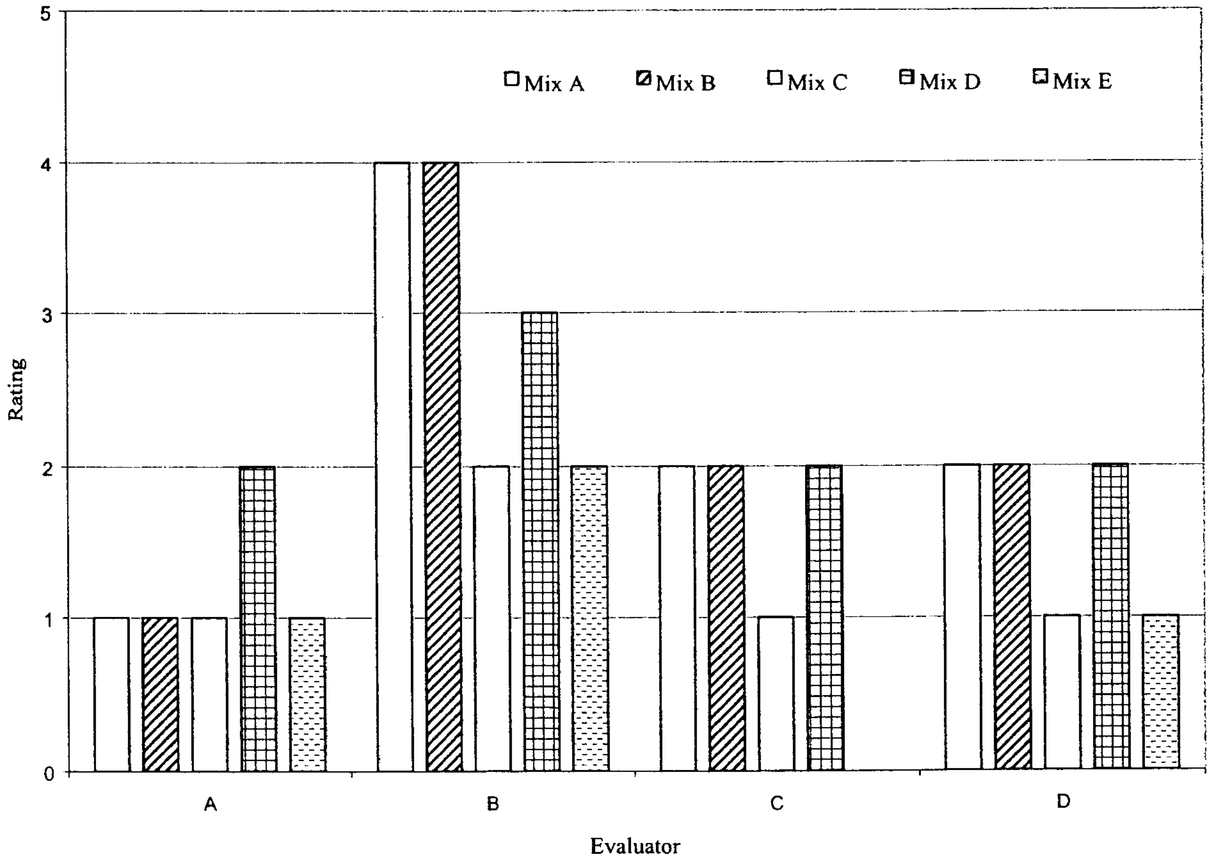

Figure 4.6 Comparison of Visual Rating Results by Evaluators for Specimens Scaled with CMA

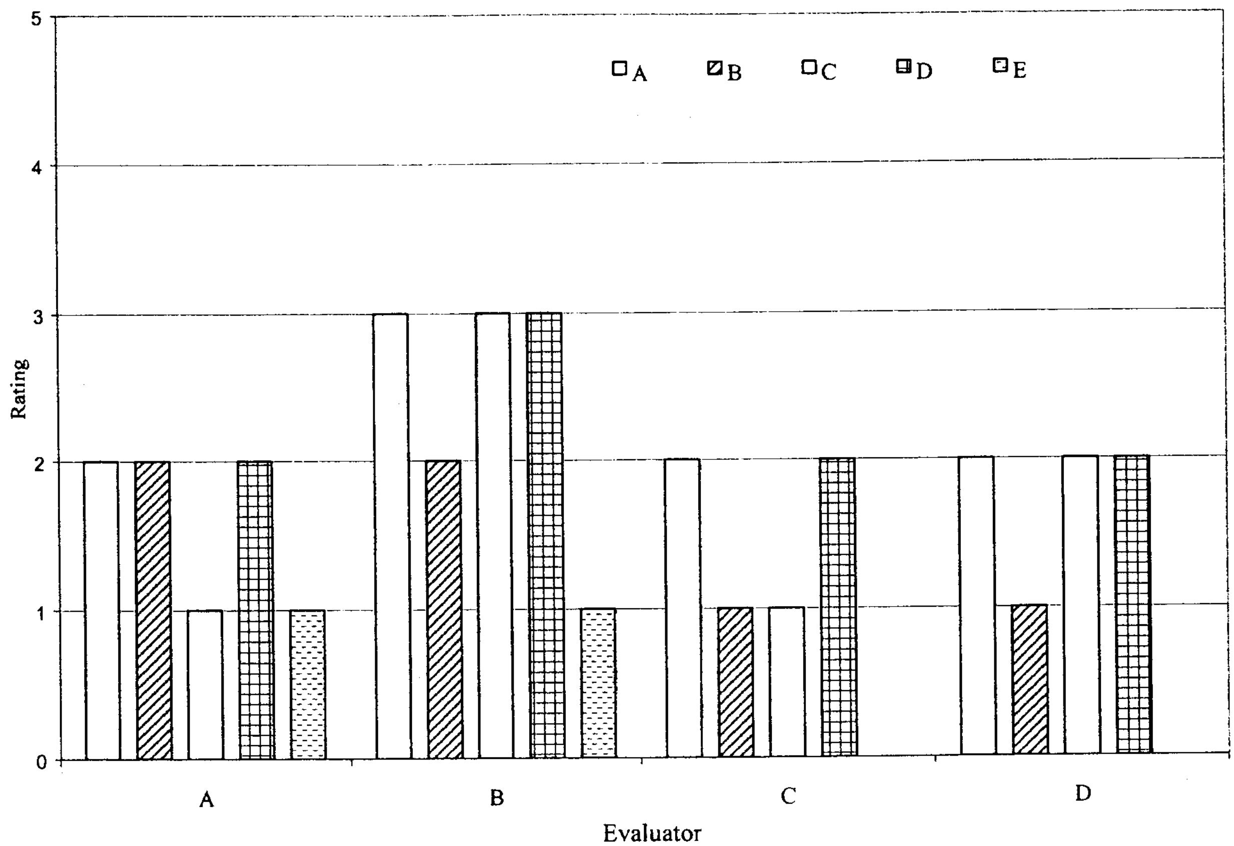

Figure 4.7 Comparison of Visual Rating Results by Evaluators for Specimens Scaled with $MgCl_2$

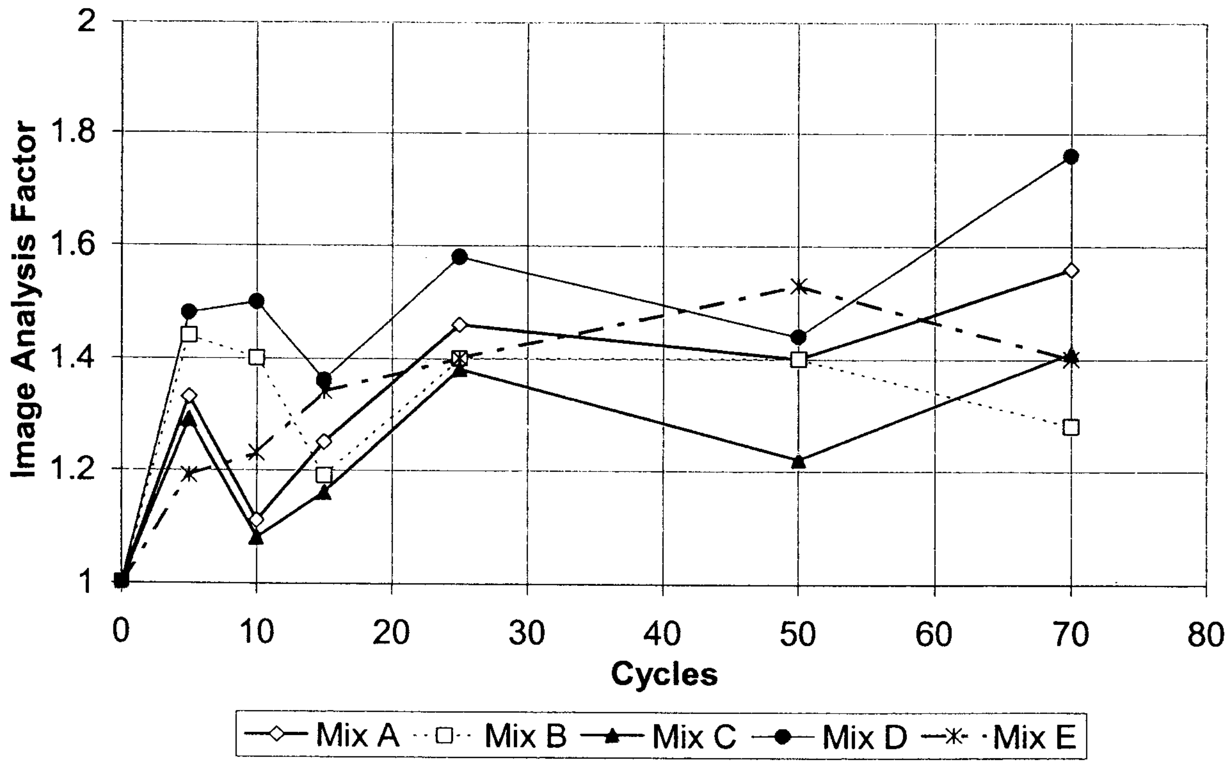

Figure 4.8 Image Analysis Results of Scaling by CMA

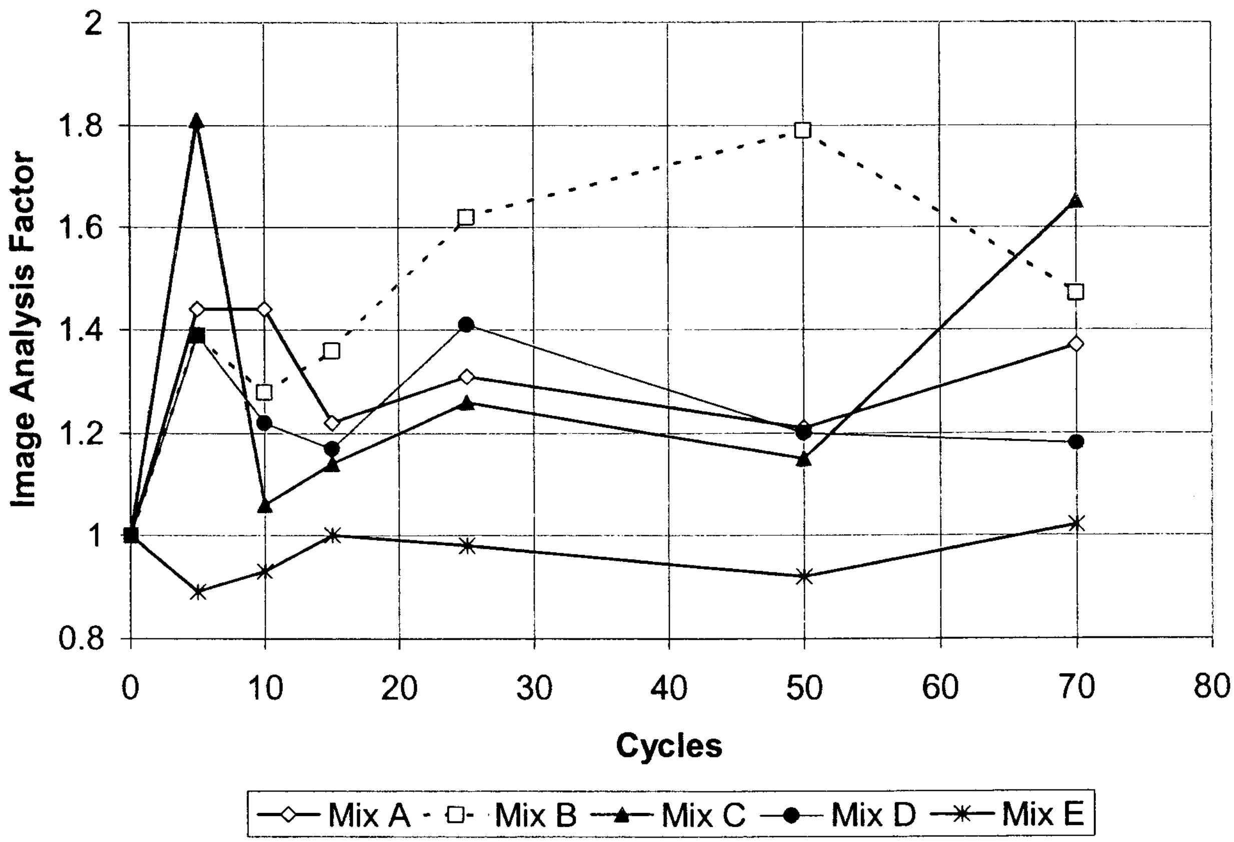

Figure 4.9 Image Analysis Results of Scaling by $MgCl_2$

Table 4.7 Compressive Strength Test Results.

Mix	Compressive Strength @ 56 days (psi) (Fracture at failure)					Design Strength (psi)
	1	2	3	Average	STD	
A	4152 (Cone)	4034 (Cone and Shear)	4207 (Cone)	4131	88	4000 @ 28 days compressive
B	6007 (Shear)	6031 (Cone and Shear)	5915 (Cone and Shear)	5984	61	2500 @1 day compressive
C	3687 (Shear)	3603 (Column)	3618 (Shear)	3636	45	650 @ 14 day flexural
D	3558 (Shear)	3535 (Shear)	3576 (Shear)	3556	21	4000 @ 28 days compressive
E	4464 (Cone)	4782 (Column)	4683 (Cone)	4643	163	650 @ 3 days flexural

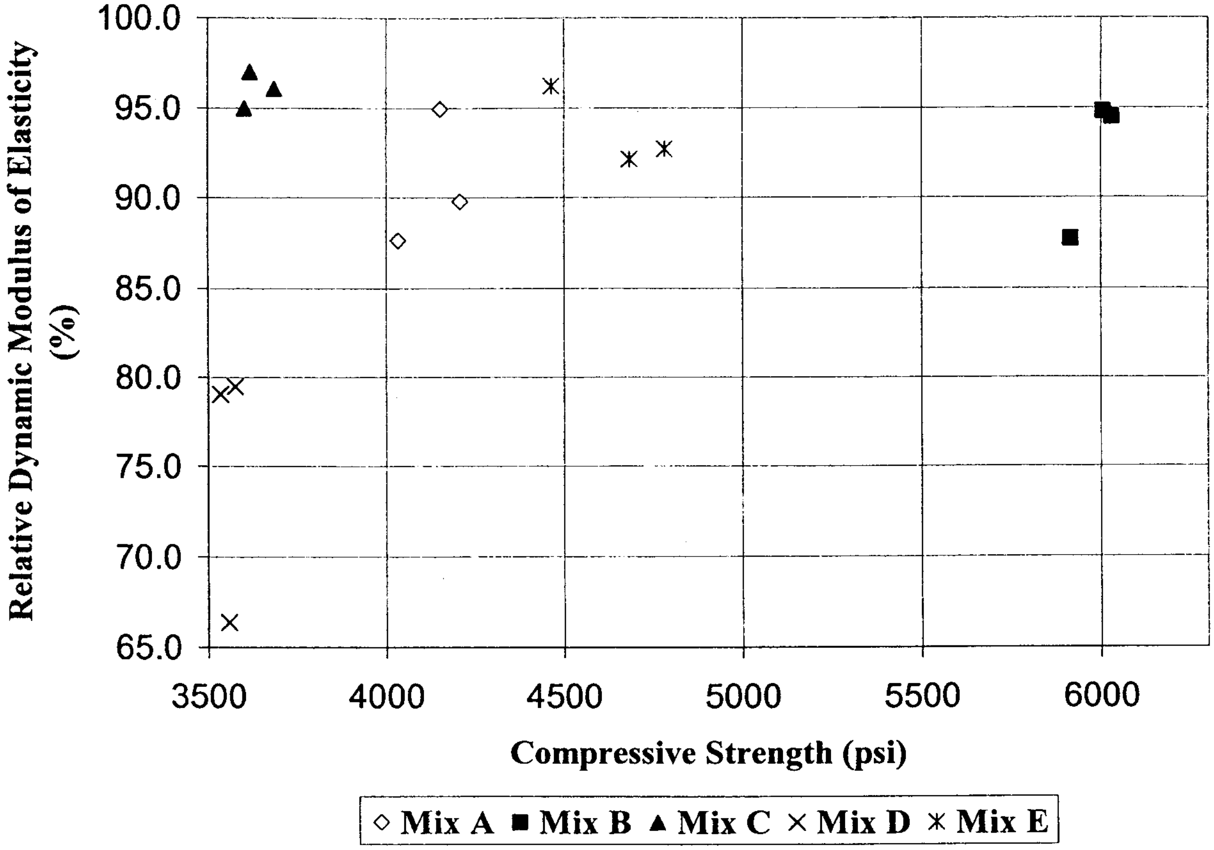

Figure 4.10 Relative Dynamic Modulus of Elasticity and Compressive Strength Comparison

4.7 Freeze Thaw Cycles in the State of Washington

The use of concrete with a certain performance grade at a geographic location depends on field exposure conditions. The FHWA has developed recommendations for the application of concrete grades according to exposure levels as shown previously in Table 1.3. Consequently, one of the tasks of the current study is to determine the freeze-thaw field exposure levels in the State of Washington and assign performance grades within the state based on these levels. The focus is on freeze-thaw because it is identified by WSDOT as the main cause of mix deterioration. Also, the exposure levels can be determined by analyzing available climatic data.

4.7.1 Climate Divisions in WA State

There are ten different climate divisions in the state of Washington (see Figure 4.13). Many counties span more than one climate zone. The climate division names and corresponding map number are given in Table 4.8. The counties associated with each climate division are also listed in the table. Only weather stations and counties with sufficient data were analyzed and are represented in this report.

The original climatic data was obtained from the following website http://www.ncdc.noaa.gov/. Minimum and maximum temperature data taken from January 1, 1998 to December 31, 1999 was analyzed to create the map. The number of freeze-thaw cycles at different locations within the state was determined and the recommend HPC performance grades were assigned for these sites. A temperature that drops below 29 degrees Fahrenheit and then increases to more than 35 degrees Fahrenheit defines a cycle.

4.7.3 Recommended HPC Grade for Each Station Analyzed

The average number of freeze-thaw cycles per year was determined for a number of weather stations in the state. Maximum and minimum temperature data collected over a two-year period for these weather stations was used to determine the average number of freeze-thaw cycles per year. The FHWA HPC performance grades were determined for each weather station based on Goodspeed's article (1996) (Table 1.3) and is shown in the following table and map. Table 4.9 includes the county, weather station name, and elevation where the data was collected. It also includes the corresponding climate division, freeze-thaw cycles per year, and the recommended HPC Grade for the station. A general performance grade was determined for each climate division. This grade does not apply to all cities and counties within the climate division, but it provides a general picture of where significant freezing and thawing occurs in the state. The FHWA performance grade is based on the number of freeze-thaw cycles per year. However, it is known that the length of the freezing cycle effects performance. Longer freezing periods cause more damage than shorter freezing periods. Exposure conditions and performance grade defined by FHWA does not reflect damage caused by long cycle lengths. For example, climate zone 8 has a performance grade of 1, however, long freezing periods occur in this region and pavements with higher durability may be needed.

4.7.4 Freeze-Thaw Zones in WA State

The map in Figure 4.12 is based on the performance grade (assigned in the previous table) for each climate zone. This grade is not representative of every weather station in the division, but rather it provides a general idea of the locations of the different freeze-thaw exposure conditions are. It is recommended that FHWA HPC performance grade 1 concrete is used in the light color zones and grade 2 is used in the dark color zones.

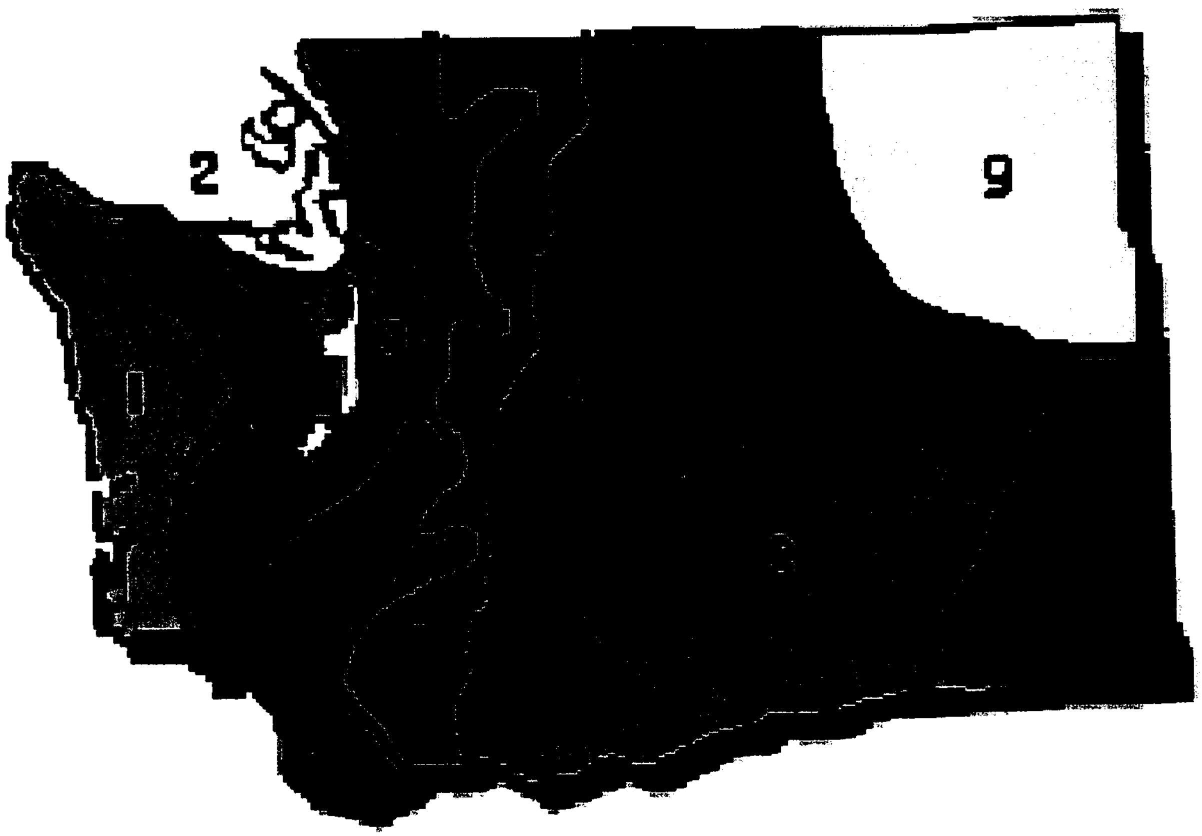

Figure 4.11 Climate Zones in WA State

Table 4.8 Climate Divisions by County

1 West Olympic Coastal	2 NE Olympic San Juan	3 Puget Sound Lowlands	4 E Olympic Cascade Foothills	5 Cascade Mountains West
CLALLAM	CLALLAM	KING	CLALLAM	KING
GRAYS	SAN JUAN	KITSAP	CLARK	KITTITAS
HARBOR	ISLAND			
JEFFERSON	SKAGIT	LEWIS	COWLITZ	PIERCE
MASON	SNOHOMISH	PIERCE	GRAYS HARBOR	SKAMANIA
PACIFIC	WHATCOM	SKAGIT	JEFFERSON	WHATCOM
		SNOHOMISH	KING	
		THURSTON	LEWIS	
		WHATCOM	MASON	
			PIERCE	
			SKAGIT	
			SKAMANIA	
			SNOHOMISH	
			WAHKIAKUM	
			WHATCOM	

6 East Slope Cascade	7 Okanogan Big Bend	8 Central Basin	9 Northeastern	10 Palouse Blue Mountains
CHELAN	CHELAN	ADAMS	FERRY	ASOTIN
KITTITAS	DOUGLAS	BENTON	PEND OREILLE	COLUMBIA
KLICKITAS	GRANT	CHELAN	SPOKANE	GARFIELD
OKANOGAN	LINCOLN	FRANKLIN	STEVENS	WHITMAN
	OKANOGAN	GRANT		
		KITTITAS		
		KLICKITAT		
		WALLA		
		WALLA		
		YAKIMA		

Table 4.9a Recommended Freeze-Thaw FHWA HPC Performance Grades Climate Divisions 1 and 2

COUNTY	STATION NAME	CLIMATE DIVISION	ELEV (m.)	FREEZE THAW CYCLES PER YEAR	RECOMMENDED HPC GRADE	RECOMMENDED PERFORMANCE GRADE FOR CLIMATE DIVISION
CLALLAM	FORKS 1 E	1	106.7	9	1	
	QUILLAYUTE STATE AIRPORT	1	54.6	14	1	
GRAYS HARBOR	ABERDEEN	1	3	1	N/A	
	ABERDEEN 20 NNE	1	132.6	1.5	N/A	
	GRAYLAND	1	3	5	1	
	HOQUIAM AP	1	3.7	2.5	N/A	
	HUMPTULIPS SALMON HATCHERY	1	42.7	16.5	1	
JEFFERSON	CLEARWATER	1	24.4	18.5	1	
	PORT TOWNSEND	1	21	1	N/A	
MASON	CUSHMAN POWERHOUSE 2	1	6.4	1.5	N/A	
PACIFIC	GRAYS RIVER HATCHERY	1	30.5	11.5	1	
	LONG BEACH EXP STN	1	9.1	6	1	
	RAYMOND 2 S	1	9.1	15.5	1	1
CLALLAM	PORT ANGELES	2	27.4	3.5	1	
	SEQUIM 2 E	2	15.2	26	1	
SAN JUAN ISLAND	COUPEVILLE 1 S	2	15.2	3.5	1	
	OLGA 2 SE	2	24.4	2	N/A	
SKAGIT	ANACORTES	2	6.1	3	1	
	MOUNT VERNON 3 WNW	2	4.3	3.5	1	
SNOHOMISH	EVERETT	2	185.9	10.5	1	
WHATCOM	BELLINGHAM 3 SSW	2	4.6	5.5	1	1

Table 4.9b Recommended Freeze-Thaw FHWA HPC Performance Grades
Climate Division 3

COUNTY	STATION NAME	CLIMATE DIVISION	ELEV (m.)	FREEZE THAW CYCLES PER YEAR	RECOMMENDED HPC GRADE	RECOMMENDED PERFORMANCE GRADE FOR CLIMATE DIVISION
KING	KENT	3	9.1	5	1	
	SEATTLE SAND PT WSFO	3	18.3	3	1	
	SEATTLE-TACOMA INTL AIRPORT	3	121.9	2.5	N/A	
KITSAP	BREMERTON	3	33.5	3	1	
LEWIS	CENTRALIA	3	56.4	2	N/A	
PIERCE	MC MILLIN RESERVOIR	3	176.5	9.5	1	
	TACOMA 1	3	7.6	3.5	1	
SKAGIT	SEDRO WOOLLEY	3	18.3	9.5	1	
SNOHOMISH	MONROE	3	36.6	6	1	
THURSTON	OLYMPIA AIRPORT	3	62.8	20.5	1	
WHATCOM	BELLINGHAM KVOS	3	91.4	3	1	
	BLAINE	3	18.3	13.5	1	
	CLEARBROOK	3	19.5	10	1	1

4.9c Recommended Freeze-Thaw FHWA HPC Performance Grades
Climate Divisions 4 and 5

COUNTY	STATION NAME	CLIMATE DIVISION	ELEV (m.)	FREEZE THAW CYCLES PER YEAR	RECOMMENDED HPC GRADE	RECOMMENDED PERFORMANCE GRADE FOR CLIMATE DIVISION
CLALLAM	ELWHA R S	4	109.7	2.5	N/A	
CLARK	BATTLE GROUND	4	86.6	16	1	
	VANCOUVER 4 NNE	4	64	13.5	1	
COWLITZ	LONGVIEW	4	3.7	3.5	1	
GRAYS HARBOR	ELMA	4	21.3	14.5	1	
JEFFERSON	QUILCENE 2 SW	4	37.5	5.5	1	
	BARING	4	231.6	12	1	
	LANDSBURG	4	163.1	10.5	1	
	MUD MOUNTAIN DAM	4	398.7	22.5	1	
	PALMER 3 ESE	4	280.4	2	N/A	
	SNOQUALMIE FALLS	4	134.1	8.5	1	
LEWIS	GLENOMA	4	256	22.5	1	
	PACKWOOD	4	323.1	24	1	
	TOLEDO	4	99.1	11	1	
MASON	SHELTON	4	6.7	17.5	1	
PIERCE	BUCKLEY 1 NE	4	208.8	9	1	
SKAGIT	CONCRETE PPL FISH STN	4	59.4	3	1	
SKAMANIA	SKAMANIA FISH HATCHERY	4	134.1	17.5	1	
SNOHOMISH	STARTUP 1 E	4	51.8	6.5	1	
WAHKIAKUM	CATHLAMET 6 NE	4	54.9			
WHATCOM	DIABLO DAM	4	271.6	8	1	
	NEWHALEM	4	160	3	1	1
KING	CEDAR LAKE	5	475.5	14.5	1	
KITTITAS	STAMPEDE PASS	5	1206.4	32	1	
PIERCE	LONGMIRE RAINIER NPS	5	841.9	66	2	
	RAINIER PARADISE RNGER S	5	1654.1	60.5	2	
SKAMANIA	CARSON FISH HATCHERY	5	345.6	23	1	
	COUGAR 6 E	5	200.9	2.5	N/A	
WHATCOM	ROSS DAM	5	376.7	7.5	1	
	UPPER BAKER DAM	5	210.3	12.5	1	1

4.9d Recommended Freeze-Thaw FHWA HPC Performance Grades
Climate Divisions 6 and 7

COUNTY	STATION NAME	CLIMATE DIVISION	ELEV (m.)	FREEZE THAW CYCLES PER YEAR	RECOMMENDED HPC GRADE	RECOMMENDED PERFORMANCE GRADE FOR CLIMATE DIVISION
CHELAN	ENTIAT FISH HATCHERY	6	292.6	53.5	2	
	HOLDEN VILLAGE	6	981.5	98.5	2	
	LEAVENWORTH 3 S	6	343.8	82	2	
	PLAIN	6	591.3	78	2	
	STEHEKIN 4 NW	6	387.1	30.5	1	
KITTITAS	CLE ELUM	6	585.2	66.5	2	
KLICKITAT	APPLETON	6	712	53	2	
KLICKITAT	DALLESPORT 9 N	6	586.1	15.5	1	
KLICKITAT	GLENWOOD 2	6	563.9	88.5	2	
KLICKITAT	SATUS PASS 2 SSW	6	795.5	59.5	2	
OKANOGAN	MAZAMA	6	661.4	72	2	
	WINTHROP 1 WSW	6	534.9	79.5	2	2
CHELAN	CHELAN	7	341.4	17	1	
DOUGLAS	CHIEF JOSEPH DAM	7	249.9	40	1	
	WATERVILLE	7	798.6	70	2	
GRANT	COULEE DAM 1 SW	7	518.2	28.5	1	
	HARTLINE	7	582.2	49.5	1	
LINCOLN	DAVENPORT	7	743.7	75.5	2	
	HARRINGTON 1 NW	7	667.5	76.5	2	
	ODESSA	7	466.3	55.5	2	
	WILBUR	7	679.7	72	2	
OKANOGAN	CONCONULLY	7	707.1	37	1	
	METHOW 2 S	7	356.6	70	2	
	TONASKET 4 NNE	7	292.6	45	1	2

4.9e Recommended Freeze-Thaw FHWA HPC Performance Grades
Climate Division 8

COUNTY	STATION NAME	CLIMATE DIVISION	ELEV (m.)	FREEZE THAW CYCLES PER YEAR	RECOMMENDED HPC GRADE	RECOMMENDED PERFORMANCE GRADE FOR CLIMATE DIVISION
ADAMS	LIND 3 NE	8	496.8	45.5	1	
ADAMS	OTHELLO 6 ESE	8	362.7	35.5	1	
ADAMS	RITZVILLE 1 SSE	8	557.8	66.5	2	
BENTON	BENTON CITY 2 NW	8	207			
	KENNEWICK	8	118.9	10	1	
	MCNARY DAM	8	110	5	1	
	PROSSER	8	253	38	1	
	RICHLAND	8	113.7	22	1	
CHELAN	WENATCHEE	8	195.1	22.5	1	
	WENATCHEE PANGBORN FIELD	8	374.6	39	1	
FRANKLIN	CONNELL 1 W	8	310.9	34	1	
	ELTOPIA 8 WSW	8	213.4	31.5	1	
	HATTON 9 SE	8	460.2	24.5	1	
GRANT	EPHRATA AP FCWOS	8	383.7	44	1	
	PRIEST RAPIDS DAM	8	140.2	19.5	1	
	QUINCY 1 S	8	388.3	43.5	1	
	SMYRNA	8	170.7	50.5	2	
KITTITAS	ELLENSBURG	8	451.1	75	2	
KLICKITAT	GOLDENDALE	8	505.1	53	2	
WALLA WALLA	ICE HARBOR DAM	8	112.2	20.5	1	
	WALLA WALLA CITY COUNTY AP	8	355.4	4	1	
	WHITMAN MISSION	8	192.6	42	1	
YAKIMA	MOXEE CITY 10 E	8	472.4	57.5	2	
	SELAH 2 NE	8	341.4	105	2	
	SUNNYSIDE	8	227.7	14.5	1	
	WAPATO	8	256.3	53	2	
	YAKIMA AIR TERMINAL	8	324.3	87	2	
	YAKIMA NO 2	8	350.5	26	1	1

4.9f Recommended Freeze-Thaw FHWA HPC Performance Grades
Climate Divisions 9, 10, 99

COUNTY	STATION NAME	CLIMATE DIVISION	ELEV (m.)	FREEZE THAW CYCLES PER YEAR	RECOMMENDED HPC GRADE	RECOMMENDED PERFORMANCE GRADE FOR CLIMATE DIVISION
FERRY	REPUBLIC	9	795.5	92.5	2	
PEND OREILLE	BOUNDARY DAM	9	548.6	61.5	2	
	NEWPORT	9	650.7	80.5	2	
SPOKANE	SPOKANE INTERNATIONAL AIR PORT	9	718.1	42	1	
	SPOKANE WFO	9	727.6	73	2	
STEVENS	CHEWELAH	9	509	75.5	2	
	COLVILLE	9	505.1	47.5	1	
	NORTHPORT	9	411.5	48	1	
	WELLPINIT	9	759	66	2	
	LA CROSSE	9	452	60	2	2
ASOTIN	ANATONE	10	1089.1			
	ASOTIN 14 SW	10	1066.8			
COLUMBIA	DAYTON 1 WSW	10	474.6	22.5	1	
GARFIELD	POMEROY	10	579.1	53	2	
WHITMAN	PULLMAN 2 NW	10	775.7	39.5	1	
	ROSALIA	10	731.5	56	2	
	SAINT JOHN	10	592.8	39	1	
	WHIDBEY ISLAND NAS	99	10.1	3	1	1

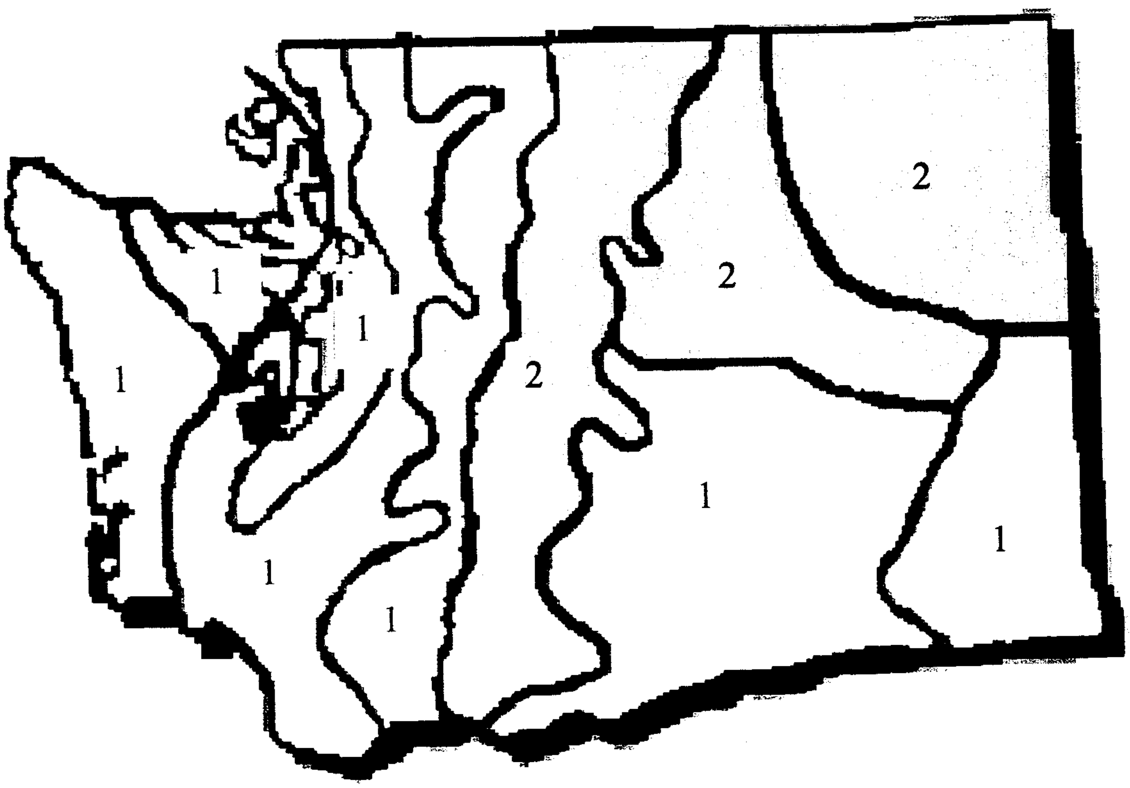

Figure 4.12 Freeze-Thaw Zones in WA State

CHAPTER 5: CONCLUSIONS AND GUIDELINES

5.1 Conclusions

The main objective of this study is to evaluate the durability and strength of typical pavement concrete mixes used in the State of Washington. Determination of the level of durability of existing mix designs will give WSDOT a starting point in developing performance-based specifications for new levels of concrete durability. Also, the results of this study will enable mix designs to be selected by matching the performance grade with field exposure conditions.

The testing methods used in this study conform in most part to the standard ASTM methods and the recommendations provided by the FHWA for evaluating the properties of high performance concrete (HPC). However, it was found that the method for measuring the fundamental frequency of concrete as described by ASTM to evaluate the mix deterioration due to freeze-thaw cycles is time consuming. Consequently, another procedure that uses a piezoelectric film as a pick up device for longitudinal frequency was used in this study. This method was found to be simple, inexpensive and to yield reliable measurements of concrete frequency. All mixes satisfied different HPC grades for freeze-thaw durability. Four of the mixes met HPC performance grade 2, and the fifth mix met performance grade 1. Including 5 to 6% air entrainment and maintaining a water/cement ratio below 0.35 in the mix was found to improve freeze-thaw durability. Also, fly ash may be added to the mix to improve freeze-thaw resistance. The compressive strength measurements have shown that there was no direct relationship between the mix strength and freeze-thaw durability for the mixes tested in this research.

The abrasion resistance was measured using a device assembled at WSU that meets the ASTM standard procedure specifications. All mixes had excellent abrasion resistance irrespective of their composition. It is believed that this resistance was mainly due to the hardness of the aggregate used in these mixes. It was noticed, however, that abrasion resistance was usually evaluated in the literature after subjecting the mixes to higher loads and for longer times than those specified in the FHWA definition of HPC and used in this study. This might suggest that the loading levels currently used in defining HPC are not high enough to distinguish among mixes with different abrasion durability.

The scaling resistance of the mixes was evaluated using visual inspection, as outlined in the standard ASTM procedure, and a new quantitative method based on image analysis techniques. The visual inspection was done independently by four individuals. The variability of the results from the four evaluators demonstrated the subjectivity of the visual inspection. It was found to be difficult to rate scaling prior to reaching severe levels that are described by visibility of coarse aggregates on the surface.

The new scaling parameter utilizes the variation of gray intensities on images of concrete surface. The variation of gray intensity increases with the deterioration of the paste on the surface. This method was found to capture scaling at earlier stages before coarse aggregates became visible at the surface.

All mixes evaluated in this study experienced high resistance to scaling after 70 cycles and achieved a performance grade of 3. This was attributed mainly to the air entrainment in these mixes and their low w/c ratio.

In terms of the resistance to chloride permeability, only one mix met a HPC grade. The other four mixes had high chloride permeability. The results suggest that the use of these mixes in reinforced pavement might cause problem in steel corrosion due to chloride ion penetration. In general, based on the literature and our testing results, low chloride permeability can be achieved by low w/c ratio and including fly ash. It is believed that a low water/cement ratio is the controlling factor for obtaining good permeability results.

Climactic data was analyzed in order to determine freeze-thaw exposure conditions in the state. This information was used to assign pavement performance grades within the state according to actual field conditions.

5.2 General Guidelines for Developing HPC Mix Designs

The following general guidelines will help improve a mix designs resistance to freezing and thawing, chloride penetration, scaling, and abrasion, as well improving compressive strength. Additional construction and placing recommendations may be found in ACI 201.2R-92 "Guide to Durable Concrete".

1. Include 5 to 6% air-entrainment for freeze-thaw durability, to prevent chloride penetration, and to increase resistance to scaling.
2. Keep the w/c ratio below 0.35 to improve durability and strength.
3. As an addition to the cement content include fly ash or other pozzolans in the mix design to improve freeze-thaw durability and resist chloride penetration.
4. Use Type III Cement to improve early age compressive strength.
5. Add superplasticizers to reduce water/cement ratio, which increases strength, given a certain mix design.

CHAPTER 6: REFERENCES

ACI Committee 201. (2000). "Guide to Durable Concrete." *ACI J. Proc.* (ACI 201.2R-77), 74(12), 1977, 573-609.

Aitcin, P.C. (1998). *High Performance Concrete.* London. E & FN Spon.

Askeland, D.R. (1994). The Science and Engineering of Materials. Boston, MA. PWS Publishing Company

Attiogbe, E. K.; Nmai, C. K.; and Gay, F. T. (1992). "Air-void system parameters and freeze-thaw durability of concrete containing superplasticizers." *Concrete International.*, 14(7), 57-61.

Bilodeau, A.; Carette, G.G.; Malhotra, V.M.; and Langley, W.S. (1991). "Influence of curing and drying on salt scaling resistance of fly ash concrete." *Durability of Concrete. Second International Concrete*, Montreal Canada, ACI SP-126, 1, 201-228.

Bilodeau, A. and Malhotra, V.M. (1994). "High-performance concrete incorporating large volumes of ASTM class F fly ash." *High-Performance Concrete. Proc., ACI International Conference.*, Singapore, ACI SP-149, 177-193.

Bilodeau, A., Sivasundaram, V., Painter, K.E., Malhotra, V.M. (1994). "Durability of concrete incorporating high volumes of fly ash from sources in the U.S." *ACI Materials Journal*, 91(1), 3-12.

Bowser, J. d., Krause, G. L., and Tadros, M. K. (1996). "Freeze-thaw durability of high-performance concrete masonry units." *ACI Materials Journal*, 93(4), 386-394.

De Almeida, I.R. (1994). "Abrasion Resistance of high strength concrete with chemical and mineral admixtures." *Durability of Concrete. Proceeding., Third International Conference*, Nice, France, ACI SP-145, 1099-1113.

Ellis, W.E. Jr. and Riggs, E.H. (1991). "Comparative results of utilization of fly ash, silica fume and GGBFS in reducing the chloride permeability of concrete." *Durability of Concrete. Second International Conference.*, Montreal, Canada, ACI SP-126, 1, 443-458.

Gagne, R.; Pigeon, M.; and Aitchin, P.-C. (1991). "Deicer salt scaling resistance of high strength concretes made with different cements." *Concrete Durability. Second International Concrete*, Montreal Canada, ACI SP-126, 1, 185-199.

Galeota, D.; Giammatteo, M.M.; Marino, R.; and Volta, V. (1991). "Freezing and thawing resistance of non air-entrained and air-entrained concretes containing a high percentage of condensed silica fume." *Durability of Concrete. Second International Conference*, Montreal, Canada, American Concrete Institute, Detroit, MI, 1, 249-261.

Gjorv, O.E.; Baerland, T.; and Ronning, H.R. (1990). "Abrasion resistance of high-strength concrete pavements." *Concrete International: Design and Construction*, 12(1), 45-48.

Goodspeed, C.H.; Vanikar, S.; Cook, R.A. (1996). "High-Performance Concrete Defined for Highway Structures." *Concrete International*, 18(2), 62-67.

Halliday, D.; Resnick, R.; Walker, J. (1993). *Fundamentals of Physics.* New York.

Kashi, Mohsen G. and Weyers, Richard E. (1989). "Freezing and thawing durability of high strength silica fume concrete." *Structural Materials. Proc., Sessions at the ASCE Structures Congress '89*, San Francisco, CA; Ed. By James F. Orofino; ASCE, New York, 138-148.

Langely, W.S., Carette, G.G., and Malhotra, V.M. (1989). "Structural concrete incorporating high volumes of ASTM Class F fly ash." *ACI Materials Journal,* 86(5), 507-514.

Laplante, P.; Aitcin, P.C.; and Vezina, D. (1991). "Abrasion resistance of concrete." *Journal of Materials in Civil Engineering*, 3(1), 19-28.

Li, Y.; Langan, B.W.; Ward, M.A. (1994). "Freezing and thawing: Comparison between non-air-entrained and air-entrained high-strength concrete." *High-Performance Concrete. Proc., ACI Int. Conf.*, Singapore, American Concrete Institute, Detroit, MI, ACI SP-149, 545-560.

Malhotra, V.M. (1990). "Durability of concrete incorporating high-volume of low-calcium (ASTM class F) Fly ash." *Cement and Concrete Composites*, 12(4), 271-277.

Malhotra, V.M. and Carino, N.J. (2000). *CRC Handbook on Nondestructive Testing of Concrete.* CRC Press. Boca Raton, FL.

McDonald, D. B. and Perenchio, W.F. (1997). "Effects of salt type on concrete scaling." *Concrete International*, 19(7), 23-26.

Naik, T. R. and Ramme, B. W. (1990). "High early strength concrete containing large quantities of fly ash." *Serviceability and Durability of Construction Materials. Proceedings of First Materials. Engineering Congress*, Denver, CO, Suprenant; 2, 1039-1050.

Naik, T. R.; Singh, S. S.; Hossain, M. M. (1994a). "Permeability of concrete containing large amounts of fly ash." *Cement and Concrete Research,* 24(5), 913-922.

Naik, T. R.; Singh, S. S.; Hossain, M. M. (1994b). "Abrasion resistance of concrete as influenced by inclusion of fly ash." *Cement and concrete Research.*, 24(2), 303-312.

Naik, T. R.; Singh, S. S.; Hossain, M. M. (1995). "Abrasion resistance of high-strength concrete made with Class C fly ash." *ACI Materials Journal,* 92(6), 649-659.

Nasser, K.W. and Lai, P.S.H. (1992). "Resistance of fly ash concrete to freezing and thawing." *Fly Ash, Silica Fume, Slag, and Natural Pozzolans in Concrete. Proceeding of the Fourth International Conference,* Istanbul, Turkey, ACI SP-132, 1, 205-226.

Ozyildirim, C. (1998). "Permeability specification for high performance concrete decks." *Transportation Research Record*, 1610, 1-5.

Pigeon, M., Gagne, R., Aitcin, P-C., and Banthia, N. (1991) "Freezing and thawing tests of high-strength concretes." *Cement and Concrete Research,* 12(5), 844-852.

Pitt, J.M.; Seshadri, M.; and Covey, D.L. (1992). "Reliability-based design for freeze-thaw concrete." Materials Performance and Prevention of Deficiencies and Failures." *Proceeding of the Materials Engineering Congress*, ASCE, 462-475.

Rear, K. and Chin, D. (1990). "Non-chloride accelerating admixtures for early compressive strength." *Concrete International 12*(10), 55-58.

Ross, R.J.; Degroot, R.; Nelson, W. (1994). "Technique for nondestructive evaluation of biologically degraded wood." *Society of Experimental Mechanics, Journal of Experimental Tech.*,18(5), 29-32.

Siebel, E. (1989). "Air-void characteristics and freezing and thawing resistance of superplasticized air-entrained concrete with high workability." *Superplasticizers and Other Chemical Admixtures in Concrete. Proc. Third Int.Conf.*, Ottawa, Canada, American Concrete Institute, ACI SP-119, 297-319.

Stark, D. (1989). "Effect of length of freezing period on durability of concrete." *PCA Res. and Development Bulletin* RD096T, Portland Cement Association, 1-9.

Torii, Kazuyuki and Kawamura, Mitsunori. (1991). "Pore structure and chloride permeability of surface layers of concrete." *Transactions of the Japanese Concrete Institute*, 13, 195-202.

Tucker, B.J., Bender, D.A., Wolcott, M.P. (1999). "Predicting flexural strength of wood-plastic composites using nondestructive evaluation." *Proceedings of the Society for Experimental Mechanics Annual Conference,* Cincinnati, OH.

Van Dam, T., Aldrich, E. (1998). "Prevention of materials-related distress in concrete pavements in cold regions." *Ninth International Conference on Cold Regions Engineering.,* Duluth, Minnesota, 489-500.

Zia, P., Leming, M.L., Ahmad, S.H., Schemmel, J.J., Elliott R.P., and Naaman A.E. (1993). "Mechanical Behavior of High Performance Concretes, Volume 1: Summary Report." *Strategic Highway Research Program, National Research Council,* Washington, D.C., XI 98, pp. SHRP-C-361.

Zhang, Min-Hong and Gjorv, Odd E. (1991). "Permeability of high-strength lightweight concrete." *ACI Materials Journal*, 88(5), 463-469.

APPENDIX A: DYNAMIC MODULUS OF ELASTICITY

A1. Mix Design A - Specimen One

Date	Cycle	Trial	Fundamental Longitudinal Frequency (Hz)	Dynamic Modulus of Elasticity (psi)	Weight (lb)	Average Length (in)	Average Cross Section b (in)	Average Cross Section t (in)	Visual Observations
5/14/00	0	1	4473	4.28E+06	15.500	16.0	4.0	3.0	
		2	4473	4.28E+06	15.500	16.0	4.0	3.0	
		3	4473	4.28E+06	15.500	16.0	4.0	3.0	
5/18/00	30	1	4448	4.26E+06	15.600	16.0	4.0	3.0	
		2	4443	4.25E+06	15.600	16.0	4.0	3.0	
		3	4448	4.26E+06	15.600	16.0	4.0	3.0	
5/23/00	60	1	4434	4.23E+06	15.600	16.0	4.0	3.0	No apparent changes
		2	4424	4.21E+06	15.600	16.0	4.0	3.0	
		3	4434	4.23E+06	15.600	16.0	4.0	3.0	
5/26/00	92	1	4438	4.24E+06	15.600	16.0	4.0	3.0	Scaling has begun on sides
		2	4429	4.22E+06	15.600	16.0	4.0	3.0	
		3	4438	4.24E+06	15.600	16.0	4.0	3.0	
6/1/00	120	1	4453	4.27E+06	15.600	16.0	4.0	3.0	Scaling has gotten worse on one side
		2	4448	4.26E+06	15.600	16.0	4.0	3.0	
		3	4429	4.22E+06	15.600	16.0	4.0	3.0	
6/12/00	155	1	4424	4.19E+06	15.500	16.0	4.0	3.0	Scaling has gotten worse on one side
		2	4365	4.08E+06	15.500	16.0	4.0	3.0	
		3	4438	4.21E+06	15.500	16.0	4.0	3.0	
6/16/00	179	1	4429	4.17E+06	15.400	16.0	4.0	3.0	Scaling has gotten worse on BOTH sides
		2	4448	4.20E+06	15.400	16.0	4.0	3.0	
		3	4434	4.18E+06	15.400	16.0	4.0	3.0	
6/23/00	212	1	4443	4.20E+06	15.400	16.0	4.0	3.0	Scaling has progressed
		2	4419	4.15E+06	15.400	16.0	4.0	3.0	
		3	4395	4.11E+06	15.400	16.0	4.0	3.0	
6/29/00	242	1	4424	4.16E+06	15.400	16.0	4.0	3.0	Scaling has progressed
		2	4424	4.16E+06	15.400	16.0	4.0	3.0	
		3	4429	4.17E+06	15.400	16.0	4.0	3.0	
7/4/00	272	1	4424	4.16E+06	15.400	16.0	4.0	3.0	Scaling has progressed
		2	4448	4.20E+06	15.400	16.0	4.0	3.0	
		3	4448	4.20E+06	15.400	16.0	4.0	3.0	
7/10/00	302	1	4424	4.13E+06	15.300	16.0	4.0	3.0	Scaling has progressed
		2	4409	4.10E+06	15.300	16.0	4.0	3.0	
		3	4414	4.11E+06	15.300	16.0	4.0	3.0	
7/14/00	322	1	4419	4.18E+06	15.499	16.0	4.0	3.0	Scaling has progressed
		2	4414	4.17E+06	15.499	16.0	4.0	3.0	
		3	4409	4.16E+06	15.499	16.0	4.0	3.0	
7/5/00	353	1	4414	4.15E+06	15.449	16.0	4.0	3.0	Scaling has progressed
		2	4424	4.17E+06	15.449	16.0	4.0	3.0	
		3	4429	4.18E+06	15.449	16.0	4.0	3.0	

A2. Mix Design A – Specimen Two

Date	Cycle	Trial	Fundamental Longitudinal Frequency (Hz)	Dynamic Modulus of Elasticity (psi)	Weight (lb)	Average Length (in)	Average Cross Section b (in)	Average Cross Section t (in)	Visual Observations
5/14/00	0	1	4478	4.37E+06	15.800	16.0	4.0	3.0	
		2	4473	4.36E+06	15.800	16.0	4.0	3.0	
		3	4473	4.36E+06	15.800	16.0	4.0	3.0	
5/18/00	30	1	4424	4.27E+06	15.800	16.0	4.0	3.0	
		2	4434	4.29E+06	15.800	16.0	4.0	3.0	
		3	4434	4.29E+06	15.800	16.0	4.0	3.0	
5/23/00	60	1	4404	4.23E+06	15.800	16.0	4.0	3.0	Large blowout.
		2	4390	4.20E+06	15.800	16.0	4.0	3.0	Scaling visible.
		3	4404	4.23E+06	15.800	16.0	4.0	3.0	
5/26/00	92	1	4380	4.18E+06	15.800	16.0	4.0	3.0	
		2	4390	4.20E+06	15.800	16.0	4.0	3.0	
		3	4370	4.16E+06	15.800	16.0	4.0	3.0	
6/1/00	120	1	4409	4.24E+06	15.800	16.0	4.0	3.0	
		2	4409	4.24E+06	15.800	16.0	4.0	3.0	
		3	4395	4.21E+06	15.800	16.0	4.0	3.0	
6/12/00	155	1	4395	4.21E+06	15.800	16.0	4.0	3.0	Scaling has
		2	4399	4.22E+06	15.800	16.0	4.0	3.0	progressed.
		3	4390	4.20E+06	15.800	16.0	4.0	3.0	
6/16/00	179	1	4404	4.20E+06	15.700	16.0	4.0	3.0	Scaling has
		2	4395	4.19E+06	15.700	16.0	4.0	3.0	progressed
		3	4385	4.17E+06	15.700	16.0	4.0	3.0	
6/23/00	212	1	4375	4.15E+06	15.700	16.0	4.0	3.0	Scaling has
		2	4390	4.18E+06	15.700	16.0	4.0	3.0	progressed
		3	4380	4.16E+06	15.700	16.0	4.0	3.0	significantly
6/29/00	242	1	4346	4.07E+06	15.600	16.0	4.0	3.0	Scaling has
		2	4336	4.05E+06	15.600	16.0	4.0	3.0	progressed
		3	4360	4.09E+06	15.600	16.0	4.0	3.0	
7/4/00	272	1	4390	4.15E+06	15.600	16.0	4.0	3.0	Scaling has
		2	4360	4.09E+06	15.600	16.0	4.0	3.0	progressed
		3	4380	4.13E+06	15.600	16.0	4.0	3.0	
7/10/00	302	1	4355	4.06E+06	15.500	16.0	4.0	3.0	Scaling has
		2	4336	4.02E+06	15.500	16.0	4.0	3.0	progressed
		3	4331	4.01E+06	15.500	16.0	4.0	3.0	
7/14/00	322	1	4341	4.08E+06	15.704	16.0	4.0	3.0	Scaling has
		2	4351	4.10E+06	15.704	16.0	4.0	3.0	progressed
		3	4341	4.08E+06	15.704	16.0	4.0	3.0	
7/5/00	353	1	4351	4.09E+06	15.656	16.0	4.0	3.0	Scaling has
		2	4351	4.09E+06	15.656	16.0	4.0	3.0	progressed
		3	4346	4.08E+06	15.656	16.0	4.0	3.0	

A3. Mix Design A - Specimen Three

Date	Cycle	Trial	Fundamental Longitudinal Frequency (Hz)	Dynamic Modulus of Elasticity (psi)	Weight (lb)	Average Length (in)	Average Cross Section b (in)	Average Cross Section t (in)	Visual Observations
5/14/00	0	1	4492	4.43E+06	15.900	16.0	4.0	3.0	
		2	4487	4.42E+06	15.900	16.0	4.0	3.0	
		3	4493	4.43E+06	15.900	16.0	4.0	3.0	
5/18/00	30	1	4453	4.38E+06	16.000	16.0	4.0	3.0	
		2	4448	4.37E+06	16.000	16.0	4.0	3.0	
		3	4448	4.37E+06	16.000	16.0	4.0	3.0	
5/23/00	60	1	4429	4.33E+06	16.000	16.0	4.0	3.0	Signs of
		2	4429	4.33E+06	16.000	16.0	4.0	3.0	scaling on
		3	4434	4.34E+06	16.000	16.0	4.0	3.0	sides.
5/26/00	92	1	4404	4.28E+06	16.000	16.0	4.0	3.0	Scaling has
		2	4404	4.28E+06	16.000	16.0	4.0	3.0	progressed
		3	4409	4.29E+06	16.000	16.0	4.0	3.0	
6/1/00	120	1	4409	4.27E+06	15.900	16.0	4.0	3.0	Scaling has
		2	4399	4.25E+06	15.900	16.0	4.0	3.0	progressed
		3	4399	4.25E+06	15.900	16.0	4.0	3.0	
6/12/00	155	1	4414	4.28E+06	15.900	16.0	4.0	3.0	Scaling has
		2	4424	4.29E+06	15.900	16.0	4.0	3.0	progressed
		3	4404	4.26E+06	15.900	16.0	4.0	3.0	
6/16/00	179	1	4404	4.23E+06	15.800	16.0	4.0	3.0	Scaling has
		2	4409	4.24E+06	15.800	16.0	4.0	3.0	progressed
		3	4385	4.19E+06	15.800	16.0	4.0	3.0	
6/23/00	212	1	4395	4.21E+06	15.800	16.0	4.0	3.0	Scaling has
		2	4390	4.20E+06	15.800	16.0	4.0	3.0	progressed
		3	4409	4.24E+06	15.800	16.0	4.0	3.0	significantly
6/29/00	242	1	4370	4.16E+06	15.800	16.0	4.0	3.0	Scaling has
		2	4390	4.20E+06	15.800	16.0	4.0	3.0	progressed
		3	4399	4.22E+06	15.800	16.0	4.0	3.0	
7/4/00	272	1	4395	4.21E+06	15.800	16.0	4.0	3.0	Scaling has
		2	4395	4.21E+06	15.800	16.0	4.0	3.0	progressed
		3	4395	4.21E+06	15.800	16.0	4.0	3.0	
7/10/00	302	1	4399	4.22E+06	15.800	16.0	4.0	3.0	Scaling has
		2	4390	4.20E+06	15.800	16.0	4.0	3.0	progressed
		3	4365	4.15E+06	15.800	16.0	4.0	3.0	
7/14/00	322	1	4360	4.18E+06	15.916	16.0	4.0	3.0	Scaling has
		2	4351	4.16E+06	15.916	16.0	4.0	3.0	progressed
		3	4351	4.16E+06	15.916	16.0	4.0	3.0	
7/5/00	353	1	4375	4.19E+06	15.860	16.0	4.0	3.0	Scaling has
		2	4370	4.18E+06	15.860	16.0	4.0	3.0	progressed
		3	4385	4.21E+06	15.860	16.0	4.0	3.0	

A4. Mix Design B - Specimen One

Date	Cycle	Trial	Fundamental Longitudinal Frequency (Hz)	Dynamic Modulus of Elasticity (psi)	Weight (lb)	Average Length (in)	Average Cross Section b (in)	Average Cross Section t (in)	Visual Observations
5/14/00	0	1	4575	4.39E+06	15.2	16.0	4.0	3.0	
		2	4570	4.38E+06	15.2	16.0	4.0	3.0	
		3	4575	4.39E+06	15.2	16.0	4.0	3.0	
5/18/00	30	1	4536	4.34E+06	15.3	16.0	4.0	3.0	
		2	4541	4.35E+06	15.3	16.0	4.0	3.0	
		3	4546	4.36E+06	15.3	16.0	4.0	3.0	
5/23/00	60	1	4546	4.36E+06	15.3	16.0	4.0	3.0	Scaling visible.
		2	4551	4.37E+06	15.3	16.0	4.0	3.0	Surface is
		3	4541	4.35E+06	15.3	16.0	4.0	3.0	gritty.
5/26/00	92	1	4536	4.34E+06	15.3	16.0	4.0	3.0	
		2	4517	4.31E+06	15.3	16.0	4.0	3.0	
		3	4526	4.33E+06	15.3	16.0	4.0	3.0	
6/1/00	120	1	4526	4.33E+06	15.3	16.0	4.0	3.0	Scaling has progressed
		2	4531	4.33E+06	15.3	16.0	4.0	3.0	
		3	4517	4.31E+06	15.3	16.0	4.0	3.0	
6/12/00	155	1	4530	4.33E+06	15.3	16.0	4.0	3.0	
		2	4536	4.34E+06	15.3	16.0	4.0	3.0	
		3	4521	4.32E+06	15.3	16.0	4.0	3.0	
6/16/00	179	1	4556	4.38E+06	15.3	16.0	4.0	3.0	Scaling has progressed
		2	4526	4.33E+06	15.3	16.0	4.0	3.0	
		3	4546	4.36E+06	15.3	16.0	4.0	3.0	
6/23/00	212	1	4541	4.33E+06	15.2	16.0	4.0	3.0	Scaling has progressed
		2	4536	4.32E+06	15.2	16.0	4.0	3.0	
		3	4507	4.26E+06	15.2	16.0	4.0	3.0	
6/29/00	242	1	4365	4.00E+06	15.2	16.0	4.0	3.0	Scaling has progressed
		2	4497	4.24E+06	15.2	16.0	4.0	3.0	
		3	4497	4.24E+06	15.2	16.0	4.0	3.0	
7/4/00	272	1	4521	4.29E+06	15.2	16.0	4.0	3.0	Scaling has progressed
		2	4521	4.29E+06	15.2	16.0	4.0	3.0	
		3	4526	4.30E+06	15.2	16.0	4.0	3.0	
7/10/00 p	302	1	4512	4.27E+06	15.2	16.0	4.0	3.0	Scaling has progressed
		2	4502	4.25E+06	15.2	16.0	4.0	3.0	
		3	4502	4.25E+06	15.2	16.0	4.0	3.0	
7/14/00	322	1	4370	4.06E+06	15.4	16.0	4.0	3.0	
		2	4478	4.27E+06	15.4	16.0	4.0	3.0	No changes
		3	4497	4.30E+06	15.4	16.0	4.0	3.0	
7/5/00	353	1	4473	4.25E+06	15.393	16.0	4.0	3.0	
		2	4492	4.29E+06	15.393	16.0	4.0	3.0	No changes
		3	4487	4.28E+06	15.393	16.0	4.0	3.0	

A5. Mix Design B - Specimen Two

Date	Cycle	Trial	Fundamental Longitudinal Frequency (Hz)	Dynamic Modulus of Elasticity (psi)	Weight (lb)	Average Length (in)	Average Cross Section b (in)	Average Cross Section t (in)	Visual Observations
5/14/00	0	1	4565	4.40E+06	15.300	16.0	4.0	3.0	
		2	4556	4.38E+06	15.300	16.0	4.0	3.0	
		3	4565	4.40E+06	15.300	16.0	4.0	3.0	
5/18/00	30	1	4536	4.34E+06	15.300	16.0	4.0	3.0	
		2	4536	4.34E+06	15.300	16.0	4.0	3.0	
		3	4536	4.34E+06	15.300	16.0	4.0	3.0	
5/23/00	60	1	4531	4.33E+06	15.300	16.0	4.0	3.0	Scaling visible
		2	4536	4.34E+06	15.300	16.0	4.0	3.0	Surface is
		3	4531	4.33E+06	15.300	16.0	4.0	3.0	gritty.
5/26/00	92	1	4536	4.34E+06	15.300	16.0	4.0	3.0	
		2	4551	4.37E+06	15.300	16.0	4.0	3.0	
		3	4536	4.34E+06	15.300	16.0	4.0	3.0	
6/1/00	120	1	4507	4.26E+06	15.200	16.0	4.0	3.0	Scaling has
		2	4521	4.29E+06	15.200	16.0	4.0	3.0	progressed greatly. Grains
		3	4517	4.28E+06	15.200	16.0	4.0	3.0	visible.
6/12/00	155	1	4535	4.32E+06	15.200	16.0	4.0	3.0	
		2	4531	4.31E+06	15.200	16.0	4.0	3.0	
		3	4541	4.33E+06	15.200	16.0	4.0	3.0	
6/16/00	179	1	4502	4.25E+06	15.200	16.0	4.0	3.0	Scaling has
		2	4536	4.32E+06	15.200	16.0	4.0	3.0	progressed
		3	4551	4.34E+06	15.200	16.0	4.0	3.0	greatly.
6/23/00	212	1	4395	4.05E+06	15.200	16.0	4.0	3.0	Scaling has
		2	4404	4.07E+06	15.200	16.0	4.0	3.0	progressed
		3	4541	4.33E+06	15.200	16.0	4.0	3.0	
6/29/00	242	1	4497	4.24E+06	15.200	16.0	4.0	3.0	Scaling has
		2	4497	4.24E+06	15.200	16.0	4.0	3.0	progressed
		3	4512	4.27E+06	15.200	16.0	4.0	3.0	
7/4/00	272	1	4531	4.31E+06	15.200	16.0	4.0	3.0	Scaling has
		2	4507	4.26E+06	15.200	16.0	4.0	3.0	progressed
		3	4521	4.29E+06	15.200	16.0	4.0	3.0	
7/10/00	302	1	4521	4.26E+06	15.100	16.0	4.0	3.0	Scaling has
		2	4531	4.28E+06	15.100	16.0	4.0	3.0	progressed
		3	4526	4.27E+06	15.100	16.0	4.0	3.0	
7/14/00	322	1	4512	4.31E+06	15.338	16.0	4.0	3.0	Scaling has
		2	4502	4.29E+06	15.338	16.0	4.0	3.0	progressed
		3	4512	4.31E+06	15.338	16.0	4.0	3.0	
7/5/00	353	1	4487	4.25E+06	15.302	16.0	4.0	3.0	
		2	4512	4.30E+06	15.302	16.0	4.0	3.0	No changes
		3	4492	4.26E+06	15.302	16.0	4.0	3.0	

A6. Mix Design B - Specimen Three

Date	Cycle	Trial	Fundamental Longitudinal Frequency (Hz)	Dynamic Modulus of Elasticity (psi)	Weight (lb)	Average Length (in)	Average Cross Section b (in)	Average Cross Section t (in)	Visual Observations
5/23/00	60	1	4697	4.75E+06	15.600	16.0	4.0	3.0	Scaling visible
		2	4683	4.72E+06	15.600	16.0	4.0	3.0	Surface is gritty.
		3	4688	4.73E+06	15.600	16.0	4.0	3.0	
5/26/00	92	1	4692	4.74E+06	15.600	16.0	4.0	3.0	Scaling has
		2	4688	4.73E+06	15.600	16.0	4.0	3.0	progressed.
		3	4688	4.73E+06	15.600	16.0	4.0	3.0	
6/1/00	120	1	4658	4.64E+06	15.500	16.0	4.0	3.0	Scaling has
		2	4668	4.66E+06	15.500	16.0	4.0	3.0	progressed.
		3	4673	4.67E+06	15.500	16.0	4.0	3.0	
6/12/00	155	1	4644	4.61E+06	15.500	16.0	4.0	3.0	Scaling has
		2	4521	4.37E+06	15.500	16.0	4.0	3.0	progressed.
		3	4722	4.77E+06	15.500	16.0	4.0	3.0	
6/16/00	179	1	4453	4.24E+06	15.500	16.0	4.0	3.0	Scaling has
		2	4468	4.27E+06	15.500	16.0	4.0	3.0	progressed.
		3	4482	4.30E+06	15.500	16.0	4.0	3.0	
6/23/00	212	1	4521	4.37E+06	15.500	16.0	4.0	3.0	Scaling has
		2	4658	4.64E+06	15.500	16.0	4.0	3.0	progressed.
		3	4502	4.34E+06	15.500	16.0	4.0	3.0	
6/29/00	242	1	4682	4.69E+06	15.500	16.0	4.0	3.0	No changes
		2	4668	4.66E+06	15.500	16.0	4.0	3.0	
		3	4668	4.66E+06	15.500	16.0	4.0	3.0	
7/4/00	272	1	4521	4.37E+06	15.500	16.0	4.0	3.0	No changes
		2	4614	4.55E+06	15.500	16.0	4.0	3.0	
		3	4653	4.63E+06	15.500	16.0	4.0	3.0	
7/10/00	302	1	4521	4.37E+06	15.500	16.0	4.0	3.0	Scaling has
		2	4648	4.62E+06	15.500	16.0	4.0	3.0	progressed.
		3	4653	4.63E+06	15.500	16.0	4.0	3.0	
7/14/00	322	1	4448	4.27E+06	15.652	16.0	4.0	3.0	No changes
		2	4434	4.25E+06	15.652	16.0	4.0	3.0	
		3	4390	4.16E+06	15.652	16.0	4.0	3.0	
7/5/00	353	1	4648	4.66E+06	15.617	16.0	4.0	3.0	No changes
		2	4531	4.42E+06	15.617	16.0	4.0	3.0	
		3	4487	4.34E+06	15.617	16.0	4.0	3.0	

A7. Mix Design C - Specimen One

Date	Cycle	Trial	Fundamental Longitudinal Frequency (Hz)	Dynamic Modulus of Elasticity (psi)	Weight (lb)	Average Length (in)	Average Cross Section b (in)	Average Cross Section t (in)	Visual Observations
5/14/00	0	1	5049	5.80E+06	16.500	16.0	4.0	3.0	
		2	5044	5.79E+06	16.500	16.0	4.0	3.0	
		3	5059	5.83E+06	16.500	16.0	4.0	3.0	
5/18/00	30	1	4971	5.66E+06	16.600	16.0	4.0	3.0	
		2	4971	5.66E+06	16.600	16.0	4.0	3.0	
		3	4966	5.65E+06	16.600	16.0	4.0	3.0	
5/23/00	60	1	4980	5.65E+06	16.500	16.0	4.0	3.0	
		2	4990	5.67E+06	16.500	16.0	4.0	3.0	
		3	4980	5.65E+06	16.500	16.0	4.0	3.0	
5/26/00	92	1	4976	5.67E+06	16.600	16.0	4.0	3.0	
		2	4951	5.62E+06	16.600	16.0	4.0	3.0	
		3	4966	5.65E+06	16.600	16.0	4.0	3.0	
6/1/00	120	1	4888	5.44E+06	16.500	16.0	4.0	3.0	
		2	4951	5.58E+06	16.500	16.0	4.0	3.0	No changes
		3	4966	5.62E+06	16.500	16.0	4.0	3.0	
6/12/00	155	1	4976	5.64E+06	16.500	16.0	4.0	3.0	End is scaling due to tapping
		2	5000	5.69E+06	16.500	16.0	4.0	3.0	
		3	4976	5.64E+06	16.500	16.0	4.0	3.0	
6/16/00	179	1	5000	5.69E+06	16.500	16.0	4.0	3.0	
		2	4976	5.64E+06	16.500	16.0	4.0	3.0	No changes
		3	4980	5.65E+06	16.500	16.0	4.0	3.0	
6/23/00	212	1	5044	5.79E+06	16.500	16.0	4.0	3.0	Light scaling visible
		2	4985	5.66E+06	16.500	16.0	4.0	3.0	
		3	4980	5.65E+06	16.500	16.0	4.0	3.0	
6/29/00	242	1	4980	5.65E+06	16.500	16.0	4.0	3.0	
		2	4990	5.67E+06	16.500	16.0	4.0	3.0	No changes
		3	4980	5.65E+06	16.500	16.0	4.0	3.0	
7/4/00	272	1	4941	5.56E+06	16.500	16.0	4.0	3.0	
		2	4961	5.60E+06	16.500	16.0	4.0	3.0	No changes
		3	4937	5.55E+06	16.500	16.0	4.0	3.0	
7/10/00	302	1	4980	5.65E+06	16.500	16.0	4.0	3.0	
		2	5024	5.75E+06	16.500	16.0	4.0	3.0	No changes
		3	4976	5.64E+06	16.500	16.0	4.0	3.0	
7/14/00	322	1	4951	5.65E+06	16.709	16.0	4.0	3.0	
		2	4956	5.66E+06	16.709	16.0	4.0	3.0	No changes
		3	4961	5.68E+06	16.709	16.0	4.0	3.0	
7/5/00	353	1	4966	5.68E+06	16.696	16.0	4.0	3.0	
		2	4971	5.69E+06	16.696	16.0	4.0	3.0	No changes
		3	4976	5.70E+06	16.696	16.0	4.0	3.0	

A8. Mix Design C - Specimen Two

Date	Cycle	Trial	Fundamental Longitudinal Frequency (Hz)	Dynamic Modulus of Elasticity (psi)	Weight (lb)	Average Length (in)	Average Cross Section b (in)	Average Cross Section t (in)	Visual Observations
5/14/00	0	1	5073	5.79E+06	16.300	16.0	4.0	3.0	
		2	5034	5.70E+06	16.300	16.0	4.0	3.0	No changes
		3	5049	5.73E+06	16.300	16.0	4.0	3.0	
5/18/00	30	1	4946	5.50E+06	16.300	16.0	4.0	3.0	
		2	4956	5.52E+06	16.300	16.0	4.0	3.0	No changes
		3	4956	5.52E+06	16.300	16.0	4.0	3.0	
5/23/00	60	1	4985	5.59E+06	16.300	16.0	4.0	3.0	
		2	4985	5.59E+06	16.300	16.0	4.0	3.0	No changes
		3	4990	5.60E+06	16.300	16.0	4.0	3.0	
5/26/00	92	1	4961	5.54E+06	16.300	16.0	4.0	3.0	
		2	4956	5.52E+06	16.300	16.0	4.0	3.0	No changes
		3	4951	5.51E+06	16.300	16.0	4.0	3.0	
6/1/00	120	1	4956	5.49E+06	16.200	16.0	4.0	3.0	Light scaling visible
		2	4966	5.51E+06	16.200	16.0	4.0	3.0	
		3	4946	5.47E+06	16.200	16.0	4.0	3.0	
6/12/00	155	1	4985	5.56E+06	16.200	16.0	4.0	3.0	
		2	5000	5.59E+06	16.200	16.0	4.0	3.0	No changes
		3	5000	5.59E+06	16.200	16.0	4.0	3.0	
6/16/00	179	1	5000	5.59E+06	16.200	16.0	4.0	3.0	
		2	5000	5.59E+06	16.200	16.0	4.0	3.0	No changes
		3	5000	5.59E+06	16.200	16.0	4.0	3.0	
6/23/00	212	1	5044	5.69E+06	16.200	16.0	4.0	3.0	Scaling has progressed
		2	4990	5.57E+06	16.200	16.0	4.0	3.0	
		3	4971	5.52E+06	16.200	16.0	4.0	3.0	
6/29/00	242	1	5020	5.63E+06	16.200	16.0	4.0	3.0	
		2	4980	5.54E+06	16.200	16.0	4.0	3.0	No changes
		3	4990	5.57E+06	16.200	16.0	4.0	3.0	
7/4/00	272	1	4966	5.51E+06	16.200	16.0	4.0	3.0	
		2	4976	5.54E+06	16.200	16.0	4.0	3.0	No changes
		3	4980	5.54E+06	16.200	16.0	4.0	3.0	
7/10/00	302	1	4985	5.56E+06	16.200	16.0	4.0	3.0	Corner has popped off
		2	4990	5.57E+06	16.200	16.0	4.0	3.0	
		3	4990	5.57E+06	16.200	16.0	4.0	3.0	
7/14/00	322	1	4985	5.65E+06	16.462	16.0	4.0	3.0	Scaling has progressed
		2	4980	5.63E+06	16.462	16.0	4.0	3.0	
		3	4976	5.62E+06	16.462	16.0	4.0	3.0	
7/5/00	353	1	4966	5.60E+06	16.452	16.0	4.0	3.0	
		2	4966	5.60E+06	16.452	16.0	4.0	3.0	No changes
		3	4961	5.59E+06	16.452	16.0	4.0	3.0	

A9. Mix Design C - Specimen Three

Date	Cycle	Trial	Fundamental Longitudinal Frequency (Hz)	Dynamic Modulus of Elasticity (psi)	Weight (lb)	Average Length (in)	Average Cross Section b (in)	Average Cross Section t (in)	Visual Observations
5/14/00	0	1	5034	5.70E+06	16.300	16.0	4.0	3.0	
		2	5029	5.69E+06	16.300	16.0	4.0	3.0	
		3	5034	5.70E+06	16.300	16.0	4.0	3.0	
5/18/00	30	1	4922	5.48E+06	16.400	16.0	4.0	3.0	
		2	4912	5.46E+06	16.400	16.0	4.0	3.0	
		3	4907	5.45E+06	16.400	16.0	4.0	3.0	
5/23/00	60	1	4927	5.49E+06	16.400	16.0	4.0	3.0	
		2	4922	5.48E+06	16.400	16.0	4.0	3.0	
		3	4932	5.51E+06	16.400	16.0	4.0	3.0	
5/26/00	92	1	4902	5.44E+06	16.400	16.0	4.0	3.0	
		2	4912	5.46E+06	16.400	16.0	4.0	3.0	
		3	4907	5.45E+06	16.400	16.0	4.0	3.0	
6/1/00	120	1	4917	5.44E+06	16.300	16.0	4.0	3.0	Light scaling
		2	4907	5.42E+06	16.300	16.0	4.0	3.0	visible on one
		3	4897	5.39E+06	16.300	16.0	4.0	3.0	side and ends
6/12/00	155	1	4971	5.56E+06	16.300	16.0	4.0	3.0	No change
		2	4956	5.52E+06	16.300	16.0	4.0	3.0	
		3	4961	5.54E+06	16.300	16.0	4.0	3.0	
6/16/00	179	1	4971	5.56E+06	16.300	16.0	4.0	3.0	No change
		2	4966	5.55E+06	16.300	16.0	4.0	3.0	
		3	5005	5.63E+06	16.300	16.0	4.0	3.0	
6/23/00	212	1	4985	5.59E+06	16.300	16.0	4.0	3.0	Scaling has
		2	4961	5.54E+06	16.300	16.0	4.0	3.0	progressed
		3	4976	5.57E+06	16.300	16.0	4.0	3.0	
6/29/00	242	1	4961	5.54E+06	16.300	16.0	4.0	3.0	No change
		2	4990	5.60E+06	16.300	16.0	4.0	3.0	
		3	5000	5.62E+06	16.300	16.0	4.0	3.0	
7/4/00	272	1	4966	5.55E+06	16.300	16.0	4.0	3.0	No change
		2	4878	5.35E+06	16.300	16.0	4.0	3.0	
		3	4912	5.43E+06	16.300	16.0	4.0	3.0	
7/10/00	302	1	4966	5.55E+06	16.300	16.0	4.0	3.0	Corner has
		2	4961	5.54E+06	16.300	16.0	4.0	3.0	popped off
		3	4966	5.55E+06	16.300	16.0	4.0	3.0	(small)
7/14/00	322	1	4932	5.54E+06	16.515	16.0	4.0	3.0	No change
		2	4946	5.58E+06	16.515	16.0	4.0	3.0	
		3	4941	5.56E+06	16.515	16.0	4.0	3.0	
7/5/00	353	1	4966	5.62E+06	16.510	16.0	4.0	3.0	No change
		2	4961	5.61E+06	16.510	16.0	4.0	3.0	
		3	4961	5.61E+06	16.510	16.0	4.0	3.0	

A10. Mix Design D - Specimen One

Date	Cycle	Trial	Fundamental Longitudinal Frequency (Hz)	Dynamic Modulus of Elasticity (psi)	Weight (lb)	Average Length (in)	Average Cross Section b (in)	Average Cross Section t (in)	Visual Observations
5/14/00	0	1	4795	5.04E+06	15.900	16.0	4.0	3.0	
		2	4800	5.06E+06	15.900	16.0	4.0	3.0	
		3	4795	5.04E+06	15.900	16.0	4.0	3.0	
5/18/00	30	1	4717	4.88E+06	15.900	16.0	4.0	3.0	
		2	4707	4.86E+06	15.900	16.0	4.0	3.0	
		3	4717	4.88E+06	15.900	16.0	4.0	3.0	
5/23/00	60	1	4688	4.82E+06	15.900	16.0	4.0	3.0	
		2	4688	4.82E+06	15.900	16.0	4.0	3.0	
		3	4658	4.76E+06	15.900	16.0	4.0	3.0	
5/26/00	92	1	4658	4.76E+06	15.900	16.0	4.0	3.0	
		2	4658	4.76E+06	15.900	16.0	4.0	3.0	Scaling visible
		3	4653	4.75E+06	15.900	16.0	4.0	3.0	
6/1/00	120	1	4624	4.69E+06	15.900	16.0	4.0	3.0	
		2	4614	4.67E+06	15.900	16.0	4.0	3.0	No changes
		3	4614	4.67E+06	15.900	16.0	4.0	3.0	
6/12/00	155	1	4512	4.47E+06	15.900	16.0	4.0	3.0	
		2	4600	4.64E+06	15.900	16.0	4.0	3.0	No changes
		3	4419	4.28E+06	15.900	16.0	4.0	3.0	
6/16/00	179	1	4385	4.22E+06	15.900	16.0	4.0	3.0	
		2	4468	4.38E+06	15.900	16.0	4.0	3.0	No changes
		3	4478	4.40E+06	15.900	16.0	4.0	3.0	
6/23/00	212	1	4414	4.28E+06	15.900	16.0	4.0	3.0	
		2	4404	4.26E+06	15.900	16.0	4.0	3.0	Scaling has progressed
		3	4424	4.29E+06	15.900	16.0	4.0	3.0	
6/29/00	242	1	4341	4.13E+06	15.900	16.0	4.0	3.0	
		2	4336	4.13E+06	15.900	16.0	4.0	3.0	No changes
		3	4326	4.11E+06	15.900	16.0	4.0	3.0	
7/4/00	272	1	4375	4.20E+06	15.900	16.0	4.0	3.0	
		2	4375	4.20E+06	15.900	16.0	4.0	3.0	No changes
		3	4092	3.67E+06	15.900	16.0	4.0	3.0	
7/10/00	302	1	4370	4.16E+06	15.800	16.0	4.0	3.0	
		2	4302	4.04E+06	15.800	16.0	4.0	3.0	Scaling has progressed
		3	4326	4.08E+06	15.800	16.0	4.0	3.0	
7/14/00	322	1	4316	4.12E+06	16.011	16.0	4.0	3.0	
		2	4272	4.03E+06	16.011	16.0	4.0	3.0	Scaling has progressed
		3	4331	4.14E+06	16.011	16.0	4.0	3.0	
7/5/00	353	1	4277	4.04E+06	15.995	16.0	4.0	3.0	
		2	4326	4.13E+06	15.995	16.0	4.0	3.0	No changes
		3	4346	4.17E+06	15.995	16.0	4.0	3.0	

A11. Mix Design D - Specimen Two

Date	Cycle	Trial	Fundamental Longitudinal Frequency (Hz)	Dynamic Modulus of Elasticity (psi)	Weight (lb)	Average Length (in)	Average Cross Section b (in)	Average Cross Section t (in)	Visual Observations
5/14/00	0	1	4771	4.93E+06	15.700	16.0	4.0	3.0	
		2	4771	4.93E+06	15.700	16.0	4.0	3.0	
		3	4771	4.93E+06	15.700	16.0	4.0	3.0	
5/18/00	30	1	4727	4.84E+06	15.700	16.0	4.0	3.0	
		2	4727	4.84E+06	15.700	16.0	4.0	3.0	
		3	4736	4.86E+06	15.700	16.0	4.0	3.0	
5/23/00	60	1	4702	4.79E+06	15.700	16.0	4.0	3.0	
		2	4712	4.81E+06	15.700	16.0	4.0	3.0	
		3	4701	4.79E+06	15.700	16.0	4.0	3.0	
5/26/00	92	1	4688	4.76E+06	15.700	16.0	4.0	3.0	Scaling visible
		2	4673	4.73E+06	15.700	16.0	4.0	3.0	
		3	4678	4.74E+06	15.700	16.0	4.0	3.0	
6/1/00	120	1	4658	4.70E+06	15.700	16.0	4.0	3.0	No changes
		2	4653	4.69E+06	15.700	16.0	4.0	3.0	
		3	4658	4.70E+06	15.700	16.0	4.0	3.0	
6/12/00	155	1	4644	4.67E+06	15.700	16.0	4.0	3.0	No changes
		2	4482	4.35E+06	15.700	16.0	4.0	3.0	
		3	4561	4.51E+06	15.700	16.0	4.0	3.0	
6/16/00	179	1	4502	4.39E+06	15.700	16.0	4.0	3.0	Scaling visible
		2	4468	4.33E+06	15.700	16.0	4.0	3.0	
		3	4536	4.46E+06	15.700	16.0	4.0	3.0	
6/23/00	212	1	4448	4.29E+06	15.700	16.0	4.0	3.0	No Changes
		2	4497	4.38E+06	15.700	16.0	4.0	3.0	
		3	4482	4.35E+06	15.700	16.0	4.0	3.0	
6/29/00	242	1	4473	4.33E+06	15.700	16.0	4.0	3.0	No Changes
		2	4414	4.22E+06	15.700	16.0	4.0	3.0	
		3	4419	4.23E+06	15.700	16.0	4.0	3.0	
7/4/00	272	1	4507	4.40E+06	15.700	16.0	4.0	3.0	No Changes
		2	4546	4.48E+06	15.700	16.0	4.0	3.0	
		3	4536	4.46E+06	15.700	16.0	4.0	3.0	
7/10/00	302	1	4521	4.40E+06	15.600	16.0	4.0	3.0	No Changes
		2	4502	4.36E+06	15.600	16.0	4.0	3.0	
		3	4551	4.46E+06	15.600	16.0	4.0	3.0	
7/14/00	322	1	4502	4.42E+06	15.810	16.0	4.0	3.0	Scaling has
		2	4414	4.25E+06	15.810	16.0	4.0	3.0	progressed
		3	4399	4.22E+06	15.810	16.0	4.0	3.0	
7/5/00	353	1	4487	4.38E+06	15.782	16.0	4.0	3.0	No Changes
		2	4482	4.38E+06	15.782	16.0	4.0	3.0	
		3	4492	4.39E+06	15.782	16.0	4.0	3.0	

A12. Mix Design D - Specimen Three

Date	Cycle	Trial	Fundamental Longitudinal Frequency (Hz)	Dynamic Modulus of Elasticity (psi)	Weight (lb)	Average Length (in)	Average Cross Section b (in)	Average Cross Section t (in)	Visual Observations
5/14/00	0	1	4741	4.84E+06	15.600	16.0	4.0	3.0	
		2	4741	4.84E+06	15.600	16.0	4.0	3.0	
		3	4741	4.84E+06	15.600	16.0	4.0	3.0	
5/18/00	30	1	4697	4.78E+06	15.700	16.0	4.0	3.0	
		2	4697	4.78E+06	15.700	16.0	4.0	3.0	
		3	4697	4.78E+06	15.700	16.0	4.0	3.0	
5/23/00	60	1	4682	4.75E+06	15.700	16.0	4.0	3.0	
		2	4678	4.74E+06	15.700	16.0	4.0	3.0	
		3	4663	4.71E+06	15.700	16.0	4.0	3.0	
5/26/00	92	1	4658	4.70E+06	15.700	16.0	4.0	3.0	Scaling visible
		2	4658	4.70E+06	15.700	16.0	4.0	3.0	
		3	4658	4.70E+06	15.700	16.0	4.0	3.0	
6/1/00	120	1	4653	4.66E+06	15.600	16.0	4.0	3.0	No changes
		2	4648	4.65E+06	15.600	16.0	4.0	3.0	
		3	4648	4.65E+06	15.600	16.0	4.0	3.0	
6/12/00	155	1	4512	4.38E+06	15.600	16.0	4.0	3.0	No changes
		2	4512	4.38E+06	15.600	16.0	4.0	3.0	
		3	4512	4.38E+06	15.600	16.0	4.0	3.0	
6/16/00	179	1	4541	4.44E+06	15.600	16.0	4.0	3.0	Scaling visible
		2	4434	4.23E+06	15.600	16.0	4.0	3.0	
		3	4448	4.26E+06	15.600	16.0	4.0	3.0	
6/23/00	212	1	4419	4.20E+06	15.600	16.0	4.0	3.0	Scaling has
		2	4419	4.20E+06	15.600	16.0	4.0	3.0	progressed
		3	4526	4.41E+06	15.600	16.0	4.0	3.0	
6/29/00	242	1	4526	4.41E+06	15.600	16.0	4.0	3.0	Scaling has
		2	4365	4.10E+06	15.600	16.0	4.0	3.0	progressed
		3	4526	4.41E+06	15.600	16.0	4.0	3.0	
7/4/00	272	1	4907	5.18E+06	15.600	16.0	4.0	3.0	Scaling has
		2	4595	4.55E+06	15.600	16.0	4.0	3.0	progressed
		3	4541	4.44E+06	15.600	16.0	4.0	3.0	
7/10/00	302	1	4517	4.39E+06	15.600	16.0	4.0	3.0	No changes
		2	4517	4.39E+06	15.600	16.0	4.0	3.0	
		3	4517	4.39E+06	15.600	16.0	4.0	3.0	
7/14/00	322	1	4336	4.10E+06	15.793	16.0	4.0	3.0	Scaling has
		2	4326	4.08E+06	15.793	16.0	4.0	3.0	progressed
		3	4321	4.07E+06	15.793	16.0	4.0	3.0	slightly
7/5/00	353	1	4463	4.34E+06	15.773	16.0	4.0	3.0	No changes
		2	4502	4.41E+06	15.773	16.0	4.0	3.0	
		3	4390	4.19E+06	15.773	16.0	4.0	3.0	

A13. Mix Design E - Specimen One

Date	Cycle	Trial	Fundamental Longitudinal Frequency (Hz)	Dynamic Modulus of Elasticity (psi)	Weight (lb)	Average Length (in)	Average Cross Section b (in)	Average Cross Section t (in)	Visual Observations
5/14/00	0	1	5308	6.53E+06	16.800	16.0	4.0	3.0	
		2	5303	6.52E+06	16.800	16.0	4.0	3.0	No changes
		3	5298	6.51E+06	16.800	16.0	4.0	3.0	
5/18/00	30	1	5283	6.47E+06	16.800	16.0	4.0	3.0	
		2	5278	6.46E+06	16.800	16.0	4.0	3.0	No changes
		3	5288	6.48E+06	16.800	16.0	4.0	3.0	
5/23/00	60	1	5264	6.42E+06	16.800	16.0	4.0	3.0	
		2	5259	6.41E+06	16.800	16.0	4.0	3.0	No changes
		3	5239	6.36E+06	16.800	16.0	4.0	3.0	
5/26/00	92	1	5254	6.40E+06	16.800	16.0	4.0	3.0	
		2	5254	6.40E+06	16.800	16.0	4.0	3.0	No changes
		3	5244	6.38E+06	16.800	16.0	4.0	3.0	
6/1/00	120	1	5239	6.36E+06	16.800	16.0	4.0	3.0	
		2	5239	6.36E+06	16.800	16.0	4.0	3.0	No changes
		3	5239	6.36E+06	16.800	16.0	4.0	3.0	
6/12/00	155	1	5063	5.94E+06	16.800	16.0	4.0	3.0	
		2	5063	5.94E+06	16.800	16.0	4.0	3.0	No changes
		3	5068	5.95E+06	16.800	16.0	4.0	3.0	
6/16/00	179	1	5264	6.42E+06	16.800	16.0	4.0	3.0	
		2	5254	6.40E+06	16.800	16.0	4.0	3.0	No changes
		3	5249	6.39E+06	16.800	16.0	4.0	3.0	
6/23/00	212	1	5225	6.33E+06	16.800	16.0	4.0	3.0	
		2	5103	6.04E+06	16.800	16.0	4.0	3.0	No changes
		3	5146	6.14E+06	16.800	16.0	4.0	3.0	
6/29/00	242	1	5225	6.33E+06	16.800	16.0	4.0	3.0	
		2	5264	6.42E+06	16.800	16.0	4.0	3.0	No changes
		3	5259	6.41E+06	16.800	16.0	4.0	3.0	
7/4/00	272	1	5254	6.40E+06	16.800	16.0	4.0	3.0	
		2	5249	6.39E+06	16.800	16.0	4.0	3.0	No changes
		3	5278	6.46E+06	16.800	16.0	4.0	3.0	
7/10/00	302	1	5195	6.26E+06	16.800	16.0	4.0	3.0	
		2	5044	5.90E+06	16.800	16.0	4.0	3.0	Corner popped off (small)
		3	5234	6.35E+06	16.800	16.0	4.0	3.0	
7/14/00	322	1	5176	6.27E+06	16.953	16.0	4.0	3.0	
		2	5244	6.43E+06	16.953	16.0	4.0	3.0	No changes
		3	5039	5.94E+06	16.953	16.0	4.0	3.0	
7/5/00	353	1	5215	6.36E+06	16.936	16.0	4.0	3.0	
		2	5244	6.43E+06	16.936	16.0	4.0	3.0	No changes
		3	5234	6.40E+06	16.936	16.0	4.0	3.0	

A14. Mix Design E - Specimen Two

Date	Cycle	Trial	Fundamental Longitudinal Frequency (Hz)	Dynamic Modulus of Elasticity (psi)	Weight (lb)	Average Length (in)	Average Cross Section b (in)	Average Cross Section t (in)	Visual Observations
5/14/00	0	1	5322	6.57E+06	16.800	16.0	4.0	3.0	
		2	5317	6.55E+06	16.800	16.0	4.0	3.0	
		3	5322	6.57E+06	16.800	16.0	4.0	3.0	
5/18/00	30	1	5283	6.47E+06	16.800	16.0	4.0	3.0	
		2	5288	6.48E+06	16.800	16.0	4.0	3.0	
		3	5288	6.48E+06	16.800	16.0	4.0	3.0	
5/23/00	60	1	5293	6.50E+06	16.800	16.0	4.0	3.0	
		2	5293	6.50E+06	16.800	16.0	4.0	3.0	
		3	5278	6.46E+06	16.800	16.0	4.0	3.0	
5/26/00	92	1	5278	6.46E+06	16.800	16.0	4.0	3.0	
		2	5278	6.46E+06	16.800	16.0	4.0	3.0	
		3	5273	6.45E+06	16.800	16.0	4.0	3.0	
6/1/00	120	1	5273	6.45E+06	16.800	16.0	4.0	3.0	
		2	5273	6.45E+06	16.800	16.0	4.0	3.0	No changes
		3	5278	6.46E+06	16.800	16.0	4.0	3.0	
6/12/00	155	1	5259	6.41E+06	16.800	16.0	4.0	3.0	Corners have started to wear
		2	5264	6.42E+06	16.800	16.0	4.0	3.0	
		3	5190	6.24E+06	16.800	16.0	4.0	3.0	
6/16/00	179	1	5269	6.44E+06	16.800	16.0	4.0	3.0	Minimal scaling on one side
		2	5249	6.39E+06	16.800	16.0	4.0	3.0	
		3	5264	6.42E+06	16.800	16.0	4.0	3.0	
6/23/00	212	1	5142	6.13E+06	16.800	16.0	4.0	3.0	Scaling has progressed slightly
		2	5254	6.40E+06	16.800	16.0	4.0	3.0	
		3	5117	6.07E+06	16.800	16.0	4.0	3.0	
6/29/00	242	1	5264	6.42E+06	16.800	16.0	4.0	3.0	Scaling has progressed slightly
		2	5273	6.45E+06	16.800	16.0	4.0	3.0	
		3	5278	6.46E+06	16.800	16.0	4.0	3.0	
7/4/00	272	1	5239	6.36E+06	16.800	16.0	4.0	3.0	Scaling has progressed slightly
		2	5122	6.08E+06	16.800	16.0	4.0	3.0	
		3	5269	6.44E+06	16.800	16.0	4.0	3.0	
7/10/00	302	1	5103	6.00E+06	16.700	16.0	4.0	3.0	Scaling has progressed slightly
		2	5068	5.92E+06	16.700	16.0	4.0	3.0	
		3	5229	6.30E+06	16.700	16.0	4.0	3.0	
7/14/00	322	1	5044	5.92E+06	16.867	16.0	4.0	3.0	No changes
		2	5225	6.35E+06	16.867	16.0	4.0	3.0	
		3	5244	6.40E+06	16.867	16.0	4.0	3.0	
7/5/00	353	1	5195	6.27E+06	16.848	16.0	4.0	3.0	No changes
		2	5215	6.32E+06	16.848	16.0	4.0	3.0	
		3	5229	6.36E+06	16.848	16.0	4.0	3.0	

A15. Mix Design E - Specimen Three

Date	Cycle	Trial	Fundamental Longitudinal Frequency (Hz)	Dynamic Modulus of Elasticity (psi)	Weight (lb)	Average Length (in)	Average Cross Section b (in)	Average Cross Section t (in)	Visual Observations
5/14/00	0	1	5454	6.98E+06	17.000	16.0	4.0	3.0	No changes
		2	5454	6.98E+06	17.000	16.0	4.0	3.0	
		3	5459	6.99E+06	17.000	16.0	4.0	3.0	
5/18/00	30	1	5439	6.94E+06	17.000	16.0	4.0	3.0	No changes
		2	5434	6.93E+06	17.000	16.0	4.0	3.0	
		3	5430	6.92E+06	17.000	16.0	4.0	3.0	
5/23/00	60	1	5425	6.90E+06	17.000	16.0	4.0	3.0	No changes
		2	5430	6.92E+06	17.000	16.0	4.0	3.0	
		3	5425	6.90E+06	17.000	16.0	4.0	3.0	
5/26/00	92	1	5420	6.89E+06	17.000	16.0	4.0	3.0	No changes
		2	5405	6.85E+06	17.000	16.0	4.0	3.0	
		3	5405	6.85E+06	17.000	16.0	4.0	3.0	
6/1/00	120	1	5410	6.87E+06	17.000	16.0	4.0	3.0	No changes
		2	5405	6.85E+06	17.000	16.0	4.0	3.0	
		3	5400	6.84E+06	17.000	16.0	4.0	3.0	
6/12/00	155	1	5156	6.24E+06	17.000	16.0	4.0	3.0	One corner has popout
		2	5381	6.79E+06	17.000	16.0	4.0	3.0	
		3	5195	6.33E+06	17.000	16.0	4.0	3.0	
6/16/00	179	1	5376	6.78E+06	17.000	16.0	4.0	3.0	No changes.
		2	5366	6.76E+06	17.000	16.0	4.0	3.0	
		3	5381	6.79E+06	17.000	16.0	4.0	3.0	
6/23/00	212	1	5405	6.85E+06	17.000	16.0	4.0	3.0	Light scaling has begun on one side
		2	5176	6.29E+06	17.000	16.0	4.0	3.0	
		3	5396	6.83E+06	17.000	16.0	4.0	3.0	
6/29/00	242	1	5366	6.76E+06	17.000	16.0	4.0	3.0	No changes
		2	5381	6.79E+06	17.000	16.0	4.0	3.0	
		3	5342	6.69E+06	17.000	16.0	4.0	3.0	
7/4/00	272	1	5381	6.79E+06	17.000	16.0	4.0	3.0	No changes
		2	5386	6.81E+06	17.000	16.0	4.0	3.0	
		3	5396	6.83E+06	17.000	16.0	4.0	3.0	
7/10/00	302	1	5303	6.60E+06	17.000	16.0	4.0	3.0	Corner has popped off (small)
		2	5342	6.69E+06	17.000	16.0	4.0	3.0	
		3	5415	6.88E+06	17.000	16.0	4.0	3.0	
7/14/00	322	1	5146	6.24E+06	17.062	16.0	4.0	3.0	No changes
		2	5142	6.23E+06	17.062	16.0	4.0	3.0	
		3	5137	6.21E+06	17.062	16.0	4.0	3.0	
7/20/00	353	1	5371	6.71E+06	16.848	16.0	4.0	3.0	No changes
		2	5366	6.69E+06	16.848	16.0	4.0	3.0	
		3	5371	6.71E+06	16.848	16.0	4.0	3.0	

APPENDIX B: SCALING TEST VISUAL OBSERVATIONS

B1. Mix A

Cycle	Mix	Specimen	Inspector Ratings A	B	C	D	Chemical	Average
0	A	1	0	0	0	0	CMA	0
		2	0	0	0	0		
		3	0	0	0	0	$MgCl_2$	0
		4	0	0	0	0		
5	A	1	1	1	1	0	CMA	1
		2	1	1	1	0		
		3	0	1	1	0	$MgCl_2$	1
		4	0	1	1	0		
10	A	1	1	2	1	0	CMA	1
		2	1	2	1	0		
		3	1	1	1	0	$MgCl_2$	1
		4	0	1	1	0		
15	A	1	1	2	1	1	CMA	1
		2	1	2	1	1		
		3	1	1	1	1	$MgCl_2$	1
		4	1	2	1	1		
25	A	1	1	2	1	1	CMA	1
		2	1	2	1	1		
		3	1	2	1	1	$MgCl_2$	1
		4	1	2	1	1		
50	A	1	1	2	1	1	CMA	1
		2	2	2	1	1		
		3	1	3	1	1	$MgCl_2$	1
		4	1	2	1	1		
70	A	1	1	4	2	2	CMA	2
		2	2	3	2	2		
		3	1	3	1	2	$MgCl_2$	2
		4	1	3	2	1		

B2. Mix B

Cycle	Mix	Specimen	Inspector Ratings				Chemical	Average
			A	B	C	D		
0	B	1	0	0	0	0	CMA	0
		2	0	0	0	0		
		3	0	0	0	0	$MgCl_2$	0
		4	0	0	0	0		
5	B	1	0	1	0	0	CMA	1
		2	0	0	1	0		
		3	1	1	1	0	$MgCl_2$	0
		4	0	0	0	0		
10	B	1	1	1	0	0	CMA	1
		2	1	1	1	0		
		3	1	2	1	0	$MgCl_2$	1
		4	0	1	0	0		
15	B	1	1	1	0	1	CMA	1
		2	2	1	1	1		
		3	2	2	1	1	$MgCl_2$	1
		4	1	1	0	1		
25	B	1	1	1	0	1	CMA	1
		2	2	1	1	1		
		3	2	2	1	1	$MgCl_2$	1
		4	2	1	0	1		
50	B	1	2	2	1	1	CMA	2
		2	2	2	1	1		
		3	2	3	1	1	$MgCl_2$	1
		4	2	2	0	1		
70	B	1	2	2	1	1	CMA	2
		2	2	2	1	1		
		3	2	3	1	2	$MgCl_2$	2
		4	2	2	1	1		

B3. Mix C

Cycle	Mix	Specimen	Inspector Ratings				Chemical	Average
			A	B	C	D		
0	C	1	0	0	0	0	CMA	0
		2	0	0	0	0		
		3	0	0	0	0	$MgCl_2$	0
		4	0	0	0	0		
5	C	1	0	0	1	0	CMA	0
		2	1	0	0	0		
		3	0	0	0	0	$MgCl_2$	0
		4	0	0	1	0		
10	C	1	0	1	1	0	CMA	0
		2	1	1	0	0		
		3	0	0	0	0	$MgCl_2$	1
		4	0	1	1	0		
15	C	1	1	1	1	1	CMA	1
		2	1	1	0	1		
		3	0	1	0	0	$MgCl_2$	1
		4	1	1	1	1		
25	C	1	1	1	1	1	CMA	1
		2	1	1	0	1		
		3	1	1	0	0	$MgCl_2$	1
		4	1	1	1	1		
50	C	1	1	2	1	1	CMA	1
		2	1	2	1	1		
		3	1	1	0	1	$MgCl_2$	1
		4	1	1	1	1		
70	C	1	1	2	1	1	CMA	1
		2	1	2	1	2		
		3	1	1	1	1	$MgCl_2$	2
		4	1	3	1	1		

B4. Mix D

Cycle	Mix	Specimen	Inspector Ratings				Chemical	Average
			A	B	C	D		
0	D	1	0	0	0	0	CMA	0
		2	0	0	0	0		
		3	0	0	0	0	$MgCl_2$	0
		4	0	0	0	0		
5	D	1	0	1	1	0	CMA	0
		2	0	1	1	0		
		3	0	0	0	0	$MgCl_2$	1
		4	0	1	1	0		
10	D	1	1	2	1	0	CMA	1
		2	1	2	1	0		
		3	1	1	0	0	$MgCl_2$	1
		4	1	1	1	0		
15	D	1	2	3	1	1	CMA	1
		2	1	2	1	1		
		3	2	1	0	1	$MgCl_2$	1
		4	1	2	1	1		
25	D	1	2	3	1	1	CMA	2
		2	2	3	1	1		
		3	2	2	0	1	$MgCl_2$	2
		4	2	2	1	1		
50	D	1	2	3	1	1	CMA	2
		2	2	3	1	1		
		3	2	2	1	1	$MgCl_2$	2
		4	2	3	1	1		
70	D	1	2	3	2	2	CMA	2
		2	2	3	2	2		
		3	2	3	1	2	$MgCl_2$	2
		4	2	3	2	1		

B5. Mix E

Cycle	Mix	Specimen	Inspector Ratings				Chemical	Average
			A	B	C	D		
0	E	1	0	0	0	0	CMA	0
		2	0	0	0	0		
		3	0	0	0	0	$MgCl_2$	0
		4	0	0	0	0		
5	E	1	0	0	0	0	CMA	0
		2	0	0	0	0		
		3	0	0	0	0	$MgCl_2$	0
		4	0	0	0	0		
10	E	1	0	0	0	0	CMA	0
		2	0	0	0	0		
		3	0	1	0	0	$MgCl_2$	0
		4	0	0	0	0		
15	E	1	1	1	0	1	CMA	1
		2	1	0	0	0		
		3	1	1	0	1	$MgCl_2$	0
		4	0	0	0	1		
25	E	1	1	1	0	1	CMA	1
		2	1	0	0	0		
		3	1	1	0	1	$MgCl_2$	0
		4	1	0	0	1		
50	E	1	1	1	0	1	CMA	1
		2	1	1	0	0		
		3	1	2	0	1	$MgCl_2$	1
		4	1	0	0	1		
70	E	1	1	1	0	1	CMA	1
		2	1	1	0	0		
		3	1	2	0	1	$MgCl_2$	1
		4	1	0	0	1		

APPENDIX C: SCALING TEST IMAGE ANLYSIS RESULTS

C1. Mix A

Mix A Specimen	Cycle #	Std	Mean	Coeff. Var.	Normalized
1	0	17.4005	179.6752	0.0968	1.00
	5	18.2812	142.9832	0.1279	1.32
	10	20.1287	177.1097	0.1137	1.17
	15	19.3664	163.3872	0.1185	1.22
	25	15.9739	107.0615	0.1492	1.54
	50	20.3555	154.4261	0.1318	1.36
	70	23.9531	171.5370	0.1396	1.44
2	0	19.5219	174.8797	0.1116	1.00
	5	33.7450	171.9215	0.1963	1.76
	10	25.2434	142.6359	0.1770	1.59
	15	27.4247	161.1592	0.1702	1.52
	25	26.2479	165.2114	0.1589	1.42
	50	28.2748	170.3038	0.1660	1.49
	70	23.7107	122.3081	0.19386	1.74
3	0	19.3707	178.6070	0.1085	1.00
	5	22.7567	155.9661	0.1459	1.35
	10	20.3247	179.2380	0.1134	1.05
	15	21.5836	155.6800	0.1386	1.28
	25	18.3667	122.0921	0.1504	1.39
	50	22.4704	143.2989	0.1568	1.45
	70	23.0711	127.1745	0.1814	1.67
4	0	21.2050	177.7906	0.1193	1.00
	5	23.4097	175.8382	0.1331	1.12
	10	21.9164	141.5139	0.1549	1.30
	15	18.4436	169.2871	0.1089	0.91
	25	13.4758	94.8425	0.1421	1.19
	50	16.9220	153.3866	0.1103	0.92
	70	21.2086	177.6579	0.1194	1.00

C2. Mix B

Mix B Specimen	Cycle #	Std	Mean	Coeff. Var.	Normalized
1	0	20.1266	181.7277	0.1108	1.00
	5	28.8380	180.8842	0.1594	1.44
	10	27.2170	196.6588	0.1384	1.25
	15	23.6100	177.9162	0.1327	1.20
	25	16.7938	98.21663	0.1710	1.54
	50	23.3743	142.8109	0.1637	1.48
	70	21.4846	135.4807	0.1586	1.43
2	0	18.1618	189.6725	0.0958	1.00
	5	19.2811	170.0038	0.1134	1.18
	10	29.2567	208.1049	0.1406	1.47
	15	23.9194	173.154	0.1381	1.44
	25	26.4284	146.2641	0.1807	1.89
	50	30.4547	144.3646	0.2110	2.20
	70	30.1764	173.3332	0.1741	1.82
3	0	22.7957	189.2420	0.1205	1.00
	5	29.30788	168.6069	0.1738	1.44
	10	26.1769	139.3669	0.1878	1.56
	15	23.9888	167.1192	0.1435	1.19
	25	16.2685	106.8412	0.1523	1.26
	50	22.6014	141.9018	0.1593	1.32
	70	18.8571	138.6608	0.1360	1.13
4	0	25.3501	182.6665	0.1388	1.00
	5	38.9968	176.3675	0.2211	1.59
	10	30.0580	199.0397	0.1510	1.09
	15	28.0891	158.8841	0.1768	1.27
	25	17.7837	94.3838	0.1884	1.36
	50	24.0975	126.1552	0.1910	1.38
	70	27.2857	176.2379	0.1548	1.12

C3. Mix C

Mix C Specimen	Cycle #	Std	Mean	Coeff. Var.	Normalized, %
1	0	21.8378	176.5893	0.1237	1.00
	5	36.0361	185.0868	0.1947	1.57
	10	26.9013	192.0211	0.1401	1.13
	15	22.5931	163.2744	0.1384	1.12
	25	17.3946	101.871	0.1708	1.38
	50	23.5267	146.715	0.1604	1.30
	70	26.7709	158.8672	0.1685	1.36
2	0	22.8754	164.7987	0.1388	1.00
	5	39.7513	178.718	0.2224	1.60
	10	26.1842	175.1253	0.1495	1.08
	15	24.4475	161.3749	0.1515	1.09
	25	22.1915	133.9957	0.1656	1.19
	50	26.8399	171.5466	0.1565	1.13
	70	25.5648	149.5001	0.1710	1.23
3	0	18.5668	173.4170	0.1071	1.00
	5	20.60221	191.8836	0.1074	1.00
	10	15.5102	140.1558	0.1107	1.03
	15	21.2529	165.1967	0.1287	1.20
	25				
	50	18.8918	155.0925	0.1218	1.14
	70	28.0605	180.9884	0.1550	1.45
4	0	19.9350	172.7898	0.1154	1.00
	5	39.4966	169.2748	0.2333	2.02
	10	22.1308	184.5593	0.1199	1.04
	15	22.5779	165.5222	0.1364	1.18
	25	19.1661	124.7190	0.1537	1.33
	50	24.3427	179.8047	0.1354	1.17
	70	29.5856	124.0760	0.2384	2.07

C4. Mix D

Mix D Specimen	Cycle #	Std	Mean	Coeff. Var.	Normalized
1	0	16.7815	178.5664	0.0940	1.00
	5	23.8169	136.652	0.1743	1.85
	10	26.3591	151.8481	0.1736	1.85
	15	20.9813	154.3085	0.1360	1.45
	25	15.5347	94.32707	0.1647	1.75
	50	21.4263	142.2676	0.1506	1.60
	70	23.9807	131.6716	0.1821	1.94
2	0	27.7726	186.4108	0.1490	1.00
	5	37.6616	167.9893	0.2242	1.50
	10	35.9165	202.0865	0.1777	1.19
	15	30.8958	175.5917	0.1760	1.18
	25	27.0324	109.4576	0.2470	1.66
	50	32.1015	180.7123	0.1776	1.19
	70	28.8653	164.612	0.1754	1.18
3	0	23.0944	184.4393	0.1252	1.00
	5	20.0275	145.3428	0.1378	1.10
	10	25.5022	176.4203	0.1446	1.15
	15	25.9124	161.8499	0.1601	1.28
	25	18.5706	104.6971	0.1774	1.42
	50	23.4383	147.5562	0.1588	1.27
	70	24.9498	126.596	0.1971	1.57
4	0	22.2872	178.9410	0.1246	1.00
	5	25.2750	158.7136	0.1592	1.28
	10	22.5936	146.2846	0.1544	1.24
	15	23.3228	161.3473	0.1446	1.16
	25	29.5566	203.2873	0.1454	1.17
	50	25.7062	170.7318	0.1506	1.21
	70	26.1079	176.3427	0.1481	1.19

C5. Mix E

Mix E Specimen	Cycle #	Std	Mean	Coeff. Var.	Normalized, %
1	0	19.8569	179.6721	0.1105	0.00
	5	21.0551	160.4902	0.1312	18.71
	10	14.6207	115.7194	0.1263	14.32
	15	23.6295	158.3849	0.1492	34.99
	25	16.3325	107.0742	0.1525	38.02
	50	24.5465	143.691	0.1708	54.57
	70	23.5187	156.2774	0.1505	36.17
2	0	21.3822	170.9611	0.1251	0.00
	5	17.3000	165.8407	0.1043	-16.59
	10	19.9558	185.9736	0.1073	-14.20
	15	19.4804	170.0085	0.1146	-8.38
	25	12.9209	95.62213	0.1351	8.04
	50	20.1347	177.0266	0.1137	-9.06
	70	15.1962	133.1184	0.1142	-8.73
3	0	21.0272	174.1937	0.1207	0.00
	5	27.0437	188.7466	0.1433	18.70
	10	28.8206	180.9562	0.1593	31.94
	15	25.3820	156.9555	0.1617	33.97
	25	18.4462	107.6196	0.1714	41.99
	50	25.1507	138.1344	0.1821	50.83
	70	22.0382	126.7114	0.1739	44.08
4	0	21.4968	193.7231	0.1110	0.00
	5	19.3604	184.5281	0.1049	-5.45
	10	18.8128	168.2562	0.1118	0.76
	15	19.5401	163.6288	0.1194	7.62
	25	16.3353	167.4553	0.0976	-12.09
	50	18.1434	177.5152	0.1022	-7.89
	70	22.0632	174.9025	0.1261	13.68